POLITECNICO DI TORINO

Corso di Laurea Magistrale

in INGEGNERIA MECCANICA

Tesi di Laurea Magistrale

Front-to-total anti-roll moment distribution control to enhance vehicle cornering response

Relatori

Prof. Mauro VELARDOCCHIA

Prof. Aldo SORNIOTTI

Prof. Enrico GALVAGNO

Candidato

Marco RICCO

A.A.2017/2018

Acknowledgements

Vorrei innanzitutto ringraziare i miei genitori, Maria e Federico, per avermi sempre sostenuto e avermi dato la possibilità di intraprendere questo corso di studi universitario.

Ringrazio poi i miei amici, nuovi e vecchi, con i quali ho condiviso diverse esperienze importanti della mia vita, nonostante le strade intraprese da ognuno di noi siano totalmente diverse.

Vorrei innanzitutto ringraziale il professor. Ing. Mauro Velardocchia per avermi dato l'opportunità di intraprendere questo lavoro di tesi all'estero, nel Regno Unito.

Vorrei poi ringrazire il professor. Ing. Aldo Sorniotti, il mio supervisore Inglese, per il grande supporto datomi, per avermi assegnato questa attività di ricerca, per avermi dato la possibilità di allargare le mie competenze, sia tecniche che relazionali,e sviluppare determinate "soft skills", del tipo problem-solving.

Abstract

This Thesis has been developed at the Centre of Automotive Engineering at the University of Surrey. The aim of this work was to investigate and design a controllable suspension system to enhance vehicle cornering response.

Different simulation tests, in steady state and transient conditions, were carried out to prove the benefit, in terms of improvement of lateral vehicle dynamics, of adopting this front-to-total anti-roll moment distribution controller. This control has got a feedback part and a feedforward contribution.

The first results showed that, by varying the load transfer among the front and rear axle, there is an increase of 10% in the values of lateral acceleration achievable.

Moreover, the analysis of the tyre led to the formulation of a new linearization of the lateral forces on each axle, for the design of the feedback part of the controller, and to reformulate the classic single-trac vehicle model.

The analysis, with the new model, highlighted an expected dynamic behaviour with respect the strategy of the controller.

The final simulations showed that the most significant contribution, in steady state, was caused by the feedforward part whilst the feedback became relevant only in transient tests.

Table of contents

CHAPTER 1

1.1 Introduction

This Master's Thesis work was carried out in the Research group of the Centre of Automotive Engineering at University of Surrey. The aim of this work was to study, develop and implement an innovative active suspension controller in order to improve the dynamic behaviour of the vehicle.

In particular, the goal of this controllable suspension system is to control the roll angle and the yaw rate of the vehicle body and to permit to reach highest values of lateral accelerations. This aim is reached by using a front-to-total anti-roll moments distribution to enhance the lateral dynamics in steady-state and transient conditions.

In literature, it is possible to find several researches and several methods of how, by adopting an active suspension system, it is possible to adjust and enhance the ride comfort of the passengers; on this hand, very advanced methods were developed which make also use from the vehicle connectivity capability. Because of this, the following activity focused the attention of how to improve the handling of the vehicle, with less attention to the comfort.

All the activity was carried out in MATLAB-Simulink, one of the main software used by the Research Centres and companies in simulation.

The vehicle, used in simulation, is a validated car in MATLAB-Simulink by using experimental data. In particular, the vehicle is an electric SUV with four in-wheel torque motors, where the main characteristics are reported in Table 1.1.

This model has been used also in other activities of University of Surrey; in this way the problem the approached by studying the passive system and then controllable system with not an abstract vehicle but with a realistic model car.

Vehicle parameters	
Wheelbase [m]	2.933
Front semi-wheelbase [m]	1.559
Rear semi-wheelbase [m]	1.374
Front track width [m]	1.676
Front track width [m]	1.742
Height of centre of gravity [m]	0.72
Vehicle mass [kg]	2530
Total roll stiffness of passive components of the suspension system [Nm/rad]	108480
Total damping coefficient of passive components of the suspension system [Nms/rad]	16042

Table 1.1: main parameters of the vehicle used in simulation

1.2 Structure of the Thesis

This work presents seven chapters in total. The second chapter reports some examples of paper and patent developed in the last years, regarding systems that allow to vary, in different way the anti-roll moment between the front and rear axles. The third chapter explains how it is implemented the new controller in MATLAB-Simulink and the main equations of the vehicle dynamics. At the end, they are showed some simulation results to verify that the controller was implemented in a correct way.

The fourth chapter refers to the explanation of the quasi-static model, used for the design of the feedforward contribution and for the design of the reference yaw rate for different vehicle speeds. The fifth chapter investigates the characteristic of the tyres, adopted in this model, and presents the novel linearized formulation of the lateral forces and of the bicycle model.

The sixth chapter is about the design of the feedback contribution of the controller and the definition of the main transfer functions; the seven and last chapter they are reported the conclusion and the future works.

CHAPTER 2

2.1 Literature review

The objective task of this thesis is to find a method to improve the dynamic behaviour of a vehicle in cornering conditions by adopting a controllable suspension system. In general, as explained before and in details in the next chapter, it is possible to vary the behaviour of the vehicle by changing the load transfer and so the anti-roll moment among the front and rear axle in order to have a vehicle less or more understeer and to reach some reference and desirable dynamic response. To this end, the existing literature review is analysed to highlight some proposed methods. The follow paper/patent provide some criteria of active roll control system.

2.2 Method proposed by "TRW"

This paper makes use of the concepts of understeer, neutral steer, and oversteer to develop nonlinear controllers to influence roll moment distribution. Most of the models use linear analysis techniques; essentially, they consider as a first order approximation a well-defined relationship between the side slip angle and the lateral force. The results can change if the vertical load is changed on each tyre. A linear approach of the lateral force with the normal force, according the theory of TRW, doesn't improve the vehicle model.

In particular, in Figure 2.1, it is possible to see how a generated lateral force is a non-linear function of normal force. The data shows that due to the load transfer more lateral force is lost, in cornering conditions, on a side of an axle than is gained by the addition of that normal force to the other side.

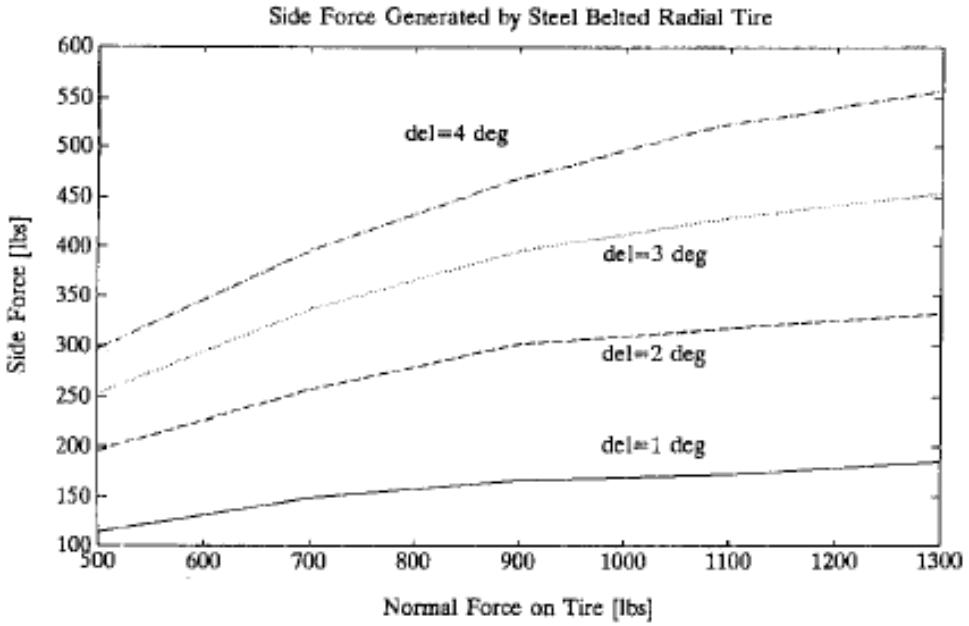

Figure 2.1: Lateral force as a function of vertical load for different values of slip angle

By these considerations, this paper assumes a higher order dependence of side force on normal force and suggests this empirical tire model by this following equation:

$$Y_i = C_1 \alpha_i N_i + C_2 \alpha_i N_i^2$$

Where:

- Y_i is the side force generated by the i-th tyre
- α_i is the slip angle of the i-th tyre
- N_i is the normal force on the i-th tyre
- C_1 and C_1 are empirical constants to be determined from the data

The front and rear axle lateral forces are assumed by TRW as sum of side forces on each tyre, by the following expressions:

$$Y_F = Y_1 + Y_2$$

$$Y_R = Y_3 + Y_4$$

$$\alpha_1 \approx \alpha_2 = \alpha_F$$

$$\alpha_3 \approx \alpha_4 = \alpha_R$$

By arranging all the calculation, this paper presents the side forces on the front and rear axle as:

$$Y_F = \alpha_F[C_1(N_1 + N_2) + C_2(N_1^2 + N_2^2)]$$

$$Y_R = \alpha_R[C_1(N_3 + N_4) + C_2(N_3^2 + N_4^2)]$$

$$\alpha_F = \delta_W - \frac{ar + v}{u}$$

$$\alpha_R = \frac{br - v}{u}$$

The model of the paper has two degrees of freedom: the yaw rate, r, and lateral velocity v and the vehicle runs at constant speed u. The system of equations is:

$$\begin{cases} m(\dot{v} + ur) = Y_1 + Y_2 + Y_3 + Y_4 \\ J_z\dot{r} = a(Y_1 + Y_2) - b(Y_3 + Y_4) \end{cases}$$

Where:

- J_z is the yaw moment of inertia
- m is the mass of the vehicle
- a and b are the distances from the vehicle centre of mass to the front and rear axle respectively

The side force developed by the front and rear tyres can be combined to yield the side force generated by the front and rear axle. The model becomes

$$\begin{cases} \dot{v} = \frac{1}{m}(Y_F + Y_R) - ur \\ \dot{r} = a\frac{1}{J_z}Y_F - B\frac{1}{J_z}Y_R \end{cases}$$

The normal forces associated with each tyre can be written as:

$$N_1 = W\frac{b}{2(a+b)} + mur\frac{h}{t}(1 + \varepsilon)$$

$$N_2 = W\frac{b}{2(a+b)} - mur\frac{h}{t}(1 + \varepsilon)$$

$$N_3 = W\frac{a}{2(a+b)} + mur\frac{h}{t}(1 - \varepsilon)$$

$$N_4 = W\frac{a}{2(a+b)} - mur\frac{h}{t}(1-\varepsilon)$$

Where:

- W is the vehicle weight
- h is the height of the centre of mass
- t is the track of the vehicle
- The term mur is the steady state inertia force acting on the centre of mass
- The term $\frac{h}{t}$ can be thought as the vehicle aspect ratio
- ε is the roll moment distribution coefficient
- $N_i, i = 1, \ldots, 4$ are the normal forces on the four tyres

TWR defines ε as the ratio between the difference between the front and rear axles roll moment and the sum between the front and rear axles roll moment:

$$\varepsilon = \frac{M_F - M_R}{M_F + M_R}$$

$$-1 \leq \varepsilon \leq 1$$

Inserting the normal force expression in the lateral forces one and rearranging all the terms:

$$Y_F = \alpha_F \left[C_1 W \frac{b}{a+b} + \frac{1}{2} C_2 W^2 \left(\frac{b}{a+b}\right)^2 + 2C_2 \left(mu\frac{h}{t}\right)^2 (1+\varepsilon)^2 r^2 \right]$$

$$Y_R = \alpha_R \left[C_1 W \frac{a}{a+b} + \frac{1}{2} C_2 W^2 \left(\frac{a}{a+b}\right)^2 + 2C_2 \left(mu\frac{h}{t}\right)^2 (1+\varepsilon)^2 r^2 \right]$$

At this point the authors introduce the following notations:

$$C_F = C_1 W \frac{b}{a+b} + \frac{1}{2} C_2 W^2 \left(\frac{b}{a+b}\right)^2$$

$$C_R = C_1 W \frac{a}{a+b} + \frac{1}{2} C_2 W^2 \left(\frac{a}{a+b}\right)^2$$

$$C_\varepsilon = 2C_2 \left(mu\frac{h}{t}\right)^2$$

Where:

- C_F and C_R correspond to the cornering stiffness

- C_ε is the non-linear term

The lateral forces Y_F and Y_R are re-written as follow:

$$Y_F = \alpha_F[C_F + C_\varepsilon(1+\varepsilon)^2 r^2]$$

$$Y_R = \alpha_R[C_R + C_\varepsilon(1-\varepsilon)^2 r^2]$$

With C_F and C_R correspond to the familiar cornering stiffness of the linearized model. By replacing $\alpha_F$and $\alpha_R$expressions there is:

$$Y_F = \left(\delta_w - \frac{ar+v}{u}\right)[C_F + C_\varepsilon(1+\varepsilon)^2 r^2]$$

$$Y_R = \frac{br-v}{u}[C_R + C_\varepsilon(1-\varepsilon)^2 r^2]$$

Then by using all these equations, the updated system of motion of this work becomes as;

$$\begin{cases} \dot{v} = -ur + \left(\delta_w - \frac{ar+v}{u}\right)\left(\frac{C_F}{m} + \frac{C_\varepsilon}{m}(1+\varepsilon)^2 r^2\right) + \left(\frac{br-v}{u}\right)\left(\frac{C_R}{m} + \frac{C_\varepsilon}{m}(1-\varepsilon)^2 r^2\right) \\ \dot{r} = \left(\delta_w - \frac{ar+v}{u}\right)\left(\frac{aC_R}{J_z} + \frac{aC_\varepsilon}{J_z}(1+\varepsilon)^2 r^2\right) - \left(\frac{br-v}{u}\right)\left(\frac{bC_R}{J_z} + \frac{bC_\varepsilon}{J_z}(1+\varepsilon)^2 r^2\right) \end{cases}$$

2.3 Patent no.: 5,948,027

The Patent presented By Oliver, Jr. et in Sep.7, 1999, provides a method of enhancing vehicle stability in a vehicle having an active roll control system with front and rear suspensions each including an anti-roll bar, and the control system being capable of providing an adjustable anti-roll moment at the front and rear anti-roll bars.

The following flow diagram, in Figure 2.2, gives an idea of the implementation of the present invention:

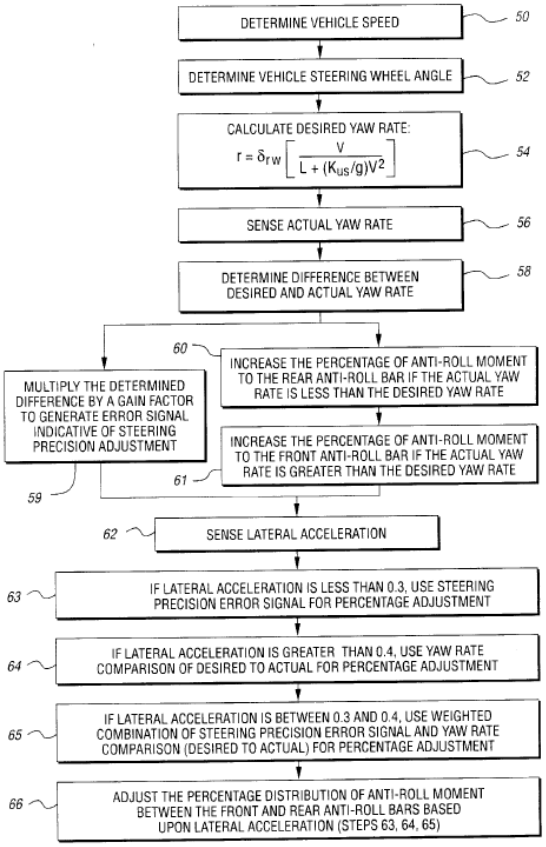

Figure 2.2: Flow diagram of control system of the Patent implemented method

The main steps are: determination of the vehicle speed, v, determination of the steering wheel angle, computation of the desired yaw rate according the following formula:

$$r_{ss} = \delta_{rw}\left[\frac{v}{L+\left(\frac{k_{US}}{g}\right)*v^2}\right]$$

Where:

- L is the wheel base
- g is the gravity acceleration
- k_{US} is the understeer gradient
- δ_{rw} is the road wheel angle which is directly proportional to the steering wheel angle

By setting the measured yaw rate, the authors calculate the yaw rate error as the difference between the desired yaw rate and the measured yaw rate

$$r_{error}(t) = r_{ss}(t) - r_{measured}(t)$$

Then, this invention proposes three kinds of control to improve vehicle stability in function of the lateral acceleration:

- if the lateral acceleration is greater than 0.4g a PID controller is used to decrease the percentage of anti-roll moment to the front anti-roll bar if the actual yaw rate is less than the desired yaw rate or increase the percentage of anti-roll moment to the front anti-roll bar if the actual yaw rate is major than the desired yaw rate.
- if the lateral acceleration is less than 0.3g a gain multiplies the yaw rate error for a correction indicative of the steering precision adjustment.
- if the lateral acceleration is between 0.3g and 0.4g, a weighted combination of steering precision error signal and yaw rate comparison is used between the two thresholds.

The Figure 2.3 shows the block diagram for implementing the method adopted by the patent:

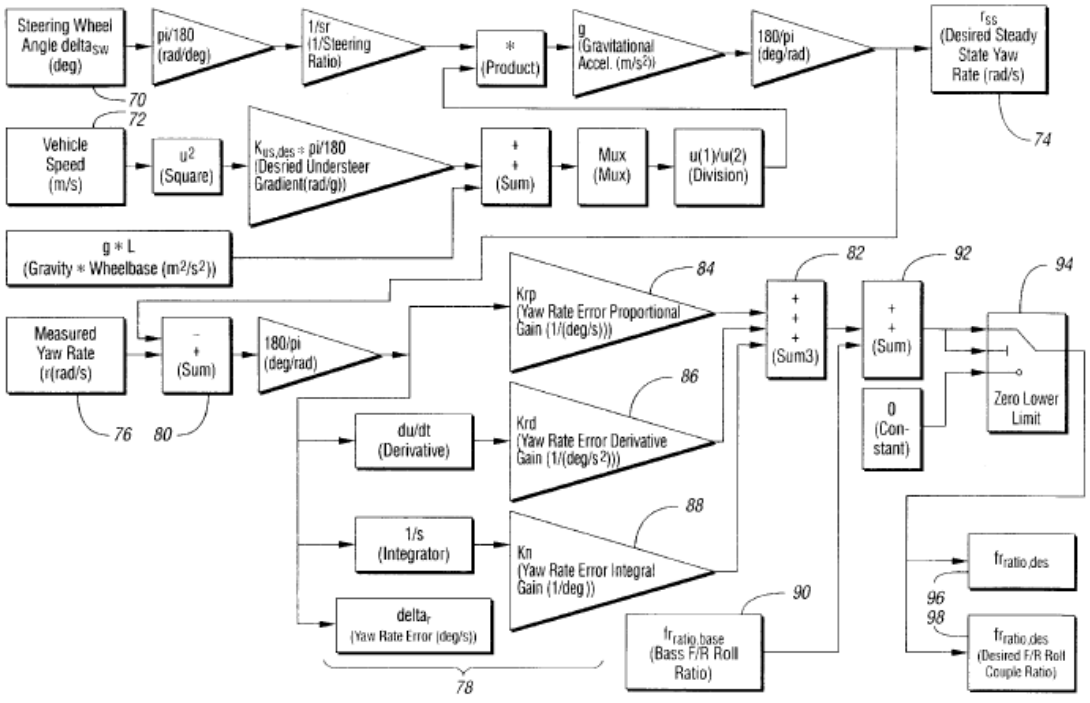

Figure 2.3: Simplified control structure of the patent

Essentially it is used a PID feedback controller loop, with a proportional gain K_{rp}, integral gain K_n and derivative gain K_{rd}, based on the error signal between the desired yaw rate and the measured yaw rate generates the yaw rate contribution of the front ratio change

$$f_{PID}(t) = K_{rp} * r_{error}(t) + \int_0^t K_n * r_{error}(\tau)d\tau + K_{rd} * \frac{d}{dt}(r_{error}(t))$$

The output f_{PID}, for example of the PID controller, is added with the base roll couple ratio of the passive vehicle, as equation:

$$f = f_{PID} + f_{r\ ratio,base}$$

$$\text{With } f_{r\ ratio,base} = \frac{M_{FRONT}}{M_{REAR}}$$

At the end there is a block 94 that compares the f to zero and picks the larger of two, thereby preventing a negative roll couple ratio. The output is the new desired roll couple distribution.

Patent no.: US 6,471,218 B1

This patent, by Burdock et.at, discuss a method of active-roll control system in which the anti-roll bars are with actuators which can provide a torque in the anti-roll bars to control vehicle body roll. For example, if there is a condition for which the vehicle is oversteering, the actuators supply pressure on front-axle in order that the front-wheels tend to break away. In Figure 2.4 it represented an example of strategy to understand how the system works:

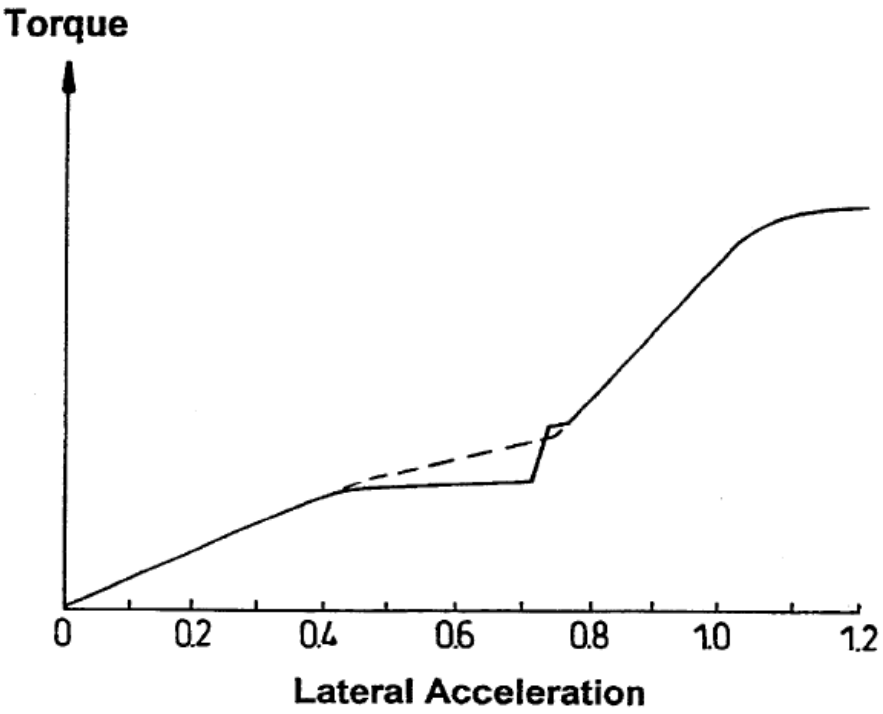

Figure 2.4: First torque characteristic of the actuators

For normal conditions the characteristic is the broken line and the control unit arranges to apply an equal torque between the front and rear axle. This system would be suitable for that vehicle which oversteers for values of lateral acceleration greater than 0.8g; in this case the rear axle tends to lose grip. In this situation the control provides a torque that sets up a vertical vibration in the wheels, by causing that both the front and rear axles break away at the same time.

In Figure 2.5, it is showed a second characteristic of the actuator used in this patent. In this case a mean torque component which increase smoothly as a function a of lateral acceleration and a pulsed torque which is present for high values of lateral acceleration. When the pulse torque starts, for value of lateral acceleration equal to 0.7g, it provokes a raise of the mean torque; in this way the front and rear axles break away at the same time it is done to prevent the oversteering behaviour of the vehicle at the tightest point of the turn.

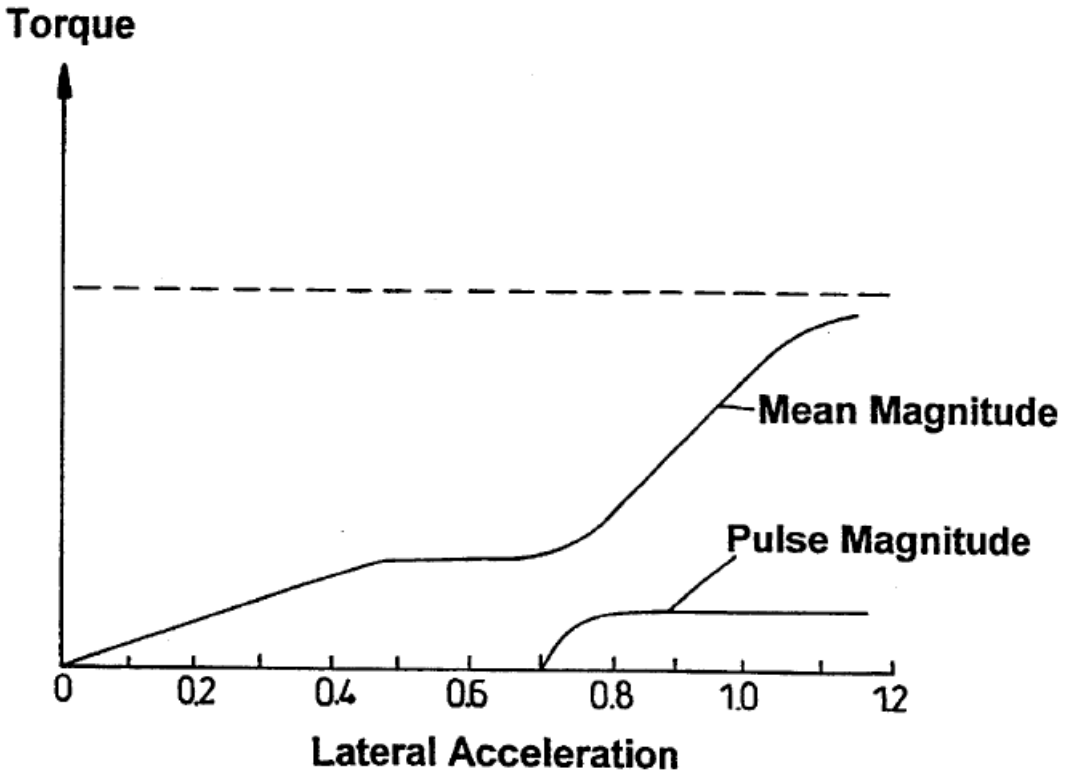

Figure 2.5: Second torque characteristic of the actuators

CHAPTER 3

3.1 Introduction

In general, in the vehicle dynamics it is possible to enhance the vehicle cornering response by using a controllable suspension system which allows the variation of the load transfer distribution among the front and rear axles; thus, major levels of lateral acceleration can be reached close to the cornering limit. This is because of the typical automotive tyre is characterized by a non-linear behaviour.

The load transfer distribution, due to lateral acceleration while cornering, changes as a function of the roll stiffness distribution and it is expressed by the following equations:

$$\Delta F_{z,F,a_y} = \frac{ma_y}{T_F}\left(\frac{bd}{L} + \frac{k_{ROLL,F}H_{ROLL}}{k_{ROLL,F} + k_{ROLL,R}}\right)$$

$$\Delta F_{z,R,a_y} = \frac{ma_y}{T_R}\left(\frac{ad}{L} + \frac{k_{ROLL,R}d_{ROLL}}{k_{ROLL,F} + k_{ROLL,R}}\right)$$

The total load transfer is the sum of the load transfer on the rear and front axle and it is given by:

$$\Delta F_{z,total,a_y} = \frac{ma_y}{T_F}\left(\frac{bd}{L} + \frac{k_{ROLL,F}H_{ROLL}}{k_{ROLL,F} + k_{ROLL,R}}\right) + \frac{ma_y}{T_R}\left(\frac{ad}{L} + \frac{k_{ROLL,R}H_{ROLL}}{k_{ROLL,F} + k_{ROLL,R}}\right)$$

$$= \frac{ma_y}{T}\left[\frac{(a+b)d}{L} + \frac{\left(k_{ROLL,F} + k_{ROLL,R}\right)H_{ROLL}}{k_{ROLL,F} + k_{ROLL,R}}\right] = \frac{ma_y}{T}(d + H_{ROLL}) =$$

$$= \frac{ma_y h_{CG}}{T}$$

The Figure 3.1, in a first approximation of conditions of pure cornering, represents the shape of the cornering stiffness as a function of the vertical load and shows the effect of the load transfer distribution in cornering on change of the cornering stiffness on that axle considered.

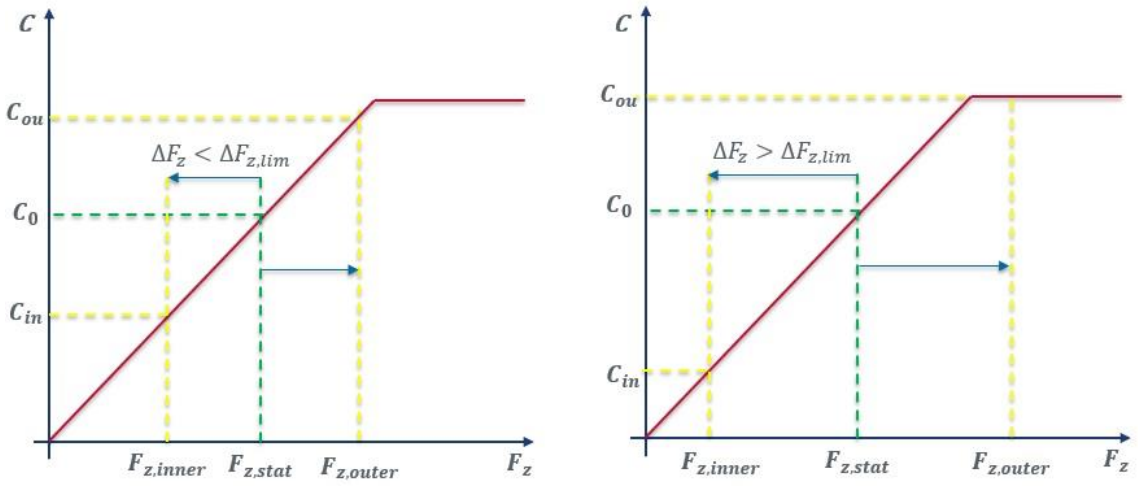

Figure 3.1: Variation of the cornering stiffness as a function of the vertical load

The load transfer, when it is caused by high values of lateral acceleration, provokes an increase of the vertical load on the outer wheel of that axle and a reduction of the vertical load on the inner wheel; the overall effect is the reduction of the cornering stiffness of that axle, because the reduction of the cornering stiffness on the inner wheel is greater than the increase of the cornering stiffness of the outer wheel.

In formulas, in case of pure cornering it is possible to write:

$$C_{axle} = \left(C_0 + \Delta F_z \frac{\partial C}{\partial F_z}\right) + \left(C_0 - \Delta F_z \frac{\partial C}{\partial F_z}\right) \cong 2C_0$$

$$\Delta C_{outer} = \Delta C_{inner} = \Delta F_z \frac{\partial C}{\partial F_z}$$

The contributes ΔC_{outer} and ΔC_{inner} compensate each other in case of small lateral load transfers.

For medium and high values of lateral accelerations $\Delta C_{outer} < \Delta C_{inner}$ and so:

$$C_{axle} = (C_0 + \Delta C_{outer}) + (C_0 - \Delta C_{inner}) < 2C_0$$

The reduction of the cornering stiffness on the axle has impact on the slope of the understeer characteristic, which represents the dynamic steering angle as a function of lateral acceleration as reported an example in Figure 3.2. The slope, on linear region of the understeer characteristic, is called understeering gradient and it is a function of the cornering stiffnesses on the rear and front axle. It is defined by the following expression:

$$k_{US} = \frac{mg}{L^2}\left(\frac{a}{C_F} - \frac{b}{C_R}\right)$$

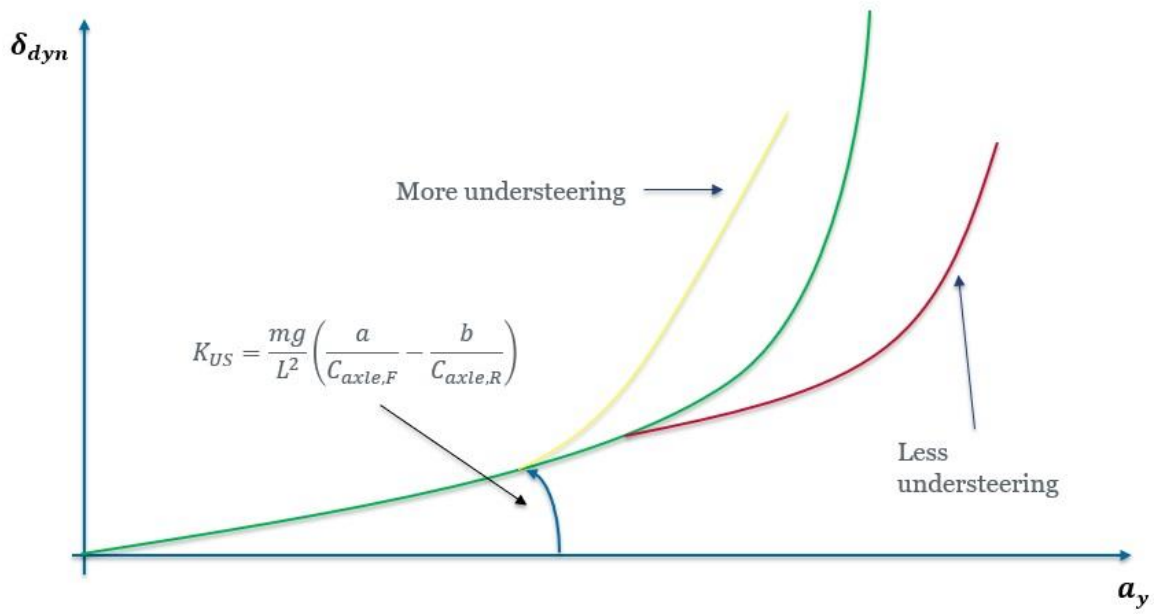

Figure 3.2: Example of understeering characteristics of a vehicle

The increase of the roll stiffness of the front suspension system, at medium-high lateral accelerations, provokes a reduction of the cornering stiffness on the front axle, an increase of the slip angle values for generating the same lateral force, a reduction of the rear load transfer and a reduction of the rear slip angle for provoking the same lateral force.

At the end, k_{US} increases and it is needed more steering wheel angle to reach the maximum value of lateral acceleration and the vehicle becomes more understeer.

Vice versa, by increasing the roll stiffness on the rear suspension system, the behaviour is the opposite of the previous one and the vehicle tends to be more oversteer. In this case K_{US} decreases and it is needed less steering wheel angle to have the same value of lateral acceleration.

3.2 Front-to-total anti-roll moment distribution control

In this part of the chapter, it is presented the implementation of the front-to-total anti-roll moment distribution control with a reference understeer characteristic.

The Figure 3.3 shows the overall structure of the controller implemented in MATLAB-Simulink. The inputs of the system are: the steering wheel angle, the body longitudinal speed, the body roll rate, the measured body yaw rate, the body longitudinal acceleration, whilst the outputs of the system are: the active anti-roll force front right, the active anti-roll force front left, the active anti-roll force rear right and the active anti-roll force rear left.

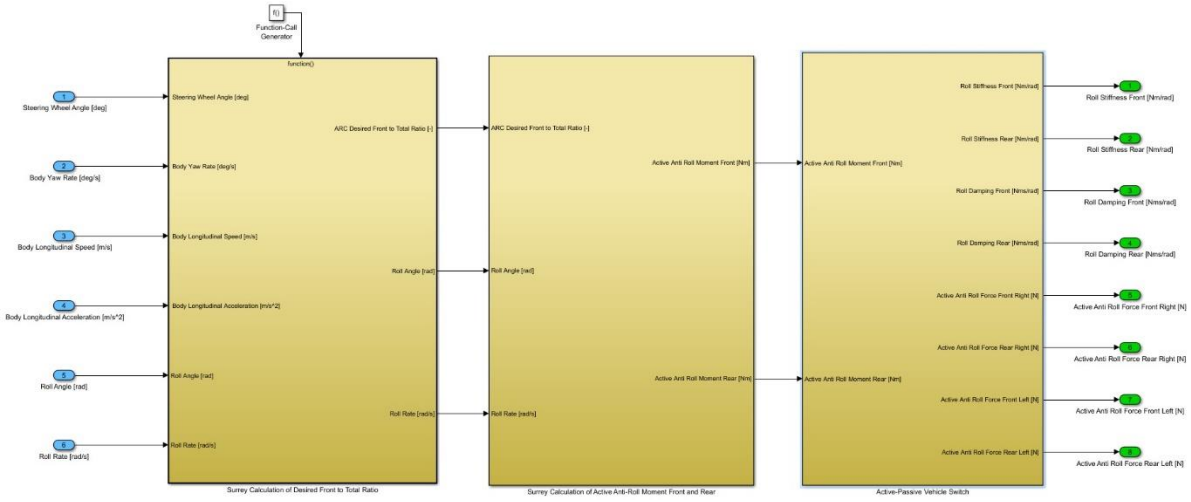

Figure 3.3: Main blocks of the front-to-total roll stiffness distribution control

The first block permits to calculate the desired front-to-total ratio by using a PID controller; the second block permits to calculate the active anti-roll moment on the front axle and the active anti-roll moment on the rear axle and at the end the third block calculates the active anti-roll forces of the actuators on each wheel.

Several points of novelty are in the implementation of the front-to-total distribution anti-roll moment.

First of all, the controller includes a feedforward contribution and a feedback part contribution; the feedforward contribution is very important because it allows a less aggressive tuning of the feedback part and a control action smoother; moreover, it is less affected from the noise disturbances with respect to the feedback part. The feedforward contribution is not-linear and it is designed through a non-linear quasi static model. The overall procedure is explained in chapter 4.

The reference yaw rate for the vehicle is not linear because of the typical non-linear behaviour of the vehicle. It is designed as well by using a non-linear quasi static model.

The feedback of the controller includes an anti-wind up contribution, a gain scheduling and a different activation process as a function of lateral acceleration.

3.2.1 Controller implementation

In Figure 3.4 it is showed a simplified schematic of the control structure for the calculation of the front-to-total roll stiffness distribution ratio.

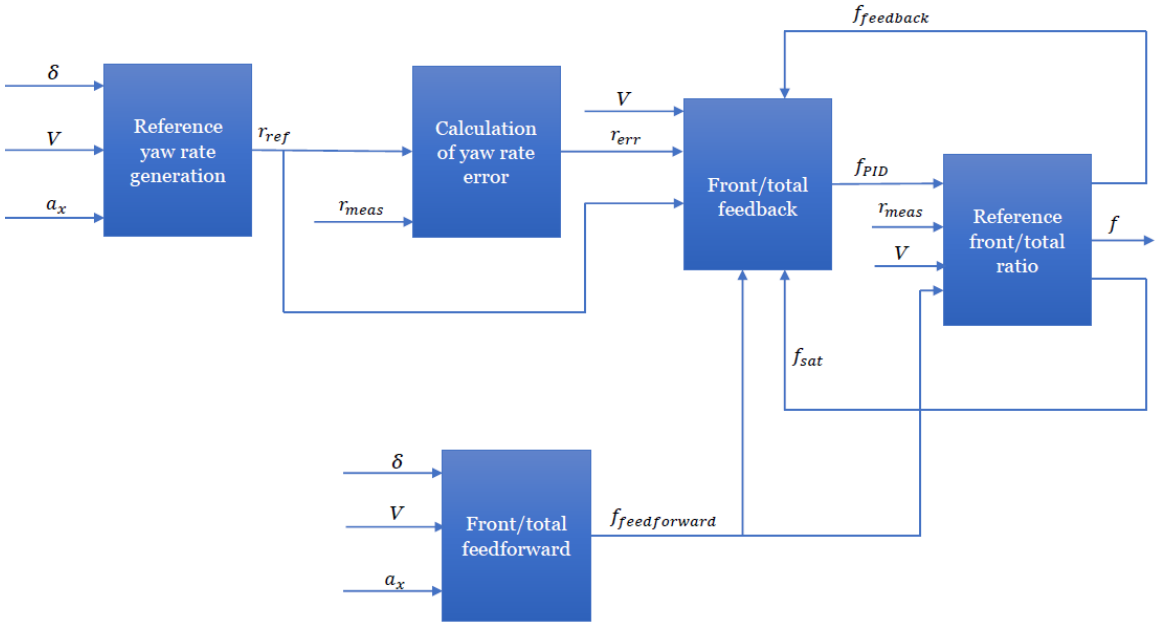

Figure 3.4: Simplified schematic of the control structure

This controller is based on the error of the yaw rate. By using a non-linear quasi static model, it is designed the look-up table that generates the reference yaw rate, in steady state condition, as a function of road wheel angle, vehicle speed and longitudinal acceleration.

$$r_{ref,ss} = r_{ref,ss}(\delta_{rw}, V, a_x)$$

Then a discrete transfer function produces a realistic and desirable yaw rate dynamics, as showed in the Figure 3.5:

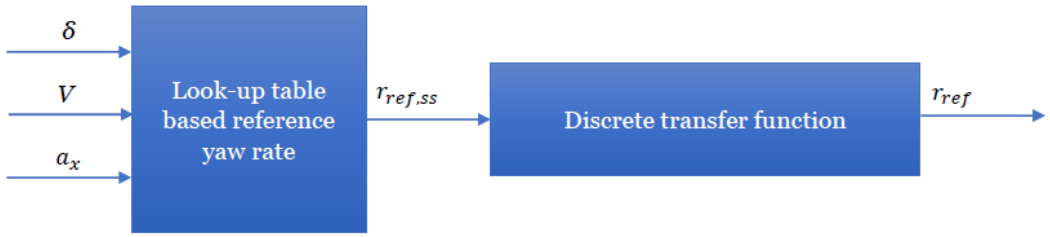

Figure 3.5: Calculation of the reference yaw rate

The output of the controller is the sum of the feedforward steady-state roll stiffness ratio $f_{feedforward}$ and the feedback contribution $f_{feedback}$:

$$f = f_{feedforward} + f_{feedback}$$

This factor f is the ratio between the stiffness anti-roll moment on the front axle and the total stiffness anti-roll moment and it is defined as:

$$f = \frac{M_{ANTI-ROLL,STIFF,F}}{M_{ANTI-ROLL,STIFF,TOT}}$$

By using a non-linear quasi-static model, as it is done for the reference yaw rate, it is designed a look-up table that generates the front-to-total feedforward contribution for steady state conditions as a function of road wheel angle, vehicle speed and longitudinal acceleration. The Figure 3.6 represents the block for the calculation of the feedforward ratio.

$$f_{feedforward} = f_{feedforward}(\delta_{rw}, V, a_x)$$

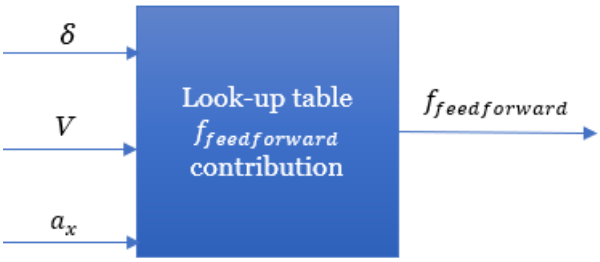

Figure 3.6: Calculation of the feedforward contribution

The feedback part would act only in transient conditions; to avoid the activation of it below certain lateral accelerations, a look-up table generates a weight factor as a function of the equivalent lateral acceleration based on yaw rate. The weight factor is given by the following system:

$$w_{a_y} = \begin{cases} 0 & if\ |rV| < a_{y,th,1} \\ \dfrac{rV - a_{y,th,1}}{a_{y,th,2} - a_{y,th,1}} & if\, a_{y,th,1} < |rV| < a_{y,th,2} \\ 1 & if |rV| > a_{y,th,2} \end{cases}$$

For the design of the front to-total anti-roll moment the values of $a_{y,th,1}$ and $a_{y,th,2}$ are respectively 0.3g and 0.6g.

The feedback contribution is scaled with the weight factor, as by the next expression:

$$f_{feedback} = w_{a_y} f_{PID}$$

The yaw rate error r_{error}, used in the control strategy and in the feedback controller, is defined as the difference between the reference and measured yaw rate multiplied by the sign of the reference yaw rate, as by this equation:

$$r_{error} = (r_{measured} - r_{reference}) sign(r_{reference})$$

It is considered also the signed of the reference yaw rate, because the vehicle must have the same behaviour if the driver is cornering to the left or to the right; in other words, the behaviour of the car has to be symmetric.

The Figure 3.7 below shows as the controller acts for different levels of lateral acceleration.

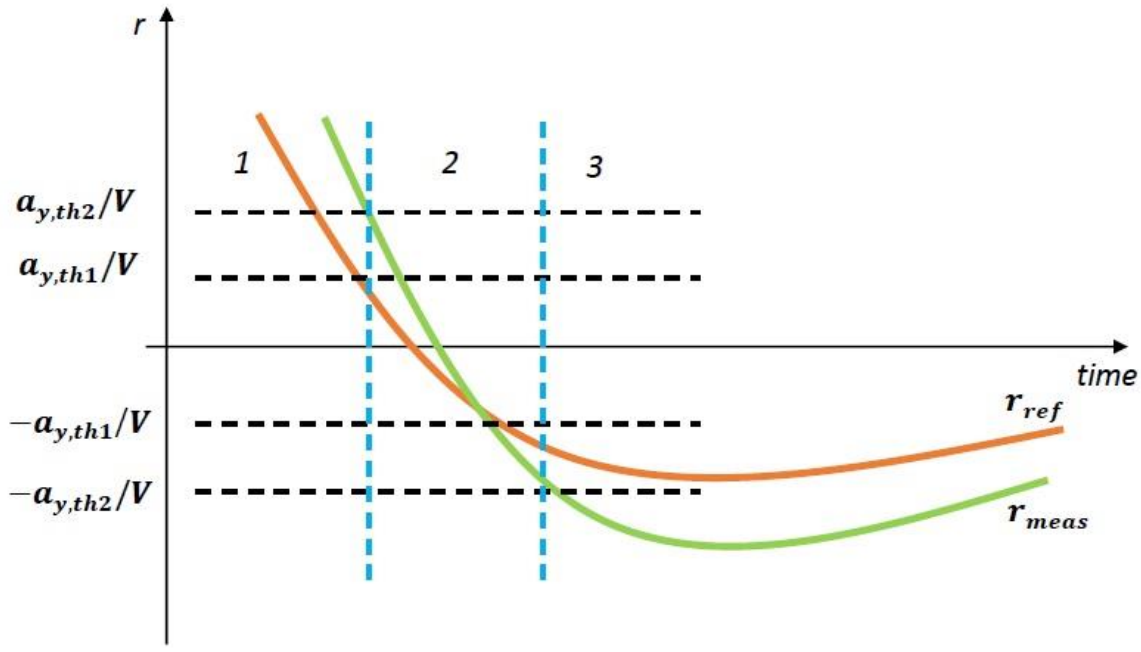

Figure 3.7: Example of strategy of the controller based of the yaw rate error

In the figure above, it is possible to identify three zones of interest:

- a first zone, where the measured yaw rate $r_{measured}$ and the reference yaw rate $r_{reference}$ have the same sign and the vehicle, in this case is oversteering; in fact $r_{measured}$ is greater than $r_{reference}$ with respect to the reference. The controller is fully active when yaw rate is above $\frac{a_{y,th2}}{V}$
- a second zone, where the measured yaw rate and the reference yaw rate are close to zero. The controller is not active $\left(f_{feedback} = 0\right)$ when $-\frac{a_{y,th1}}{V} < r < \frac{a_{y,th1}}{V}$ and is progressively activated when the yaw rate is $-\frac{a_{y,th2}}{V} < r < -\frac{a_{y,th1}}{V}$ and $\frac{a_{y,th1}}{V} < r < \frac{a_{y,th2}}{V}$
- a third zone, where the measured and the reference yaw rate have the same sign again. The vehicle is oversteering with respect to the reference. The controller is fully active when yaw rate is below $-\frac{a_{y,th2}}{V}$.

The feedback contribution is based on a PID controller with a proportional gain K_P, an integral gain K_I, an anti-wind up gain K_{AW} and a derivative gain K_D based on the yaw rate error. The expression of the output of the PID controller is:

$$f_{PID} = f_P + f_D + f_I + f_{AW}$$

The proportional gain is scheduled with vehicle speed:

$$K_P = K_P(V)$$

The f_P contribution is given by the following expression:

$$f_P = K_P r_{error}$$

The derivative and integral gains are always scheduled with vehicle speed:

$$K_D = K_D(V)$$

$$K_I = K_I(V)$$

The f_D and f_I contributions of the controller are given by the following expressions:

$$f_D = K_D \frac{dr_{error}}{dt}$$

$$f_I = K_I \int r_{error}(t)dt$$

In the controller it is also included an anti-windup contribution to prevent the increase of the integral contribution when the control action is saturated. The equation of this contribution is the following:

$$f_{A.W} = \int \left(f_{saturation}(t) - f_{feedforward}(t) - r_{feedback}(t)\right) dt$$

The integral and anti-windup terms of integrator controller include a reset condition, based on the reference yaw rate and its time derivative:

$$K_{I,reset} r_{reference} + \frac{dr_{reference}}{dt} > K_{I,reset,threshoald}$$

3.2.2 Calculation on the front and rear anti-roll moments

The Figure 3.8 gives an idea how they are calculated the anti-roll moments on the rear and on the front axle.

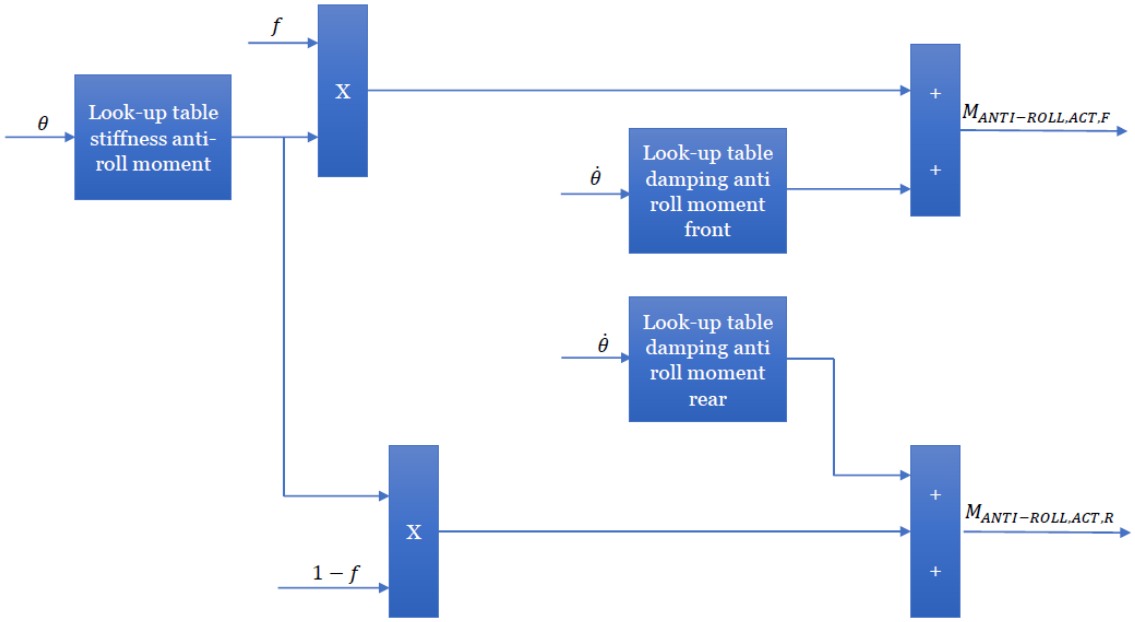

Figure 3.8: Scheme for the derivation of the anti-roll moment on the front-rear axles

This part of the model includes two look-up tables for the definition of the stiffness anti-roll moment, of the damping anti-roll moment on the front axle and the damping anti roll moment on the rear axle.

The total stiffness anti-roll moment, in case of active vehicle through this controllable suspension system, is varied through the parameter f, which is the output of the controller. In this way it is possible to have more roll stiffness on the front axle or on the rear axle to correct, respectively, the potential and dangerous oversteer or understeer behaviour of the vehicle.

In this case, the front-to-total ratio parameter f doesn't permit to vary the damping contribution of the moment; thus the rear and front damping anti-roll moments remain constant.

The following expressions give the front anti-roll moment and the rear anti-roll moment due to the control action:

$$M_{ANTI-ROLL,ACT,F} = f M_{ANTI-ROLL,STIFF,TOT} + M_{ANTI-ROLL,DAMP,F}$$

$$M_{ANTI-ROLL,ACT,R} = (1-f) M_{ANTI-ROLL,STIFF,TOT} + M_{ANTI-ROLL,DAMP,R}$$

From the definition of $M_{ANTI-ROLL,ACT,F}$ and $M_{ANTI-ROLL,ACT,F}$, it is possible to calculate the it is possible to calculate the active anti-roll forces on each wheel, by the expressions:

$$F_{ANTI-ROLL,ACT,FL} = -\frac{M_{ANTI-ROLL,ACT,F}}{T_F}$$

$$F_{ANTI-ROLL,ACT,FR} = \frac{M_{ANTI-ROLL,ACT,F}}{T_F}$$

$$F_{ANTI-ROLL,ACT,RL} = -\frac{M_{ANTI-ROLL,ACT,R}}{T_R}$$

$$F_{ANTI-ROLL,ACT,RR} = \frac{M_{ANTI-ROLL,ACT,R}}{T_R}$$

where T_F and T_R are respectively the front track width and the rear track width. It is important to point out that these forces contain only the contribution of the load transfer.

3.2.3 Vehicle model: implementation of the front-to-total roll stiffness distribution control vehicle model

They are reported the main blocks of the vehicle model used by the University of Surrey for the calculation of the roll angle, the front and rear axle load transfers and tyres vertical forces. The Figure 3.9 reports a simplified structure for the calculation of the roll angle.

The input of this system are the lateral acceleration a_y, the lateral forces generated by the rear right and the rear left tyres, $F_{Y,RR}$ and $F_{Y,RL}$, the active anti-roll moment on the front axle $M_{ANTI-ROLL,ACT,F}$, the active anti-roll moment on the rear axle $M_{ANTI-ROLL,ACT,R}$, the stiffness coefficients, K_F and K_R, on the front and rear axle. and the damping coefficients, D_F and D_R, on the front and rear axles.

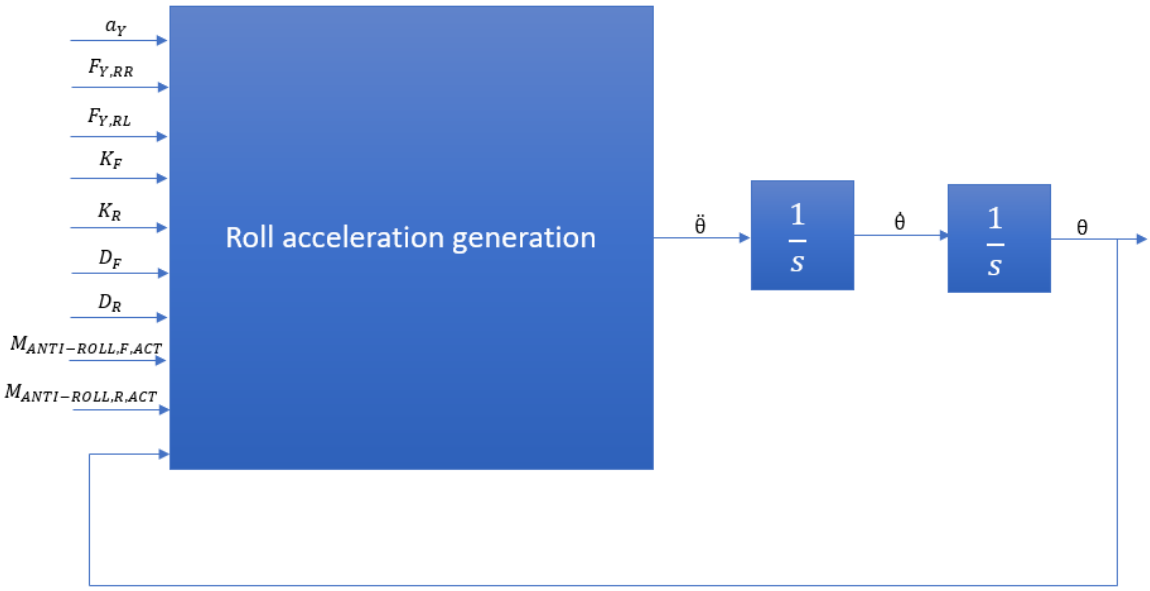

Figure 3.9: Calculation of the roll angle

The following relation express the roll moment balance around the roll axis:

$$J_X\ddot{\theta} = ma_y(h - d_F)\cos\theta + mg(h - d_F)\sin\theta - \left(F_{Y,RR} + F_{Y,RL}\right)(d_R - d_F) - M_{ANTI-ROLL,F} - M_{ANTI-ROLL,R}$$

It is possible to define the anti-roll moment contribution of the rear and front suspension system in two different ways if it is considering the passive vehicle or the active vehicle.

For the passive vehicle it possible to write the following equations:

$$M_{ANTI-ROLL,F} = K_F\theta + D_F\dot{\theta}$$

$$M_{ANTI-ROLL,R} = K_R\theta + D_R\dot{\theta}$$

For the active vehicle it also considered the contributions of the controller, thus the active anti-roll moments on the front and rear axles that are function of the front to total roll stiffness parameter, the output of the controller. The updated equations are thus:

$$M_{ANTI-ROLL,F} = K_F\theta + D_F\dot{\theta} + M_{ANTI-ROLL,ACT,F}$$

$$M_{ANTI-ROLL,R} = K_R\theta + D_R\dot{\theta} + M_{ANTI-ROLL,ACT,R}$$

The calculation of the load transfers is implemented by these equations and showed in Figure 3.10.

$$\Delta F_{Z,F} = \frac{(F_{X,FR} + F_{X,FL})d_F \sin\delta_F + (F_{Y,FR} + F_{Y,FL})d_F \cos\delta_F + M_{ANTI-ROLL,F}}{T_F}$$

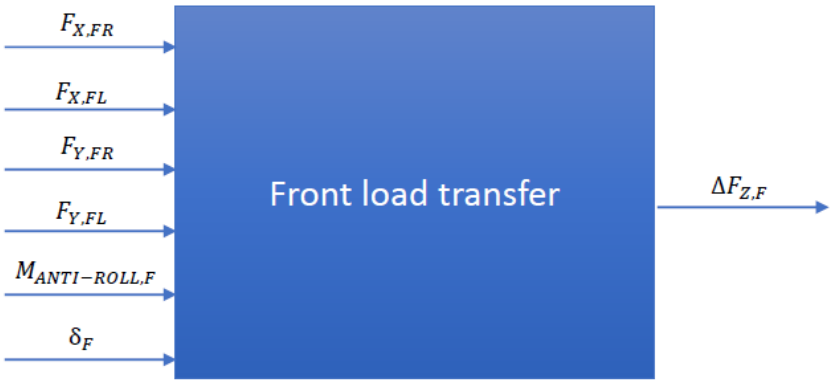

Figure 3.10: Front load transfer calculation

A similar equation is used for the calculation of the load transfer for the rear axle; in this case the rear steering angle is assumed to be zero, thus $\delta_r = 0$.

$$\Delta F_{Z,R} = \frac{(F_{Y,RR} + F_{Y,RL})d_R + M_{ANTI-ROLL,R}}{T_R}$$

For completing the analysis of the vehicle model, they are reported in the equations below the calculation of tyre vertical forces:

$$F_{Z,FR} = mg\frac{b}{2L} - ma_x\frac{h}{2L} - \Delta F_{drag} + \Delta F_{Z,F}$$

$$F_{Z,FL} = mg\frac{b}{2L} - ma_x\frac{h}{2L} - \Delta F_{drag} - \Delta F_{Z,F}$$

$$F_{Z,RR} = mg\frac{a}{2L} + ma_x\frac{h}{2L} + \Delta F_{drag} + \Delta F_{Z,R}$$

$$F_{Z,RL} = mg\frac{a}{2L} + ma_x\frac{h}{2L} + \Delta F_{drag} - \Delta F_{Z,R}$$

where the first term is the static contribution, the second term is due to the longitudinal acceleration, the third term is caused by the aerodynamic forces and the last term is the contribution of the load transfer on each axle.

3.3 Simulation results

In this part of the thesis, they are presented some preliminary controller testing in simulation with an experimentally vehicle model validated by the University of Surrey. It is focused the attention on two mains manoeuvres that are the ramp steer and the double step steer.

At this point of the work, it is not yet adopted the quasi-static model for the design of the reference yaw rate and for the design of the feedforward contribution. Some general look-up tables are used to carry out these preliminary tests to verify the correct behaviour of the system for different tunings.

3.3.1 Ramp steer test

The ramp steer is usually a test where the car is run by the driver at a constant speed; the steering angle is increased with low values of gradient with respect to the time and the manoeuvre finishes when the vehicle reaches the maximum possible lateral acceleration.

The Figure 3.11 shows the behaviour of the dynamic steering angle as a function of lateral acceleration during a ramp steer at $V = 80\ {}^{km}/_{h}$; the blue line refers to the passive vehicle whilst the others characterizes the active vehicle, with front-to-total anti-roll moment distribution controller, and are obtained decreasing of the 20 % and 10 % the reference yaw rate (red and yellow lines) and increasing of 10 % and 20 % the reference yaw rate (green and light blue lines), with respect to the passive vehicle.

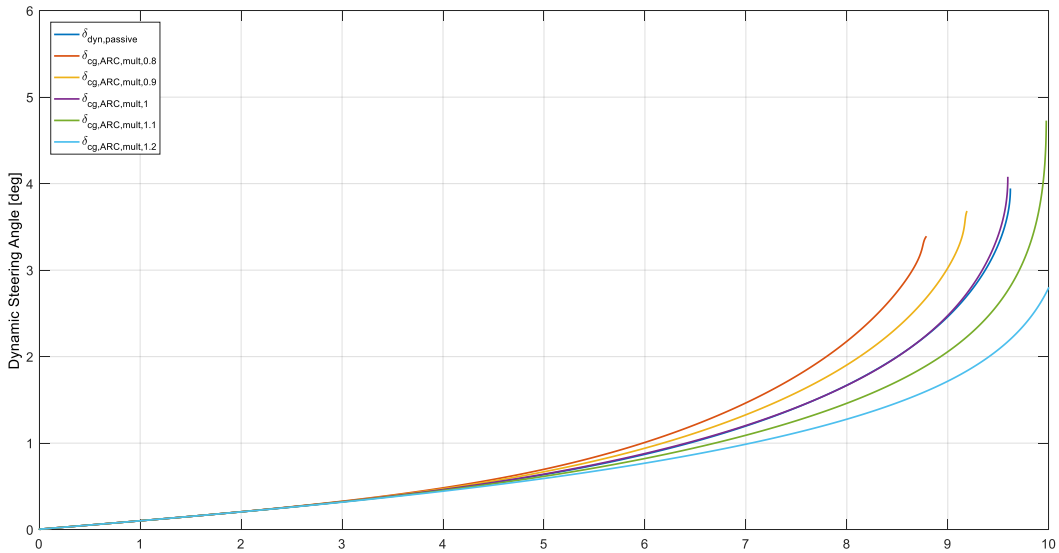

Figure 3.11: Understeer characteristics during ramp steer manoeuvre at $V = 80\ {}^{km}/_{h}$

In the Figure 3.12 it is performed a ramp steer test by considering the reference yaw rate of the passive vehicle for the active vehicle. In the first plot of Figure 3.12 it is possible to see the understeer characteristic, in the second one the front-to-total ratio (the output of the controller), in the third one the rear axle sideslip angle, in the fourth the roll angle, in the fifth the roll rate and in the last one the anti-roll moment on each axle. In this case all the behaviours of the active vehicle are overlapped with the passive vehicle.

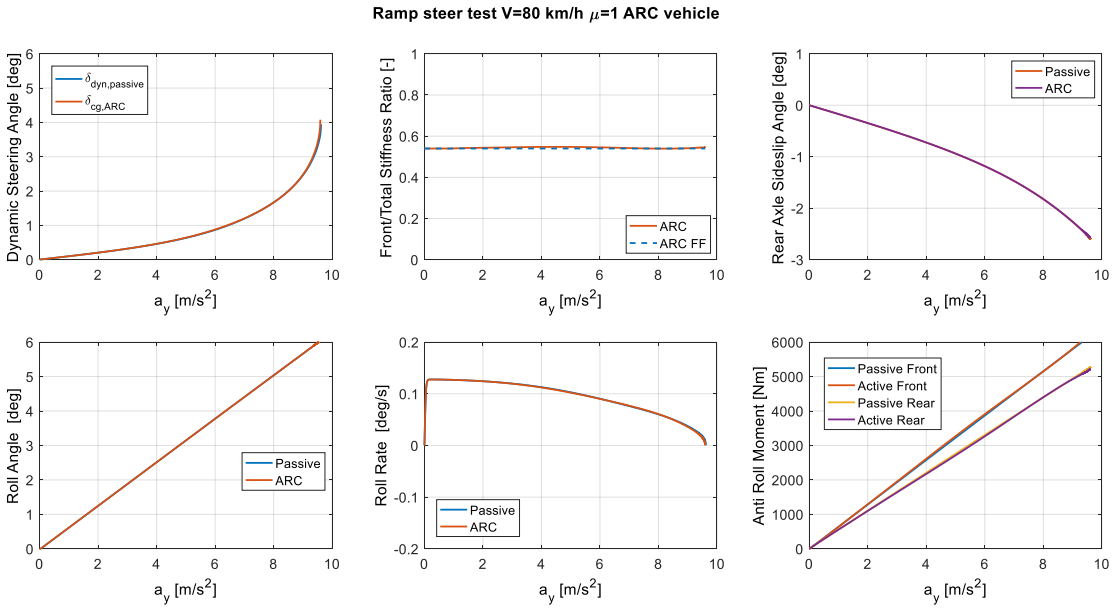

Figure 3.12: Ramp steer manoeuvre (reference yaw rate of the passive vehicle)

By decreasing of 20 % the reference yaw rate of the active vehicle, as in Figure 3.13, the vehicle tends to be more understeer; in fact, the front-to-total ratio of the active vehicle, that is represented with the red line, is more highest with respect to the passive vehicle, represented by with the blue line, which means that the anti-roll moment on the front axle is major that the anti-roll moment on the rear axle.

In the sixth plot of the same figure, it is possible to see this behaviour: the active anti-roll moment on the front axle is greater than the front anti-roll moment of the passive vehicle, whilst the active anti-roll moment on the rear axle is less than the rear anti-roll moment of the passive vehicle. This because the active vehicle tends to follow the reference.

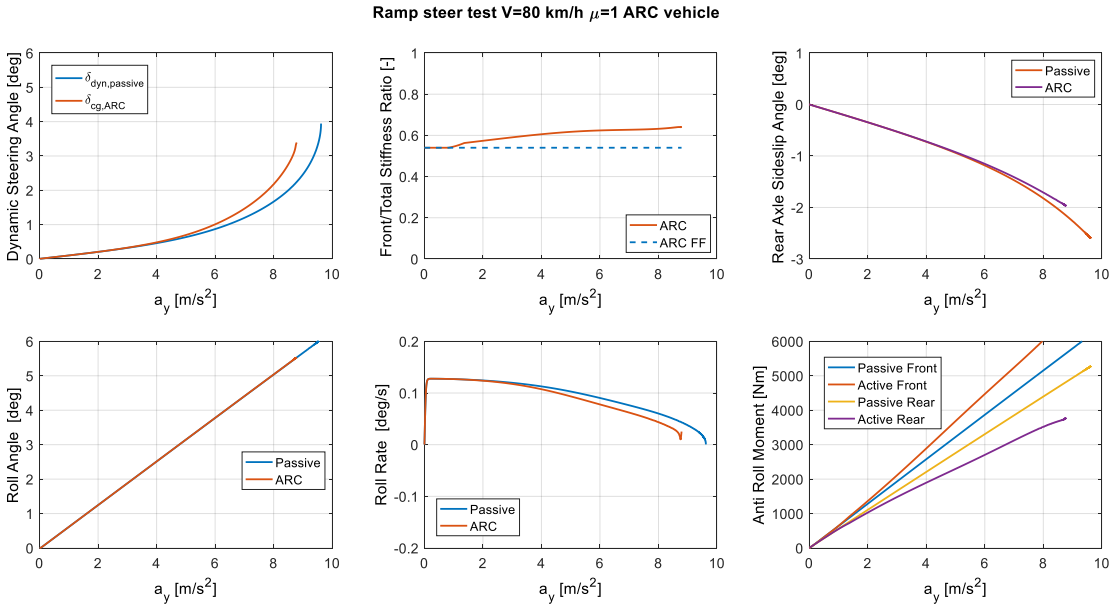

Figure 3.13: Ramp steer manoeuvre $V = 80\ {}^{km}/_{h}$ *(20% decreased reference yaw rate)*

It is possible to see the opposite behaviour in Figure 3.14; by choosing a configuration for which the reference yaw rate is increased of 20 %, the vehicle with the controllable control system is more oversteer.

In this case the active vehicle is actually less understeer than the passive vehicle, always constant, which means to have more load transfer on the rear axle. This result is also viewed in the plot of the anti-roll moment; the active anti-roll moment on the rear axle is greater than the rear anti-roll moment of the passive vehicle, whilst the active anti-roll moment on the front axle is less than the front anti-roll moment of the passive vehicle.

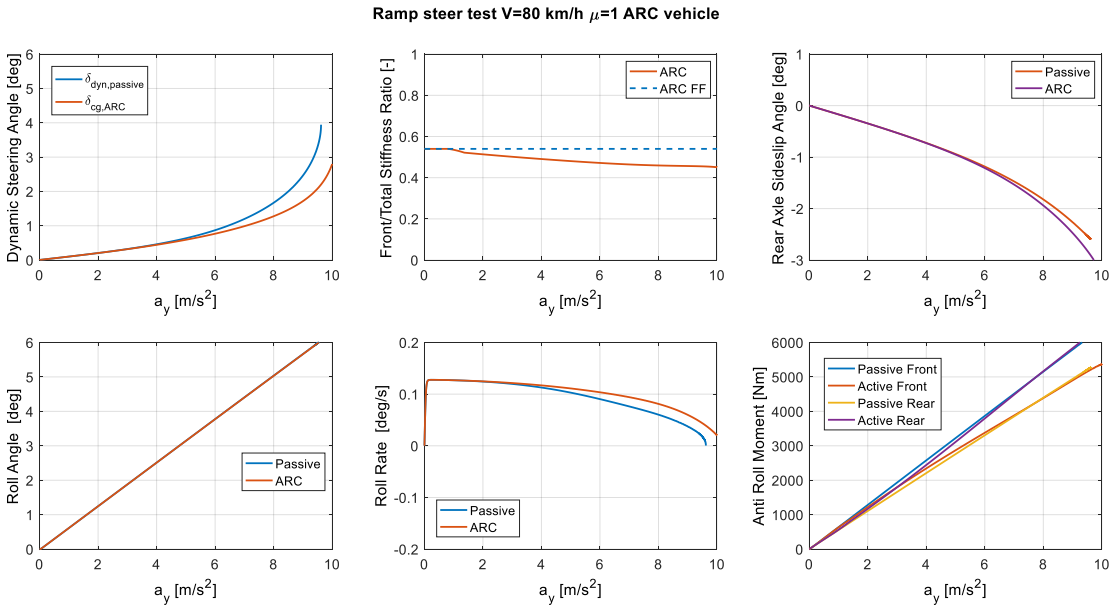

Figure 3.14: Ramp steer manoeuvre $V = 80\ {}^{km}/_{h}$ 20 % (increased reference yaw rate)

3.3.2 Double step steer test

In the double step steer test, the driver accelerates in straight line conditions to a precise value of constant speed; he tends, during the manoeuvre and so when it is applied the steering input, to keep the wheel torque demand constant at a fixed value.

In this case, a fast steering angle is applied by the driver and it is held constant for some seconds. It is followed by the second steering wheel input of the same magnitude but with reversed sign, which is always held constant for the same time as before, before returning the steering wheel angle to zero angle.

In Figure 3.15 it is simulated a double steer manoeuvre at $V = 80\ {}^{km}/_{h}$, with a maximum steering angle amplitude equal to 150 deg and in high friction conditions ($\mu = 1$). In the first plot of the figure it is showed the yaw rate of the passive vehicle, represented with the blue line, the yaw rate of the active vehicle, represented with the red line, represented the yellow line that represents the reference yaw rate and the dotted lines indicates the thresholds, in terms of yaw rate, when the controller is active. In this case the passive vehicle tends to have more oscillations with respect to the active vehicle.

In the second plot, it is possible the to see the shape of the front-to-total stiffness ratio; the feedforward contribution is essentially constant, by considering that in these preliminary

results it is not yet used the quasi-static model to design it, and the total front-to-total ratio changes in order the reach the reference yaw rate.

In the first part, when the controller is fully activated, the yaw rate of the passive vehicle is major than the reference yaw rate, thus the vehicle is oversteering; the parameter f is major than 0.5, thus the anti-roll moment on the front axle is greater than the anti-roll moment on the rear axle. This behaviour is to decrease the yaw rate of the vehicle. The shape of the anti-roll moments is plotted in the sixth plot of the same figure.

In the second plot it also reported the activation factor w_{a_y} of the controller; it is 1 when the controller is fully activated once a medium-high value of lateral acceleration is reached.

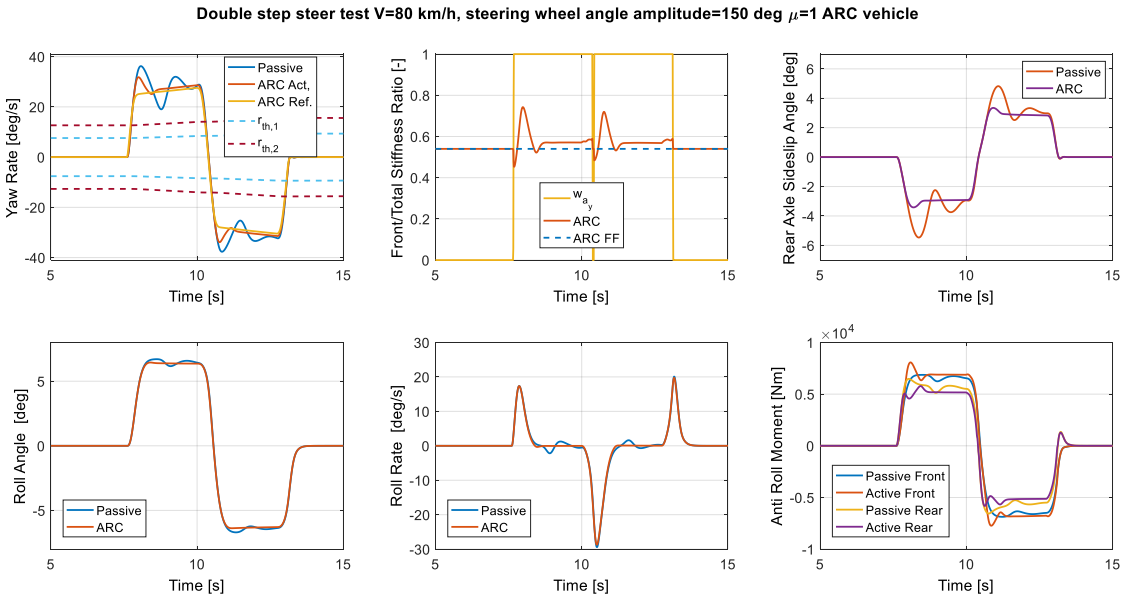

Figure 3.15: Double step steer manoeuvre

In Figure 3.16 it is reported the same simulation in the same conditions of the case above. In this simulation, however, the total roll stiffness is increased, in order to have a reduced roll angle with respect to the passive vehicle, as it is possible to see in the fourth plot of the same figure.

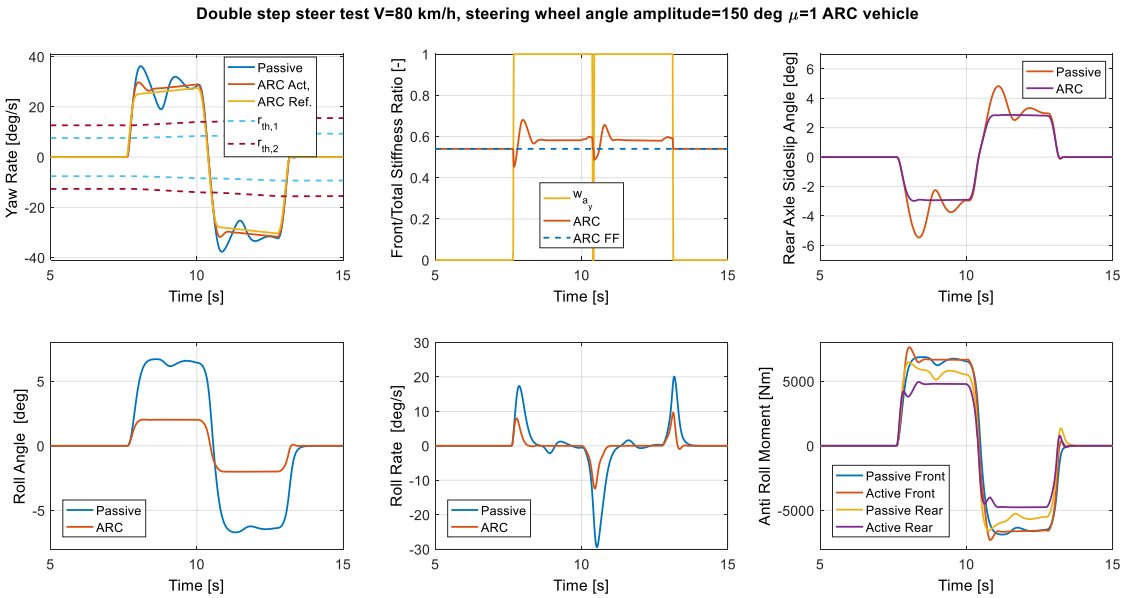

Figure 3.16: Double step steer manoeuvre (increased roll stiffness for active vehicle)

CHAPTER 4

4.1 Introduction

In chapter three it is described the operation of the front to-total anti-roll moment distribution controller. In this part of the thesis it is described the procedure for the design of the feedforward distribution controller, because the output controller is the sum of the feedforward contribution, $f_{feedforward}$, and the feedback contribution, $f_{feedback}$.

The feedforward contribution is to achieve the design cornering response, by starting from the steering angle and vehicle speed inputs mainly and without relied on the measurement of the actual yaw rate of the vehicle, that can be noisy and that can provoke oscillations on the actuation.

First-of-all, in this chapter it is presented the quasi-static model; secondly it is discussed how the quasi-static model can be used to generate the reference yaw rate for the suspension controller and the feedforward contribution of the active vehicle; at the end they are showed some simulations in the time domain, with the model in the time domain, to verify that this feedforward contribution is actually correct.

To summarise these are the tree steps:

- description of the quasi static model
- adoption of the quasi static model for the feedforward contribution design
- verification that the results of this designed procedure of feedforward contribution actually works in simulation.

4.2 Quasi-static model

The method used, for designing the feedforward ratio and then the reference yaw rate, is based on the quasi-static model: it is a model implemented in MATLAB, that doesn't require the forward time integration of the equations of the motion of the vehicle. This model was validated in other projects of the University of Surrey.

4.2.1 Implementation

The quasi static model means that the time derivatives of some of the vehicle states, in particular, the time derivative of side-slip angle $\dot{\beta}$, roll angle $\dot{\theta}$, side slip ratio, $\dot{\sigma_i}$, are assumed to be zero. These are the hypothesis adopted in the implementation of this model.

In particular, under these hypotheses, it is possible to eliminate the terms in $\dot{\beta}$ from the longitudinal force balance equation and the lateral force balance equation of the vehicle. The longitudinal balance equation is given by:

$$m(a_x - rV\sin\beta) = \sum_{i=1}^{4} F_{X,i}\cos\delta_i - \sum_{i=1}^{4} F_{Y,i}\sin\delta_i - F_{drag}$$

Essentially there is the mass, m, multiplied by the longitudinal acceleration, a_x, minus the terms related to the yaw rate of the vehicle multiplied by the component related to the sine of the sideslip angle, $rV\sin\beta$. This is equal to the sum of the longitudinal forces between the tires and the ground multiplied by the respective cosine of the steering angle, $\sum_{i=1}^{4} F_{x,i}\cos\delta_i$, minus the longitudinal components of the lateral forces, $\sum_{i=1}^{4} F_{y,i}\sin\delta_i$, minus the aerodynamic force, F_{drag}.

They are written, in a similar way, the lateral force balance equation and the yaw moment balance equation. In particular, the lateral force balance equation is:

$$m\left(a_y + a_X\tan\beta\right) = \sum_{i=1}^{4} F_{X,i}\sin\delta_i + \sum_{i=1}^{4} F_{Y,i}\cos\delta_i$$

$$a_y = Vr\cos\beta$$

The yaw moment balance equation is:

$$\sum_{i=1}^{4} F_{X,i}\sin\delta_i\, x_i + \sum_{i=1}^{4} F_{Y,i}\cos\delta_i\, x_i - \sum_{i=1}^{4} F_{X,i}\cos\delta_i\, y_i + \sum_{i=1}^{4} F_{Y,i}\sin\delta_i\, y_i + \sum_{i=1}^{4} M_{Z,i} = 0$$

In the quasi-static model, it is used a non-linear tyres formulation according to the Pacejka Magic Formula 5.2. They were used experimental data which were already validated for an electric vehicle, in which University of Surrey had been working in the last year.

It also included the roll moment balance equation, expressed by:

$$ma_y(h - d_F)\cos\theta + mg\,(h_{CG} - d_F)\sin\theta - \left(\sum_{i=3}^{4} F_{Y,i}\cos\delta_i + \sum_{i=3}^{4} F_{X,i}\sin\delta_i\right)(d_R - d_F) = M_{ANTI-ROLL,F} + M_{ANTI-ROLL,R}$$

Essentially the first contribution is the exciting component of the roll moment, $ma_y(h - d_F)\cos\theta$, then there is the component caused by the lateral offset between the centre of gravity and the centre of the roll of the car, $mg(h_{CG} - d_F)\sin\theta$; then there are the components of the lateral forces that are transmitted to the rigid links of the suspension system, $\left(\sum_{i=3}^{4} F_{y,i}\cos\delta_i + \sum_{i=3}^{4} F_{x,i}\sin\delta_i\right)(d_R - d_F)$ and all this is equal to the sum of the anti-roll moment on the front and rear axle that is caused by the flexible elements of the suspension system, $M_{anti-roll,f}$ and $M_{anti-roll,r}$.

In particular for the passive vehicle it is supposed to have a linear characteristic in terms of roll stiffness as shown in the below equations;

$$M_{ANTI-ROLL,F} = K_F\theta$$

$$M_{ANTI-ROLL,R} = K_R\theta$$

For the active vehicle there is the contribute of the passive elements of the suspension system plus the contribution caused by the controller that is the active anti-roll moment contribution. The equations are:

$$M_{ANTI-ROLL,F} = K_F\theta + M_{ANTI-ROLL,ACT,F}$$

$$M_{ANTI-ROLL,R} = K_R\theta + M_{ANTI-ROLL,ACT,R}$$

In particular, there is the variable f, the output of the controller, that starts from the total stiffness component of the anti-roll moment, and it allows to distribute it between the front and rear suspension system in order to calculate the anti-roll moment of the actuators on the front axle and the anti-roll moment of the actuators on the rear axle. It is so used the factor f that is possible to vary and to control.

The equations related to the calculation of $M_{ANTI-ROLL,ACT,F}$ and $M_{ANTI-ROLL,ACT,R}$ are:

$$M_{ANTI-ROLL,ACT,F}=f M_{ANTI-ROLL,STIFF,TOT}$$

$$M_{ANTI-ROLL,ACT,R}=(1-f) M_{ANTI-ROLL,STIFF,TOT}$$

The total anti-roll moment related to the stiffness of the control components of the active suspension system is given by a look-up table as a function of roll angle.

$$M_{ANTI-ROLL,STIFF,TOT} = M_{ANTI-ROLL,STIFF,TOT}(\theta)$$

In this model they are also included inequality constraints related to the maximum and minimum values of the front-to-total roll stiffness parameter f, because in a real vehicle, there are some actuator constraints and it is necessary to keep these constraints in a range during the design of the controller. The consideration of actuator ratio limitations is:

$$f_{min} \leq f \leq f_{max}$$

As it is possible to see there isn't included the damping contribution of the moment because one of the hypothesis is $\dot{\theta} = 0$.

There are also implemented the formula for the calculation of the vertical loads for each tire. First of all, it is calculated the total vertical load on the front axle:

$$F_{Z,F} = mg\frac{b}{L} - ma_x\frac{h}{L} - F_{drag}\frac{h}{L}$$

where there is a static load, $mg\frac{b}{l}$, the load transfer due to the longitudinal acceleration, $ma_X\frac{h}{l}$, the load transfer caused by aerodynamics, $F_{DRAG}\frac{h}{l}$. The vertical load transfer, caused by the lateral acceleration, is expressed by:

$$\Delta F_{Z,F} = \frac{\left(\sum_{i=1}^{2} F_{X,i}\sin\delta_i + \sum_{i=1}^{2} F_{Y,i}\cos\delta_i\right)d_F + M_{ANTI-ROLL,\,F}}{T_F}$$

There is the contribution given by the total lateral force component, $\left(\sum_{i=1}^{2} F_{X,i}\sin\delta_i + \sum_{i=1}^{2} F_{Y,i}\cos\delta_i\right)$, multiplied d_F, the roll centre high of the front axle: so the first part is the load transfer transferred at the rigid links of the suspension system and the second term is the load transfer given by the deformable elements of the suspension system.

By considering the sum of the static load and the load transfer caused by longitudinal acceleration and deceleration, load transfer caused by aerodynamic force, load transfer

caused by lateral acceleration, $\Delta F_{Z,F}$, it is possible calculate the vertical load on the front left and on the front right wheel, $F_{Z,FL}$ and $F_{Z,FR}$.

$$F_{Z,FL} = mg\frac{b}{2L} - ma_x\frac{h}{2L} - F_{drag}\frac{h}{2L} - \Delta F_{Z,F}$$

$$F_{Z,FR} = mg\frac{b}{2L} - ma_x\frac{h}{2L} - F_{drag}\frac{h}{2L} + \Delta F_{Z,F}$$

As if in extreme conditions it could happen that a wheel lifts, inequality constraints of the vertical load on each wheel in the quasi static model formulation are also included, so that the vertical load can be between zero and the total vertical load on the front axle.

$$0 \leq F_{Z,FL/R} \leq F_{Z,F}$$

This means that if one wheel lifts the formulation of $\Delta F_{Z,F}$ is not valid anymore because simply the total vertical load on the front axle will be in that specific wheel that is still in contact with the ground.

The same procedure is followed for the rear axle: they are calculated the total vertical load on the rear axle, the load transfer because of lateral acceleration, the vertical loads for each wheel and then inequality constraints are considered between zero, the condition so a wheel lifts, and the total vertical load on the rear axle. The overall equations are:

$$F_{Z,R} = mg\frac{a}{L} + ma_x\frac{h}{L} + F_{drag}\frac{h}{L}$$

$$\Delta F_{Z,R} = \frac{\left(\sum_{i=3}^{4} F_{X,i}\sin\delta_i + \sum_{i=3}^{4} F_{Y,i}\cos\delta_i\right)d_R + M_{ANTI-ROLL,\,R}}{T_R}$$

$$F_{Z,RL} = mg\frac{a}{2L} + ma_x\frac{h}{2L} + F_{drag}\frac{h}{2L} - \Delta F_{Z,R}$$

$$F_{Z,RR} = mg\frac{a}{2L} + ma_x\frac{h}{2L} + F_{drag}\frac{h}{2L} + \Delta F_{Z,R}$$

$$0 \leq F_{Z,RL/R} \leq F_{Z,R}$$

It is also considered the wheel torque balance equation for each wheel: there is the drive train component, the brake torque component, the longitudinal tyre force component, the rolling resistance and the inertial component. The expression for the wheel i is:

$$i_g T_{m,i} - T_{b,i} - F_{x,i}R_{l,i} - M_{y,i} - J_{w,i}\dot{\omega}_i = 0$$

The angular acceleration of the wheel, $\dot{\omega}_i$, is a function of longitudinal acceleration of the vehicle and of the slip ratio of the specific wheel: the time derivative of slip ratio in the quasi static model is zero, but the angular acceleration is different from zero.

$$\dot{\omega}_i = \frac{\dot{V}_{x,i}}{R_{e,i}}(\sigma_i + 1) + \frac{V_{x,i}}{R_{e,i}}\dot{\sigma}_i \approx \frac{\dot{V}_{x,i}}{R_{e,i}}(\sigma_i + 1)$$

Then the wheel speed is limited according to electric motor speed limitations, if there an electric vehicle as in the case, or according to the engine motor speed limitation, if there is a combustion engine vehicle. The constraint is the actual average of the two wheels speeds that are limited because there is an open differential. The inequality constraint is:

$$0 \leq \omega_i \leq \frac{\omega_{m,max}}{i_g}$$

The motor torque is also limited according to electric motor torque limitations as a function of motor speed.

$$T_{m,min}(\omega_m) \leq T_{m,i} \leq T_{m,max}(\omega_m)$$

The equations of the quasi static model can be solved without time integration: this is a significant advantage because for example it is possible to simulate situations in which the vehicle is subject to strongly longitudinal accelerations and decelerations.

Secondly this simulation model is implemented in MATLAB and it is solved by using a non-linear optimization function fmincon.

While fmincon is an optimization function, it can also be used as a solver by adopting a zero objective function and imposing the quasi-static model equations as equality constraints and the physical vehicle and actuator limitations as inequality constraints; in case of multiple valid solutions, an objective function has to be defined and fmincon is used to minimize the objective function while ensuring that constraints are respected.

In other words fmincon is an optimization function: if the system has only one possible solution to the problem if, then even if this is an optimization function, it is possible to put a zero cost function and the optimization will automatically define any solutions; if there are multiple solutions in the problem it is used fmincon in order to calculate the solutions that minimize the objective function while to ensure that the constraints are respected.

In-particular, the control inputs for the vehicle are the steering angle, imposed by the driver, the front to total roll stiffness distribution and the output of the active roll controller and finally the total torque demand imposed by the driver or the control system.

$$\delta, f, T_{tot}$$

The vehicle state variables are the speed, the longitudinal and lateral acceleration, the yaw rate, the side-slip angle, and the roll angle.

$$V, a_x, a_y\ r, \beta, \theta$$

It is possible to constrain a subset of the above variables, while the other variables can be determined by solving the quasi-static model equations. For example, if speed, the longitudinal and lateral acceleration are constrained to specific values, the required steering angle and total torque can be calculated, in-order to keep vehicle in that speed, longitudinal acceleration and lateral acceleration.

4.3 Reference yaw rate and feedforward contribution

In this part it is explained the design procedure that it is implemented in-order to define the look-up tables of the feedforward front-to-total ratio distribution in-order to achieve the reference understeering characteristic.

The first point of this procedure is that the quasi static model is solved for increasing values of lateral acceleration, for constant values of speed and longitudinal acceleration: so they are imposed V and a_x,and then it is started to solve the quasi-static model for progressive values of lateral acceleration and this procedure is stopped when no valid solutions can be found anymore, because at that point that means the maximum value of lateral acceleration of the vehicle is been achieved.

In the design procedure, the first step is to validate the quasi-static model results for the passive vehicle against dynamic simulation and experimental results for the passive vehicle.

The second step in the procedure is to determine the maximum value of lateral acceleration for neutral steering behaviour: essentially in this second step it is understood how much it

is possible to obtain in terms of cornering response improvement by using the front-to-total anti-roll moment distribution controller. In-particular, to calculate this maximum value of lateral acceleration for neutral steering behaviour, it is used an optimization procedure based on the quasi-static model that has a cost function that minimizes the absolute value of dynamic steering angle: because neutral steering condition corresponds to zero dynamic steering angle.

Once validated the model, once defined what are the limits can be achieved in terms of performance improvement by using the front to total roll stiffness distribution controller, the third step is to define the reference understeer characteristic to achieve the desired vehicle response and in-particular this reference understeer characteristic is usually less understeer than the passive vehicle. This reference understeer characteristic should not conflict with the maximum achievable response of the vehicle that has been calculated in the second step.

4.3.1 Reference yaw rate design

In terms of practicality, for the design of the reference yaw rate, the user is asked to use a graphical user interface to define the reference understeer characteristic of the vehicle by including three parameters: These three parameters are: K_{US}, the understeering gradient, that essentially it is the slope of the graph of steering angle as function of lateral acceleration and it says how much the vehicle is understeering in the linear part of the understeering characteristic. The second parameter to define the reference understeering characteristic is a_y^*, the maximum value of lateral acceleration for which the vehicle is cornering in the linear part of the understeer characteristic.

The third parameter is $a_{y,max}$, the maximum achievable lateral acceleration. In particular, there is this function expressed in the following system:

$$\delta = \begin{cases} k_{US}a_y + \dfrac{la_y}{V^2} & if\ a_y < a_y^* \\ k_{US}a_y^* + \left(a_y^* - a_{y,max}\right)k_{US}log\left(\dfrac{a_y - a_{y,max}}{a_y^* - a_{y,max}}\right) + \dfrac{la_y}{V^2} & if\ a_y^* \le a_y \le a_{y,max} \end{cases}$$

If the lateral acceleration is less than a_y^*, it is implemented the linear relationship between steering angle δ and lateral acceleration a_y; there is the contribution of $k_{US}a_y$, that says

how the vehicle is understeer plus the cinematic steering angle, $\frac{la_y}{V^2}$, the steering angle would have in condition of zero slip angle of neutral steering vehicle.

For large values of lateral acceleration there is an exponential function that gives the shape of reference understeer characteristic, in order to achieve the maximum value of lateral acceleration that it is defined by the user. These three parameters are selected to define the desired understeer characteristic.

From the previous system it is possible to get the steering angle as a function of lateral acceleration and then through this approach starting from the reference understeer characteristic delta versus ay, it is defined the steady state value of the reference yaw rate that is simply equal to the lateral acceleration over the vehicle speed. There is a procedure based on an interpolation in order to calculate the look-up table automatically of the reference yaw rate as a function of steering angle, δ, and vehicle speed, V.

The computation of the look-up table for the reference yaw rate from lateral acceleration is:

$$r_{ref,ss}(\delta, V) = \frac{a_y(\delta, V)}{V}$$

4.3.2 Feedforward contribution calculation

The fourth step of this procedure is the calculation of the feedforward contribution; according to this approach the reference yaw rate and corresponding steering angle are imposed as equality constraints in the optimization procedure and the quasi-static model is solved to determine the required front-to-total distribution ratio to achieve the reference understeer characteristic for different values of vehicle speed.

At the moment, for low values of lateral acceleration the front-to-total anti-roll moment distribution control is not very influence in the cornering response; thus it has decided to calculate the feedforward contribution for values of steering angle that correspond to lateral acceleration values, in absolute value, larger than 3 $^{m}/_{s^2}$. Moreover it is decided in this because the controller is not active for low values of lateral acceleration.

It is checked in the optimisation the feasibility of the reference yaw rate by applying all the vehicle limitations and controller limitations: the limitation on the minimum and maximum front-to-total roll stiffness distribution, the limitation of the motor torque

demand. Essentially with this quasi static model, it is possible to have a realistic simulation of the performance of the vehicle in non-linear conditions.

At the end of this procedure, a look-up table is automatically generated for the feedforward contribution ratio in steady-state conditions as a function of steering angle, δ, and vehicle speed, V. Further developments are possible.

$$f_{feedforward} = f_{feedforward}(\delta, V)$$

The final step of the procedure is to insert the look-up tables of the reference yaw rate, the feedforward stiffness ratio in a simulation model in the dynamic Simulink vehicle model and to check how the feedforward contribution does the most of the job in steady-state cornering conditions; because if the feedforward contribution is properly designed, it is responsible from most of the front-to-total roll stiffness distribution calculation in steady state cornering condition, while the feedback contribution becomes important in case of transient conditions.

In other word, if the feedforward contribution has been designed correctly, the final output of the controller, f, should be approximately equal to the feedforward contribution and the feedback contribution should be close to zero.

4.4 Simulation results

There are presented some results obtained according to this procedure; it is validated the quasi-static model, that is indicated with the blue continuous line, for example in the diagram of dynamic steering angle versus lateral acceleration of Figure 4.1, against an experimental validated simulation model used in another activity of University of Surrey.

The vehicle parameters, in this simulation, are consistent with the performance of an actual vehicle and it is not simulate an abstract car.

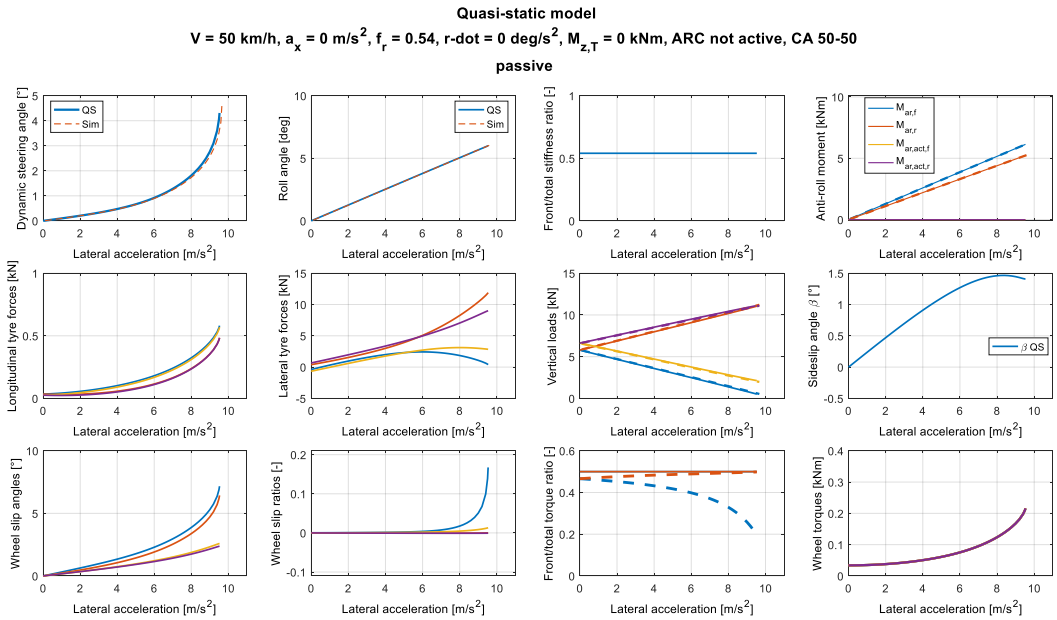

Figure 4.1: Example of validation of the quasi-static model with a ramp steer manoeuvre

In the same figure, it is possible to see some plots: in the third diagram they are represented the front and rear anti-roll moments, including the actuation contribution with the constant front-to-total roll stiffness distribution including the passive elements; in this case the passive elements of the suspension system for the active car have zero contribution.

It is possible to see the wheel torque in the twelfth plot: in this thesis, it is considered a four- wheels drive vehicle without any form of torque vectoring, so the four-wheel torques are the same and they are an increasing function of lateral acceleration; in fact when the lateral acceleration increases, there are lateral tyres slip power losses that provoke an increase of the overall wheel torque as a function of a_y; it is possible to see that the slip angles are larger in the front wheels, that means the vehicle is understeer.

This is an example of validation of the quasi-static model for 50 $^{km}/_{h}$; in the Figure 4.2, there are plotted similar results also for 100 $^{km}/_{h}$; essentially in a range from 50 $^{km}/_{h}$ to 100 $^{km}/_{h}$ there is this quasi-static model validated against the simulation model.

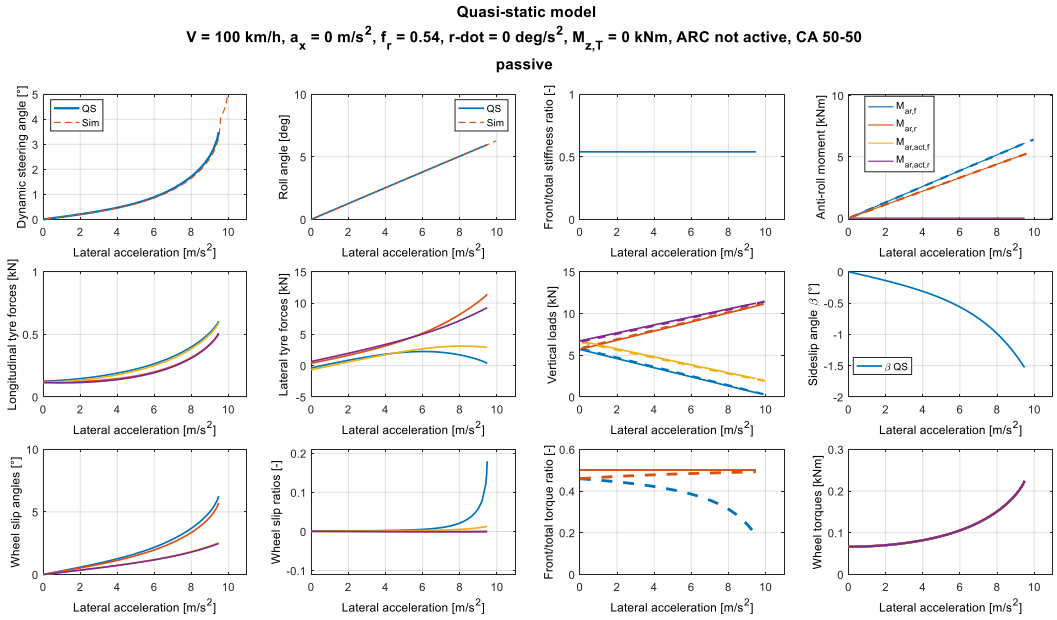

Figure 4.2: Example of validation of the quasi-static model with a ramp steer manoeuvre

The next step is how to calculate the maximum value of lateral acceleration achievable with the front-to-total anti-roll moment distribution controller.

This vehicle can achieve without any form of suspension controller, as shown in Figure 4.3, a maximum value of lateral acceleration of 9.53 $^{m}/_{s^2}$ in high friction conditions, even it is run the optimization as indicated in second step of the procedure, as explained in the last paragraph: essentially it is used the absolute value of steering angle, as a cost function, in order to try to get a neutral steering behaviour and then the optimization is run for different values of lateral acceleration, until the fmincon cost function MATLAB manages to find a solution.

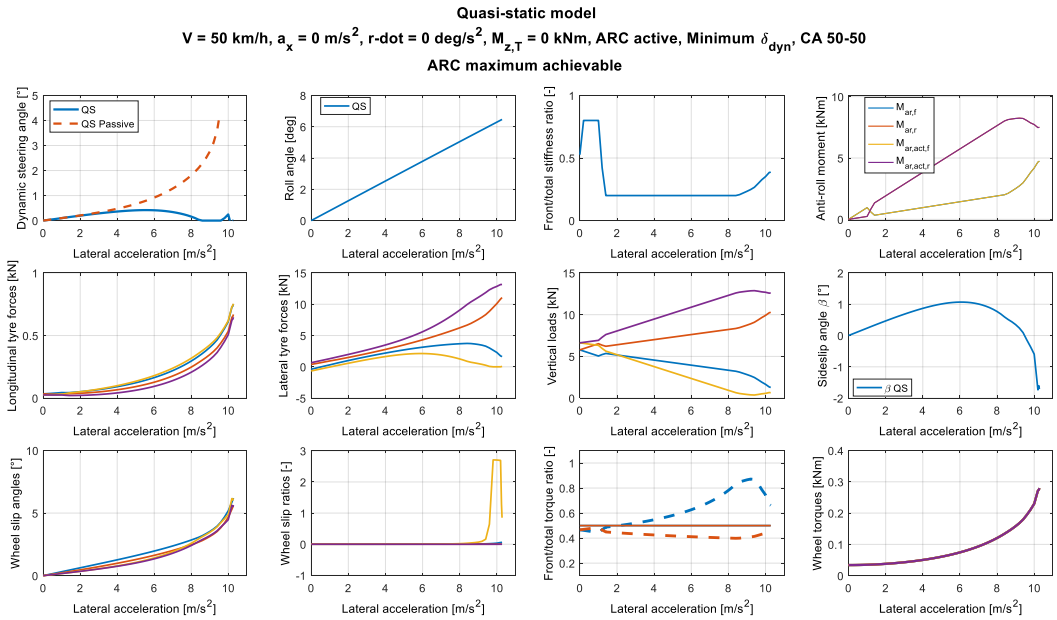

Figure 4.3: Calculation of the maximum value of lateral acceleration achievable with active vehicle

The maximum value of lateral acceleration that can be achieved, according to the vehicle parameters of this validated vehicle, is 10.28 $^{m}/_{s^2}$: there is a gain about 0.7 $^{m}/_{s^2}$ of maximum value of lateral acceleration that is very insignificant. In particular it is possible to see in the third plot of the same figure, the front-to-total stiffness ratio f, the control output of the strategy, as a function of lateral acceleration: essentially this parameter, for medium and high values of lateral acceleration, is around 0.2. This value is the lower limit selected for the actuators; if the limit is different, other results could be possible.

It also interesting in the first plot, for low values of lateral acceleration close to 3 $^{m}/_{s^2}$, the dynamic steering angle cannot to be reduced to neutral steering; and then lateral acceleration increases the achievable dynamic steering angle gets progressed lower. For values of lateral acceleration lower than 8 $^{m}/_{s^2}$, it is not possible to get exactly zero dynamic steering angle, that achieves neutral steering behaviour. This behaviour could be different depending on the values of actuator limits.

It is possible to see the same results for 100 $^{km}/_{h}$, in the Figure 4.4; it also interesting to note that on the case of 50 $^{km}/_{h}$, there is major positive sideslip angle because the kinematic component of sideslip angle is prevalent around one when the driver is cornering at lower turn radius and low speed; whilst when the driver is cornering at larger speed, the dynamic component of side slip angle becomes prevalent and the sideslip angle is negative.

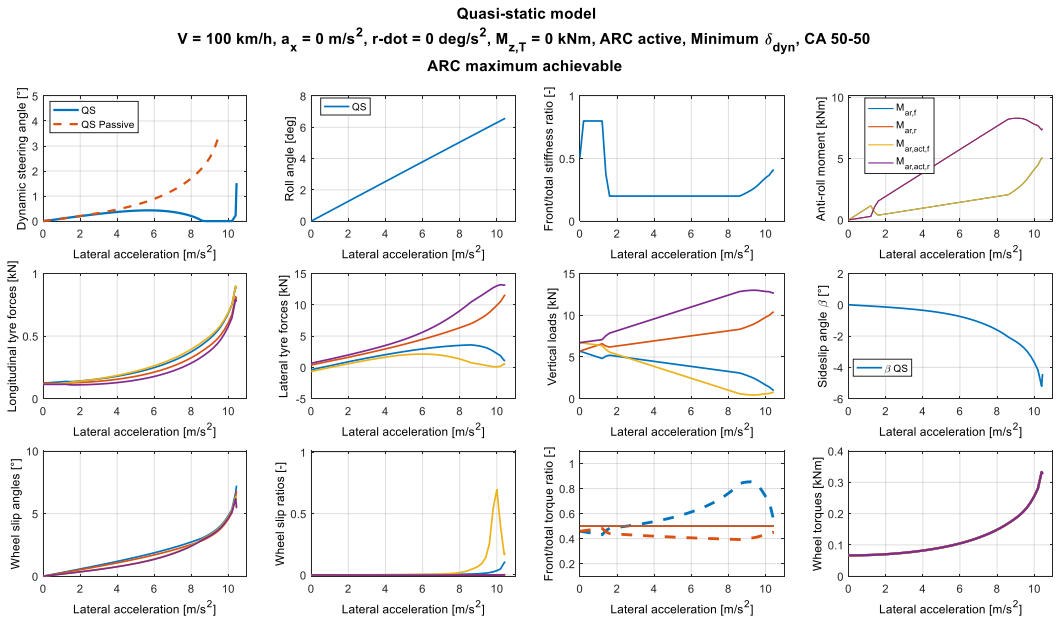

Figure 4.4: Calculation of the maximum value of lateral acceleration achievable with active vehicle

Then once reached the awareness of the limit achievable by the vehicle, there is a graphical use interface in the quasi static-model, in which the user can define for the vehicle with the controllable suspension system three parameters: k_{US}, a_y^* and $a_{y,max}$ of the vehicle.

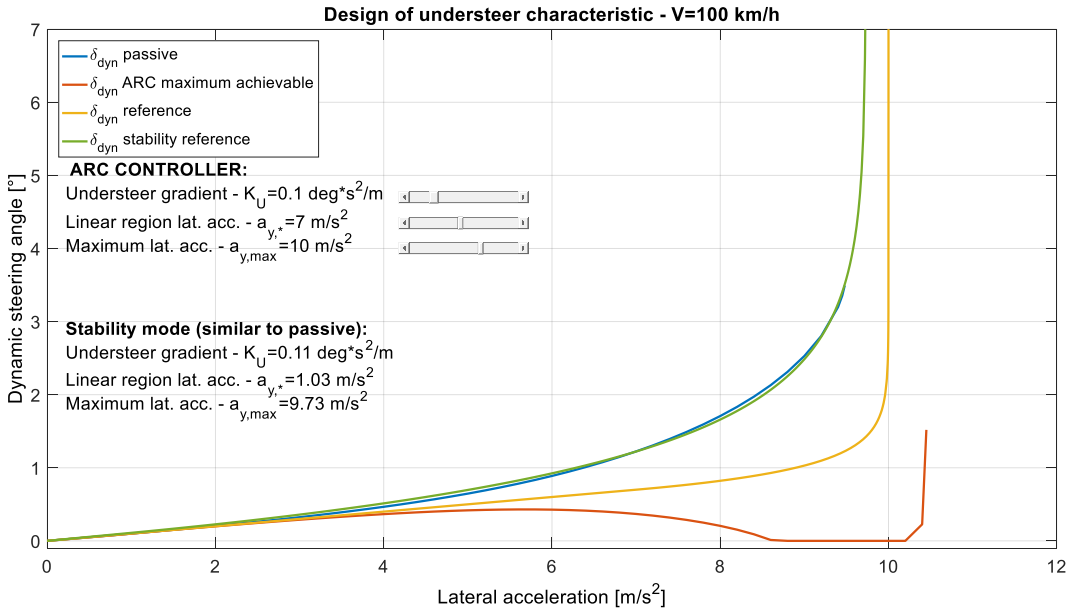

Figure 4.5: Calculation of the reference understeering characteristic for active vehicle

On this graphical interface, the user can see the values of the passive vehicle, with k_{US}= 0.11 $^{degs^2}/_{m}$, a_y^*= 1.03 $^{m}/_{s^2}$ and $a_{y,max}$=9.73 $^{m}/_{s^2}$, and then he/she can select the values for the same parameters for the vehicle with the controller: in this case it is selected a similar value of understeering gradient for the controlled vehicle and passive vehicle, it is selected a significant extension of the linear part of the understeer characteristic from 1.03 $^{m}/_{s^2}$ to 7 $^{m}/_{s^2}$ and it is also extended the maximum value of lateral acceleration from 9.73 $^{m}/_{s^2}$ to 10 $^{m}/_{s^2}$.

It is showed in Figure 4.5 the blue understeer characteristic of the passive vehicle, in orange the understeer characteristic that is the reference characteristic of the control vehicle and in there is the maximum achievable result by using the active suspension system. This is the graph that can be updated in real time when the user designs the feedforward contribution of the suspension controller.

Then it is run the optimization for calculating the feedforward component of the control action. The Figure 4.6 is about the speed of 50 $^{km}/_{h}$; it is showed the front -to-total roll stiffness ratio f, the feedforward component of the factor f, that is the result of the optimization procedure as a function of steering angle. Essentially the first part is not actually calculated because between 0 $^{m}/_{s^2}$ and 0.3 $^{m}/_{s^2}$ the controller is not active and it isn't used for shaping the understeer characteristic.

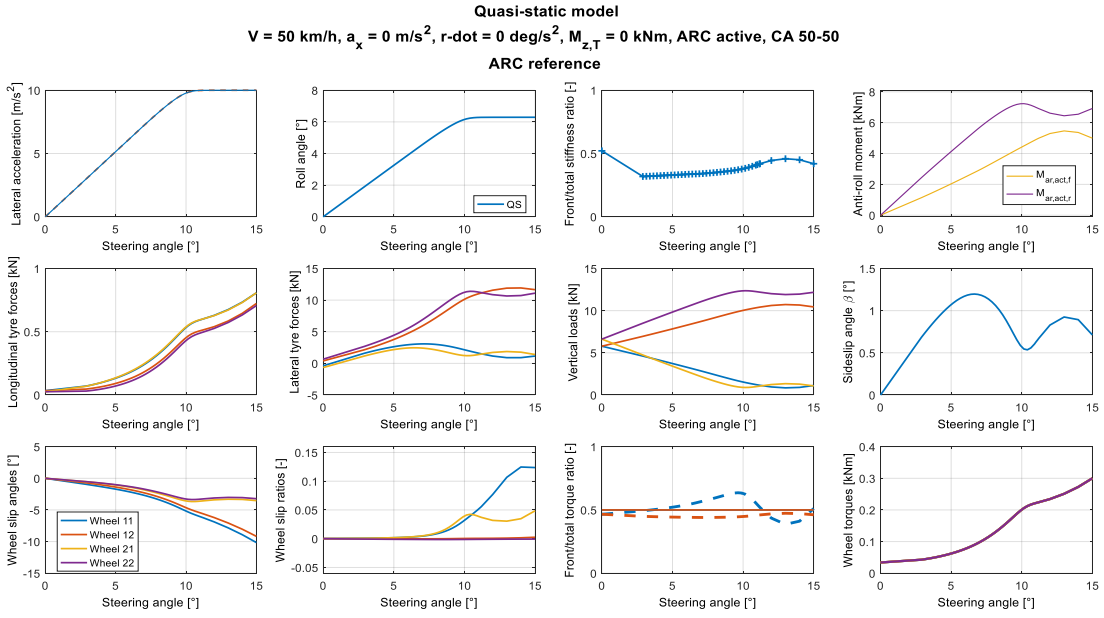

Figure 4.6: Calculation of the behaviour of lateral acceleration as a function of steering angle

At zero of lateral acceleration the static value of front-to-total roll stiffness distribution is the same of the passive vehicle and then for 3 $^{m}/_{s^2}$,forward by the crosses are located, it is possible to note the results of the optimization based on the quasi static model.

In particular, the system tends to have more roll stiffness toward the rear axle in order to reduce the understeer behaviour of the vehicle. In Figure 4.7 there are produced similar results for speeds of 100 $^{km}/_{h}$: in general, the aim is to reduce understeer and thus there is a reduction of the front-to-total roll stiffness distribution ratio.

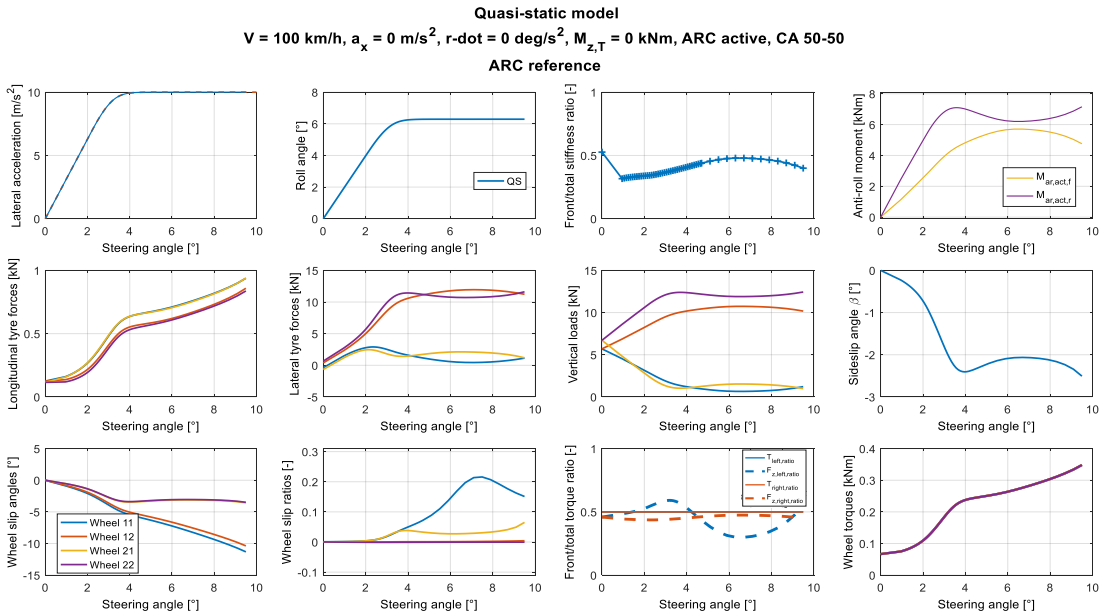

Figure 4.7: Calculation of the behaviour of lateral acceleration as a function of steering angle

At the end of this procedure, they are computed two look-up tables, as showed in Figure 4.8: one of the reference yaw rate in degree per second as a function of steering angle of the wheel in degree for different values of vehicle speed: the blue characteristics are for low speed values, the red characteristics are for high speed values and this is the typical shape of the reference yaw rate.

In the second look-up table it is represented the front-to-total roll stiffness ratio for the active suspension controller as a function of steering angle again for different values of speed.

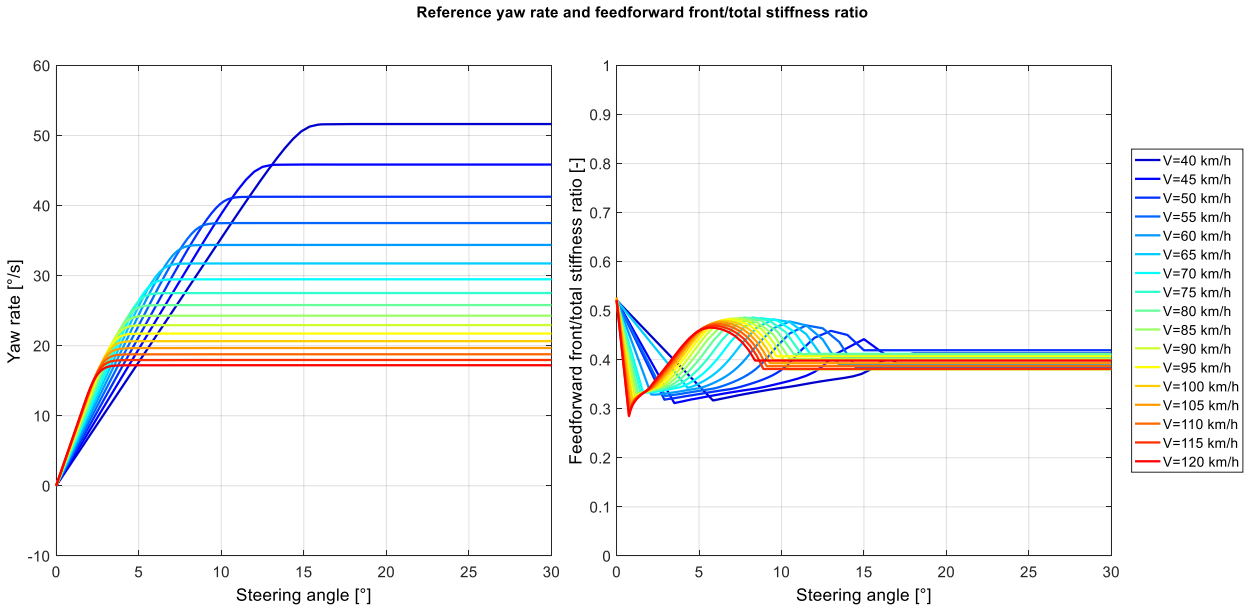

Figure 4.8: Look-up tables of the reference yaw rate and feedforward for different values of vehicle speed

The part, that is the result of the optimization, is calculated for values of steering angle for which $a_y > 0.3\ {}^{m}/_{s^2}$. The initial part is simply a linear interpolation between the first value of steering angle that corresponds to a lateral acceleration of $0.3\ {}^{m}/_{s^2}$ and the static value, that is typical of the vehicle in straight line operations; for high values of steering angle it is simply kept the constant front-to-total roll stiffness distribution equal to the last value calculated from the optimization.

The next step is to put these two look-up tables into the simulation model in the time domain and verifies that, actually, provides the reference understeer characteristic. In the graph 1 of Figure 4.9 of the dynamic steering angle as a function of lateral acceleration, the passive vehicle is characterized by the blue line whilst the vehicle with active roll control has a reference understeering characteristic that is the dashed line whilst the continuous line what it is obtained by including the active roll controller and it is coincident with the dashed line.

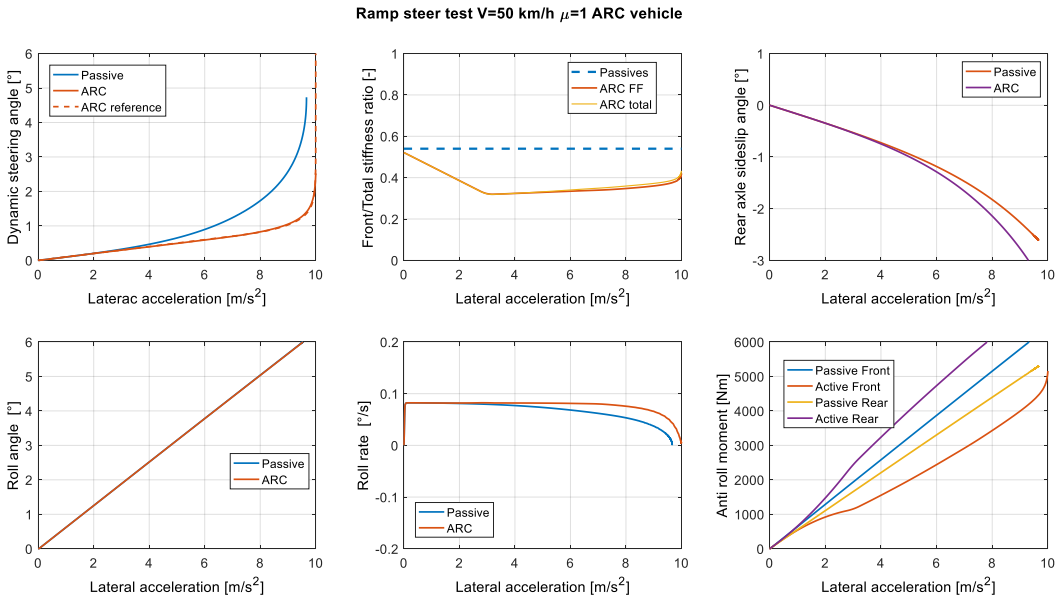

Figure 4.9: Ramp steer with dynamic Simulink vehicle model

The second plot of the same Figure is about the front-to-total stiffness ratio: the dashed line refers to the passive vehicle, the feedforward contribution is indicated in red and the total value of the front-to-total stiffness ratio during the simulation is indicated in orange. It is possible to see that the orange line is substantially coincident with the red value, which means essentially that the only feedforward contribution is providing the control action and the actuation of the feedback contribution is negligible. This was the purpose by using this feedforward contribution controller.

It is possible to note that the feedforward contribution provokes an increase of the load transfer on the rear axle, in fact the anti-roll moment on the rear is larger with the active roll control system, that is the violet line, in comparison when with the passive vehicle. For the front axle there is less load transfer for the active vehicle in comparison to the case of the passive vehicle, that is characterized by an anti-roll moment corresponding to the blue line.

The same for speed of 100 $^{km}/_{h}$ in Figure 4.10; there is a good track of the understeer characteristic in the graph 1, the total contribution and the feedforward contribution in graph 2; as expected it makes the vehicle less understeering and the absolute value of sideslip angle of the rear axle increases.

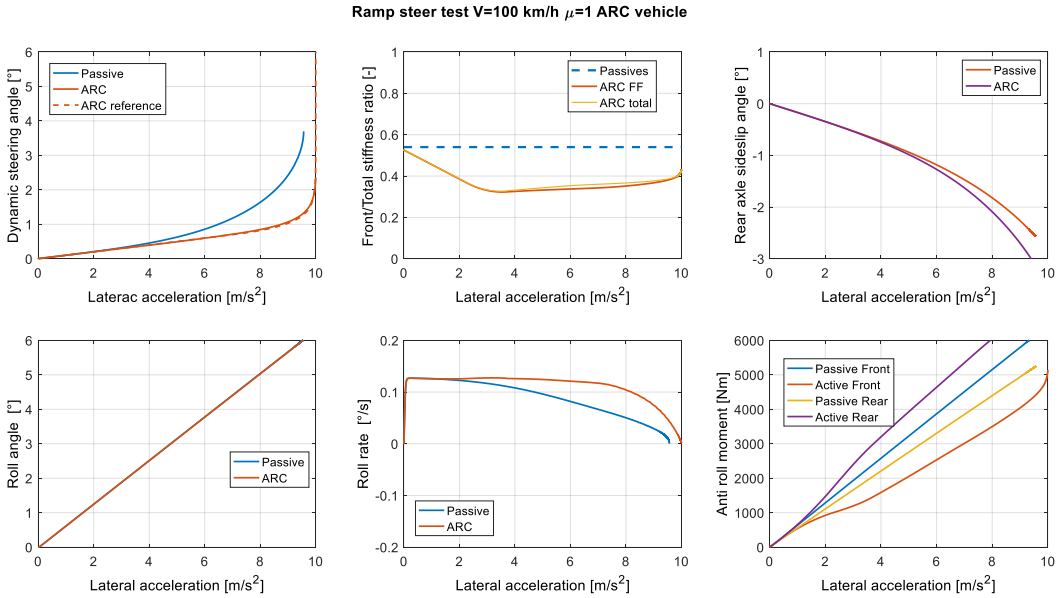

Figure 4.10: Ramp steer with dynamic Simulink vehicle model

In conclusion it is designed the non-linear feedforward front-to-total roll stiffness ratio, it is run the procedure for a validate vehicle and it is verified it in the time domain.

CHAPTER 5

5.1 Introduction

In the last chapters, the attention is focused on the controller formulation , based on the feedforward and feedback contribution, then implemented in MATLAB-Simulink; it is explained the tool, based on a non-linear quasi static model, for the offline design of the feedforward contribution: so it is designed the front to total anti-roll moment distribution by using this tool and at the end some preliminary simulation results are showed with a Simulink vehicle model including feedback and feedforward contributions.

This chapter is, first of all, about the sensitivity analysis of the dynamic steering angle characteristic of the vehicle with respect to the total value of roll stiffness of the front and rear suspension system. Secondly, it is analysed in detail the maximum values of steady state lateral acceleration that are achievable with and without the front-to-total roll stiffness distribution controller for different values of total roll stiffness or anti-roll moment of the vehicle, in order to quantify the potential benefit that is possible to reach through this new controller.

Then, since the benefit of cornering response of the vehicle caused by this controller based on the variable distribution of the front and rear anti-roll moment, depends on the non- linear tyre behaviour, it is developed a tool for the analysis of the effect of the lateral load transfer on the lateral force characteristic on the front and rear axles, in order to predict a priority what is the effect of different distributing the anti-roll moment on the front and rear axle.

At the end a novel formulation of the single-track vehicle model is discussed, that has been arranged in order to be able to design the feedback gains of the control system in the frequency domain.

5.2 Effect of total roll stiffness on the vehicle cornering response

In these analyses it is used the non-linear quasi static model and they are considered different values of the total suspension roll stiffness. It is made a sensitivity analysis on the variation of the dynamic steering angle, roll angle as a function of lateral acceleration for the passive vehicle, on the variation of minimum dynamic steering angle, needed to achieve the maximum value of lateral acceleration and on the variation of the roll angle for the active vehicle. At the end it is analysed how the front-to-total feedforward contribution changes in this sensitivity analysis.

5.2.1 Sensitivity analyses

The study is started with very low values of roll stiffness, respect what it should aspect in a vehicle application, and then they are considered more realistic roll stiffness values, providing a roll gradient about $5 - 6\ {}^{deg}/_{g}$ and lower values of roll gradient, that are more typical values of a vehicle with active suspension system.

The analysis starts by considering very wide range of anti-roll moment characteristics as a function of roll angle and for this range of anti-roll moment characteristics, it is analysed the variation of the understeering characteristic. The latter provides the dynamic steering angle, which is the difference between the total steering angle at the wheels and the kinematic steering angle, the steering angle of the vehicle with zero slip angles in the front and rear axle versus lateral acceleration.

In Figure 5.1, the blue characteristic, characterized by a very high exaggerated value of roll angle, has a penalty in terms of understeering behaviour; this vehicle is more understeering and is characterized by significant lower maximum values of lateral accelerations with respect to the other vehicles. For the other three vehicle the behaviour is a very similar in terms of understeer; in fact, it is changed the total roll stiffness of the vehicle without changing the front-to-total roll stiffness distribution.

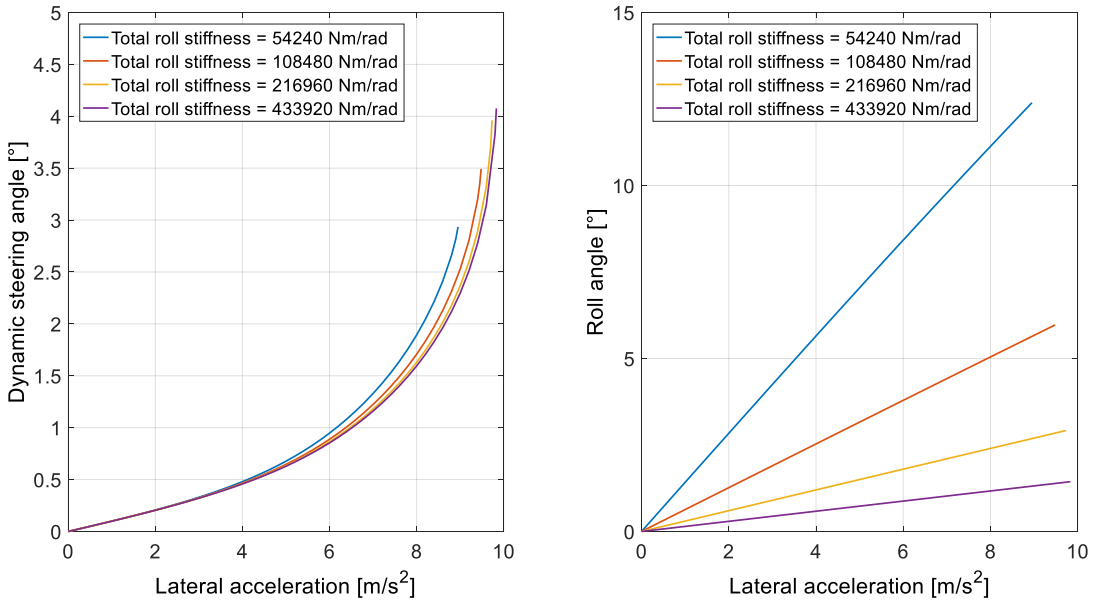

Figure 5.1: Dynamic steering angle and roll angle for the passive vehicle, as a function of lateral acceleration

This is a confirmation that through a normal active suspension system in which it is modified the total roll stiffness without plane with the front-to-total roll stiffness distribution, there isn't a great benefit in terms of vehicle corner response.

Then in this study, it is focused the attention on the front-to-total roll stiffness distribution; essentially it is considered the same value of total roll stiffness of the vehicle but then it is applied the optimisation procedure, discussed in the previous chapter, based on the quasi-static model with a cost-function based on the absolute value of the dynamic steering angle in order to find the maximum level of lateral acceleration that is achievable with the different values of total roll stiffness.

Essentially this maximum level of lateral acceleration is the maximum that can be achieved with the controller by considering different values of total roll stiffness for the front and rear suspension system. This work is carried out for three different speeds that are $V = (50, 75, 100)\ {}^{km}/_{h}$.

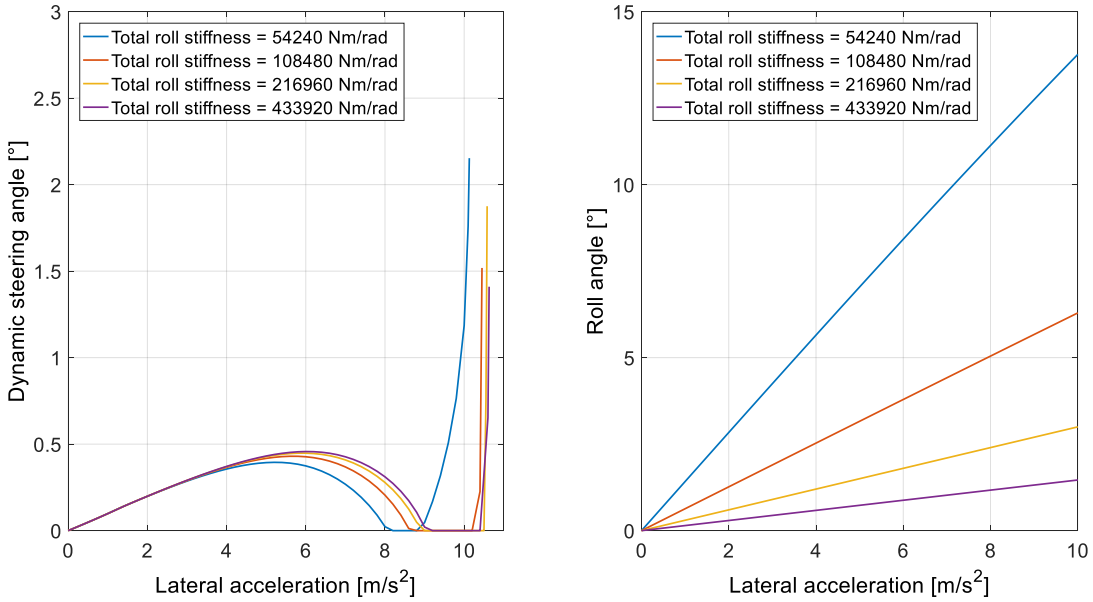

Figure 5.2: Optimisation-based calculation of the maximum value of lateral acceleration achievable with the controller

In Figure 5.3, it is possible to see in the maximum value of lateral acceleration, in the vertical axis, can be achieved according to the optimisation shown in Figure 5.2 where progressively it is increased the value of lateral acceleration and it is calculated the corresponding value of front-to-total anti-roll moment distribution, in-order to minimize this cost function until it is possible to find a solution.

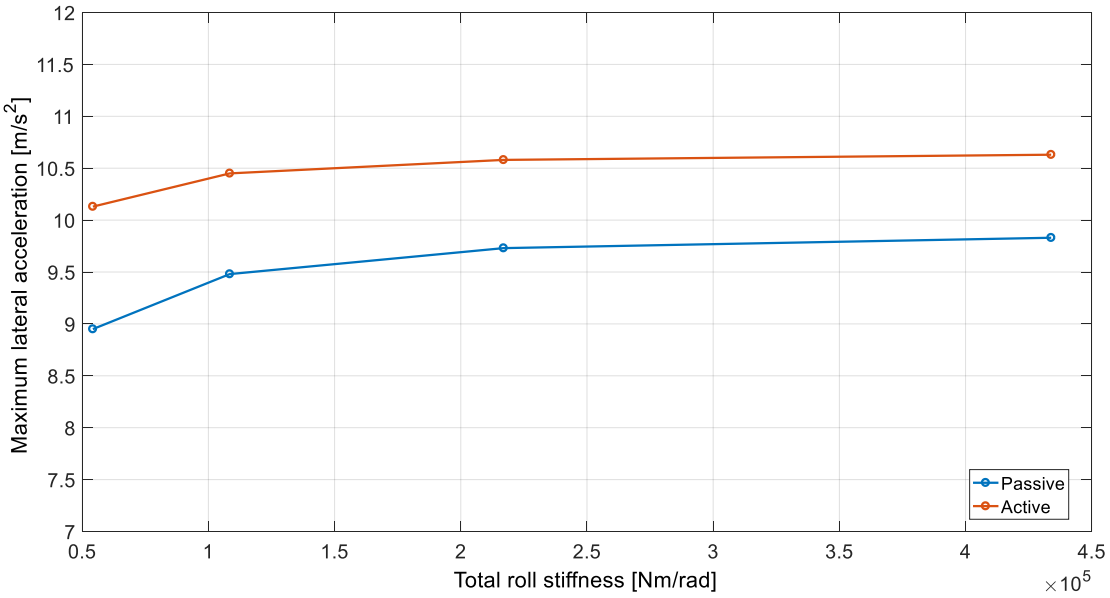

Figure 5.3: Calculation of the maximum value of a_y achievable as a function the total suspension roll stiffness

On the horizontal axis, it is plotted the total value of the sum of roll stiffness on the front and rear suspension system. The blue line corresponds to the passive vehicle, without the front to total anti-roll moment distribution controller, and the red line corresponds to the vehicle with front to total anti-roll moment distribution controller.

It is possible to note, for this specific vehicle data set, a consistent improvement can be achieved on the steady state corner response; in particular, by considering a vehicle where it is simply increased the total roll stiffness, without changing the roll stiffness distribution, which is the case of the blue line, there is a benefit in terms of cornering response caused by the reduction of the roll angle, but this benefit is much lower than the benefit that is achievable by properly distributing of front-to-total roll stiffness.

In fact, by comparing, the level that corresponds to the minimum level of maximum lateral acceleration achievable with front to total distribution controller with the maximum level of lateral acceleration that is achieved with the controller, that doesn't change the front-to- total roll stiffness distribution, there is a significant benefit with the controller that modifies the front-to-total roll stiffness distribution.

It is possible to note similar results for different speeds; there are only little differences caused by Ackermann percentage effect on the two front wheels, that is different for different speeds and caused by very marginal load transfer due to aerodynamic contribution.

Looking, for example, at the Table 5.1, referred at $V = 100\ {}^{km}/_{h}$, it is possible to see the total roll stiffness distribution, the maximum value of lateral acceleration achievable with the passive vehicle and the maximum value of lateral acceleration achievable by using the controller. There is a difference of around 1 ${}^{m}/_{s^2}$ between the passive vehicle and the controlled vehicle for low values of total roll stiffness, and a difference of around 0.8 ${}^{m}/_{s^2}$ for high values of total roll stiffness. In the last column of the table, there is the percentage increase in terms of maximum lateral acceleration with respect maximum level of lateral acceleration of the passive vehicle; the improvement is ranging between 13.2 % and 8.1 %.

$K_{ROLL,TOT}\left[{}^{Nm}/_{rad}\right]$	$a_{y,max,PASS}\left[{}^{m}/_{s^2}\right]$	$a_{y,max,ACTIVE}\left[{}^{m}/_{s^2}\right]$	${}^{\Delta a_{y,max}}/_{a_{y,max,PASS}}$ [%]
54240	8.95	10.13	+ 13.2
108480	9.48	10.45	+ 10.2
216960	9.73	10.58	+ 8.7
433920	9.83	10.63	+ 8.1

Table 5.1: Comparison of the maximum accelerations achievable with the passive and active vehicles at $V = 100\ {}^{km}/_{h}$

Similar results can be seen for the other levels of speed considered. In terms of conclusion, based on the other projects of the University of Surrey, the improvement of maximum level of lateral acceleration achievable is similar to that is possible to have by using a torque vectoring controller.

In terms of the variation of the front-to-total roll stiffness distribution as a function of the total roll stiffness, to achieve a reference understeering characteristic it is possible to see in Figure 5.4 the dynamic steering angle as a function of lateral acceleration.

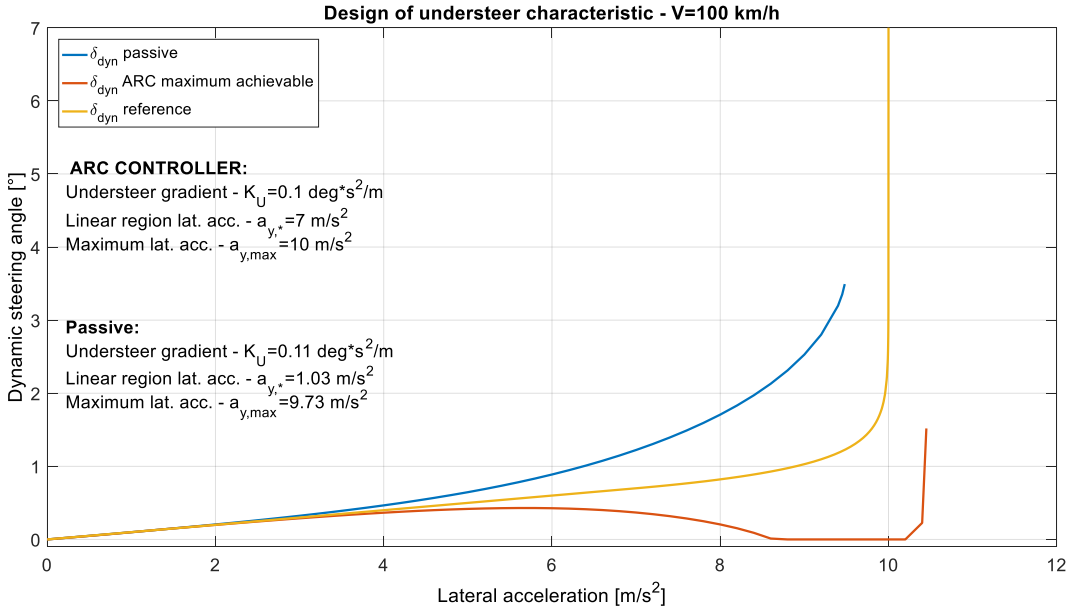

Figure 5.4: Reference understeer characteristic for the active vehicle

The blue line refers to the passive vehicle, whilst the maximum achievable level of control that is possible according to the given constraints for the active vehicle corresponds to the red line; in other words, the red line is the minimum level of vehicle understeer that is possible to achieve according to the constraints set up in the procedure. The orange line corresponds to the reference understeer characteristic of the vehicle.

As explained, it is used the non-linear quasi-static model in order to design the front-to-total roll stiffness ratio to achieve the target characteristic indicated with the orange line.

In Figure 5.5 it is plotted the feedforward front-to-total roll stiffness ratio as a function of steering angle at $V = 100\ {}^{km}/_{h}$ for different values of total suspension roll stiffness; it is possible to note that the variation of the feedforward ratio to achieve the same understeer characteristic is very marginal, especially considering the useful range of lateral accelerations corresponds to those colourful circle in the figure that correspond at different level of lateral acceleration. Actually, the difference is for values of steering angle larger than 3.5 deg, where the vehicle is characterized by the tyre saturation on the front axle.

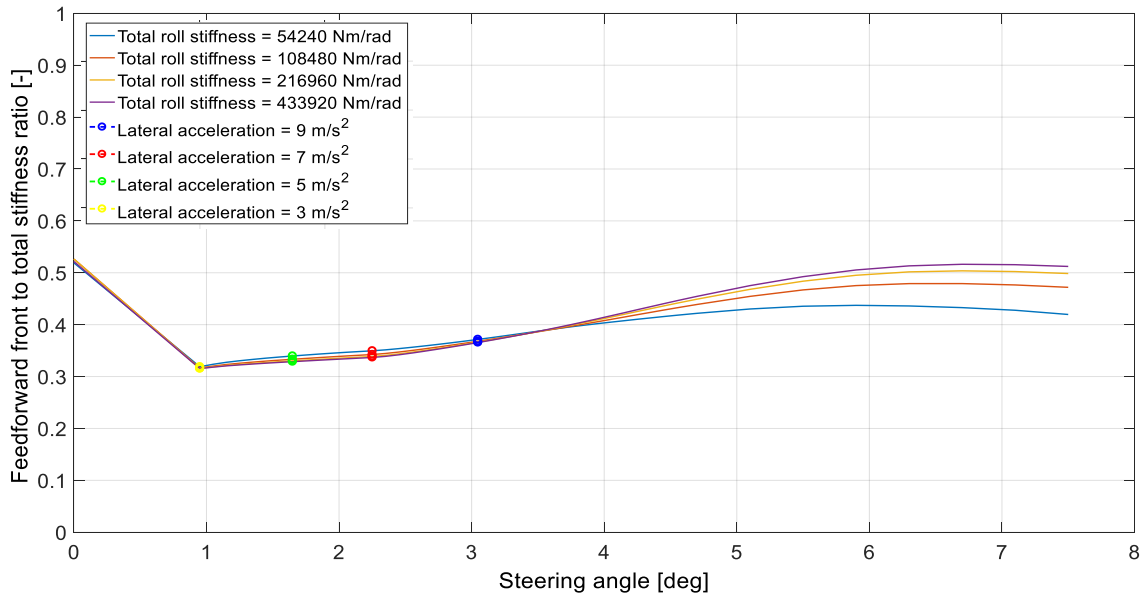

Figure 5.5: Feedforward front-to-total roll stiffness ratio for different values of total suspension roll stiffness as function of steering angle

It is possible to conclude that the total value of roll stiffness and the roll gradient imposed by the active suspension system is substantially irrelevant with respect to the required front-to-total roll stiffness ratio in order to achieve the same understeer characteristic.

Then the plot of front-to-total stiffness ratio as a function of lateral acceleration, in Figure 5.6, is a further confirmation, because the variation of the resulting characteristic with respect to the total roll stiffness of the vehicle is negligible.

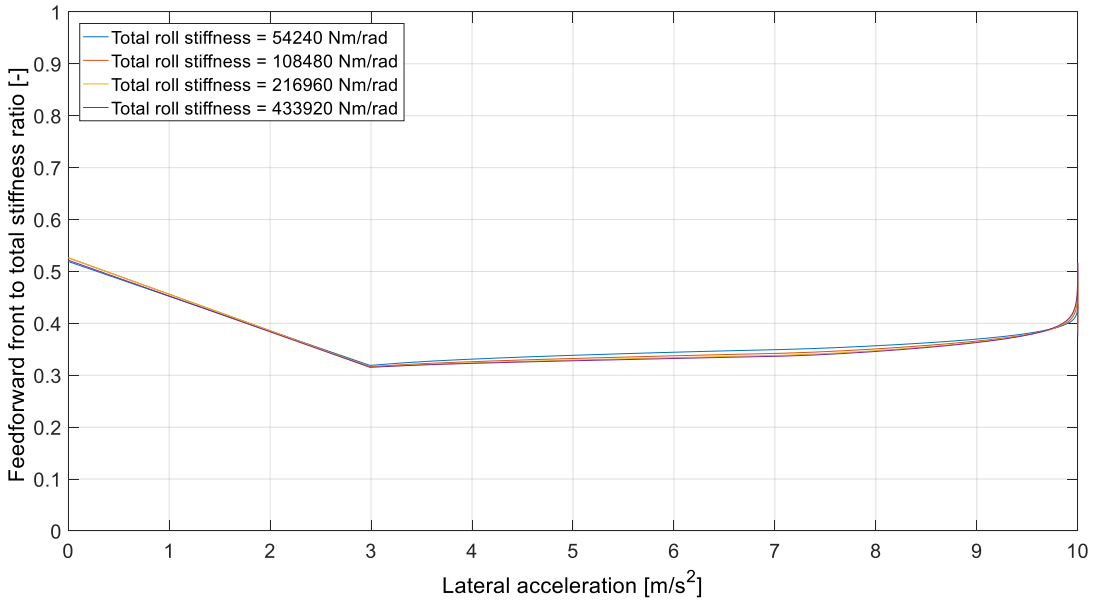

Figure 5.6: Feedforward front-to-total rol stiffness ratio for different values of total roll stiffness as a function of lateral acceleration

5.3 Effect of anti-roll moment on lateral tyre forces

The increase of load transfer on an axle produces a reduction of the cornering stiffness of that axle because the increase of cornering stiffness on the outer wheel is smaller in absolute value than the decrease of cornering stiffness on the inner wheel in that axle; this is what, in theory, is possible to find in the text on vehicle dynamics.

In this paragraph it is presented a tool suitable to plot the actual cornering stiffness on the front and rear axles for different values of anti-roll moment on that axle, in order to verify the actual behaviour of that axle for a set of Magic Formula tyre parameters. This tool is also very important to obtain linearized axle characteristics to be used in a vehicle model for frequency response analysis.

In this tool, the formulation of load transfers on the front and rear axle that are related to the front and rear anti-roll moments is given by the equations:

$$\Delta F_{Z,F} = \frac{\left(\sum_{i=1}^{2} F_{X,i}\, sin\, \delta_i + \sum_{i=1}^{2} F_{Y,i}\, cos\, \delta_i\right) d_F + M_{ANTI-ROLL,\,F}}{T_F}$$

$$\Delta F_{Z,R} = \frac{\left(\sum_{i=3}^{4} F_{X,i}\, sin\, \delta_i + \sum_{i=3}^{4} F_{Y,i}\, cos\, \delta_i\right) d_R + M_{ANTI-ROLL,\,R}}{T_R}$$

In a first approximation, by considering zero the load transfers to the rigid links of the suspension system negligible for a passenger car, since the front and rear roll centre height, d_F and d_R, are quite negligible respect to the centre of gravity height. In other way it is considered only the load transfer caused by the flexible parts and the controlled parts of the suspension system. The above equations are reformulated as:

$$\Delta F_{Z,F} \approx \frac{M_{ANTI-ROLL,\,F}}{T_F},\ \ \Delta F_{Z,R} \approx \frac{M_{ANTI-ROLL,\,R}}{T_R}$$

It is possible to calculate for different values of load transfers, caused by the anti-roll moment, the vertical forces on the individual wheels, by considering zero the longitudinal acceleration and a constant speed of the vehicle set to 100 $^{km}/_{h}$.

$$F_{Z,FL} = mg\frac{b}{2L} - ma_x\frac{h}{2L} - F_{drag}\frac{h}{2L} - \Delta F_{Z,F}$$

$$F_{Z,FR} = mg\frac{b}{2l} - ma_x\frac{h}{2l} - F_{drag}\frac{h}{2L} + \Delta F_{Z,F}$$

$$F_{Z,RL} = mg\frac{a}{2L} + ma_x\frac{h}{2L} + F_{drag}\frac{h}{2L} - \Delta F_{Z,R}$$

$$F_{Z,RR} = mg\frac{a}{2L} + ma_x\frac{h}{2L} + F_{drag}\frac{h}{2L} + \Delta F_{Z,R}$$

Under these hypothesis, the lateral forces for each tyre, based on the Pacejka Magic Formula 5.2, for a set of slip angles and with the respective vertical loads are calculated, where different values of anti-roll moment are used.

$$F_{Y,FL} = F_{Y,FL}(\alpha_{FL},\, F_{Z,FL})$$

$$F_{Y,FR} = F_{Y,FR}(\alpha_{FR},\, F_{Z,FR})$$

$$F_{F,RL} = F_{Y,RL}(\alpha_{RL},\, F_{Z,RL})$$

$$F_{Y,RR} = F_{Y,RR}(\alpha_{RR},\, F_{Z,RR})$$

For this calculation one 100 % Ackermann steering is considered, so the two wheels of the same axle are characterized by the same slip angle. The lateral forces on the front and rear

axles are given by the sum of the lateral forces on the individual respected tyres, as by the equations:

$$F_{Y,F} = F_{Y,FL} + F_{Y,FR}$$

$$F_{Y,R} = F_{Y,RL} + F_{Y,RR}$$

Then the values of C_F and C_R are obtained by using the definition of cornering stiffness as incremental ratio of lateral force with respect to slip angle, as the equations below:

$$C_F = \frac{F_{Y,FR}(\alpha_{FR} + \Delta\alpha,\ \sigma_{FR},\ \gamma_{FR},\ F_{Z,FR}) - F_{Y,FR}(\alpha_{FR},\ \sigma_{FR},\ \gamma_{FR},\ F_{Z,FR})}{\Delta\alpha} + \frac{F_{Y,FL}(\alpha_{FL} + \Delta\alpha,\ \sigma_{FL},\ \gamma_{FL},\ F_{Z,FL}) - F_{Y,FL}(\alpha_{FL},\ \sigma_{FL},\ \gamma_{FL},\ F_{Z,FL})}{\Delta\alpha}$$

$$C_R = \frac{F_{Y,RR}(\alpha_{RR} + \Delta\alpha,\ \sigma_{RR},\ \gamma_{RR},\ F_{Z,RR}) - F_{Y,RR}(\alpha_{RR},\ \sigma_{RR},\ \gamma_{RR},\ F_{Z,RR})}{\Delta\alpha} + \frac{F_{Y,RL}(\alpha_{RL} + \Delta\alpha,\ \sigma_{RL},\ \gamma_{RL},\ F_{Z,RL}) - F_{Y,RL}(\alpha_{RL},\ \sigma_{RL},\ \gamma_{RL},\ F_{Z,RL})}{\Delta\alpha}$$

The first part of the equation is related to the calculation of the cornering stiffness on the front and rear right wheels, the second part to the left wheels.

By using this tool, it is possible to plot the characteristic, as in Figure 5.7, that is the total lateral force on the front axle as a function of slip angle and of anti-roll moment on the front suspension system, that correspond to different values of lateral load transfer caused by the control of the front suspension system. This is a 3D representation of the lateral force to understand the influence of both contributes.

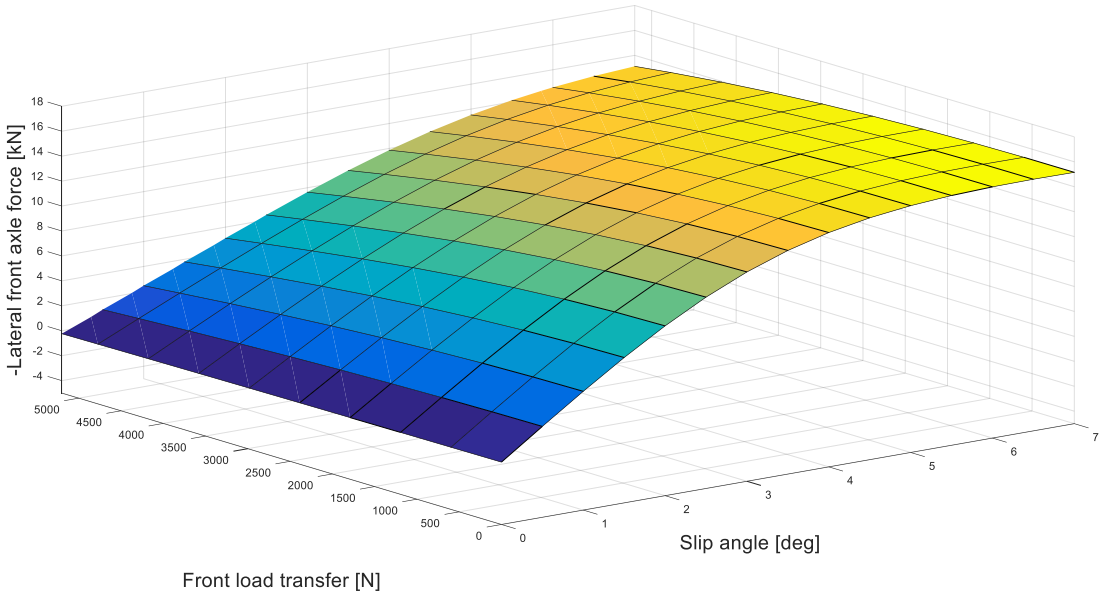

Figure 5.7: Lateral force on the front axle for different values of slip angle and front load transfer

As expected, according to the theory, when the load transfer is zero the value of lateral force is maximum, whilst when the load transfer increases there is a progressive reduction of the lateral force. Moreover, when the stiffness of the suspension system increases, there is a reduction of the cornering stiffness of that axle.

Actually, for small values of slip angle, when the anti-roll moment increases the cornering stiffness decreases, but at high values of slip angle, for example at $\alpha = 6\ deg$, the slop of the diagram is zero, but it is positive a significant value of the anti-roll moment; so, the force decreases but, actually, the cornering stiffness that is the rate of change of lateral force as a function of slip angle increases. This is a trivial thing, because on text-books the typical behaviour presented is the reduction of cornering stiffness of the axle as a function of anti-roll moment.

Since this vehicle is characterised by different tyre characteristics on the front and rear axles it is done the same job for the rear axle with similar results: for small values of slip angle the characteristics are always as expected, for medium-high values of slip angles the situation becomes complicated. As matter of fact, if the anti-roll moment on the rear axle increases there is a decrease of lateral force but there is an increase of cornering stiffness because the slope of the blue characteristic for example is larger then the slope of the characteristic at zero load transfer.

In Figure 5.8 there is the plot of the cornering stiffness on the front axle as a function of slip angles for different values of load transfer: it is possible to note, as said before, that for small slip angles, the cornering stiffness is a decreasing function of the load transfer caused by the anti-roll moment. However, for these specific tyre characteristics, that are reasonable because validated with the quasi-static against the corner behaviour of an actual vehicle measured in experimental tests in other activities of University of Surrey, the cornering stiffness is larger with high levels of load transfer for high values of slip angle.

For example, as possible to see from Figure, there is the transition from one situation to the other with $\alpha = 3 - 4\ deg$.

For the design of the feedback gains on frequency domain the cornering stiffness will be approximated linearly as a function of load transfer; the variation of the cornering stiffness will be modelled on the respective axle.

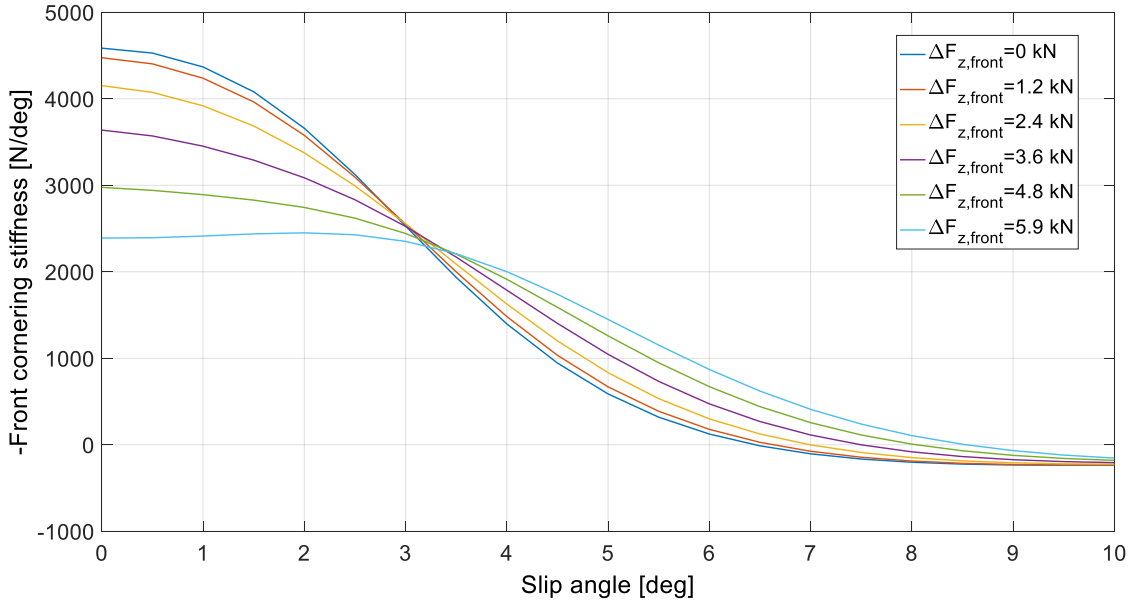

Figure 5.8: Cornering stiffness on the front axle as a function for different values of load transfer

5.4 Novel formulation of the single-track vehicle model

As pointed out in the last paragraph, the variation of cornering stiffness on the front and rear axle is not as expected in sense of reduction of cornering stiffness with the increase of load transfer in all conditions. In fact, for high values of slip angle, the absolute value of cornering stiffness is an increase function of the anti-roll moment, which is unexpected by considering the theory in textbooks, but it is justifiable looking the actual behaviour of the tyres.

As consequence, in this paragraph it is explained a novel formulation of linearization of the single-track vehicle model.

5.4.1 Single-track vehicle model

The front-to-total anti-roll moment distribution controller is useful to enhance the vehicle cornering response and to control the roll of the vehicle. At this point the problem is to create a link between the yaw/lateral dynamics and the roll dynamics.

The Figure 5.9 represents a simplified schematic of a single-track vehicle model with all the sign conventions adopted during this work of thesis. For example, the yaw rate, r, and the steering angle, δ, are positives when the driver is cornering to the right.

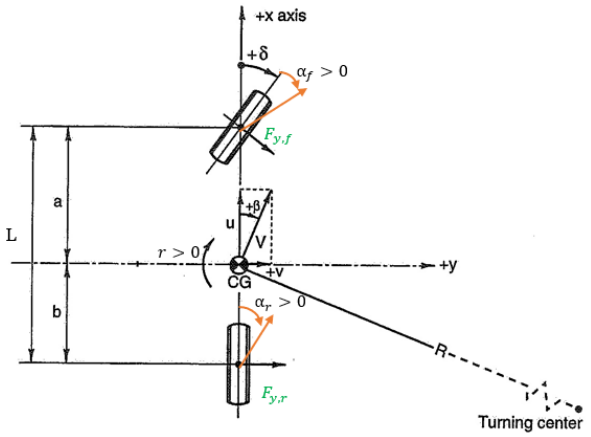

Term	Symbol	Units	Sign
Yawing velocity	r	radian/sec.	+ for clockwise
Lateral velocity	v, v_F, v_R	ft./sec.	+ to right
Longitudinal velocity	u	ft./sec.	+ for forward
Steer angle front wheels	δ	radian	+ for clockwise
Slip angles	α_F, α_R	radian	+ for slip to right
Vehicle slip angle at CG	β	radian	+ for slip to right
Cornering stiffnesses (two tires)	C_F, C_R	N /radian	always –
Total cornering stiffness ($C_F + C_R$)	C	N /radian	always –

Figure 5.9: Signs convention used in the formulation

It is possible to define the yaw moment balance equation, around the Z axis, as:

$$J_z\dot{r} = F_{Y,F}a - F_{Y,R}b$$

The lateral balance equation is the second main equation of the single-track vehicle model given by:

$$mV(\dot{\beta} + r) = F_{Y,F} + F_{Y,R}$$

The lateral forces are express as a function of slip angle, $F_Y = F_Y(\alpha)$

$$F_{Y,F} = C_F \alpha_F$$

$$F_{Y,R} = C_R \alpha_R$$

The slip angles, α_F and α_R, are defined as a function of steering angle, sideslip angle of the vehicle and yaw rate:

$$\alpha_F = \beta + \frac{a}{V} r - \delta$$

$$\alpha_R = \beta - \frac{b}{V} r$$

According the previous equations, it is possible to write the standard system equations of the single-track vehicle model:

$$\begin{cases} mV(\dot{\beta} + r) = F_{Y,F} + F_{Y,R} \\ J_z \dot{r} = F_{Y,F} a - F_{Y,R} b \end{cases}$$

This system can be written in matrix form as:

$$\begin{cases} \dot{\boldsymbol{x}}(\boldsymbol{t}) = \boldsymbol{A}\boldsymbol{x}(\boldsymbol{t}) + \boldsymbol{B}\boldsymbol{u}(\boldsymbol{t}) \\ \boldsymbol{y}(\boldsymbol{t}) = \boldsymbol{C}\boldsymbol{x}(\boldsymbol{t}) + \boldsymbol{D}\boldsymbol{u}(\boldsymbol{t}) \end{cases}$$

Where $\boldsymbol{x}(\boldsymbol{t})$ is the vector of the state variables, $\boldsymbol{u}(\boldsymbol{t})$ is the input vector and $\boldsymbol{y}(\boldsymbol{t})$ is the output vector.

5.4.2 Linearization of the lateral forces

In Figure 5.10, it is showed the lateral force on the axle as a function of slip angle of the front axle.

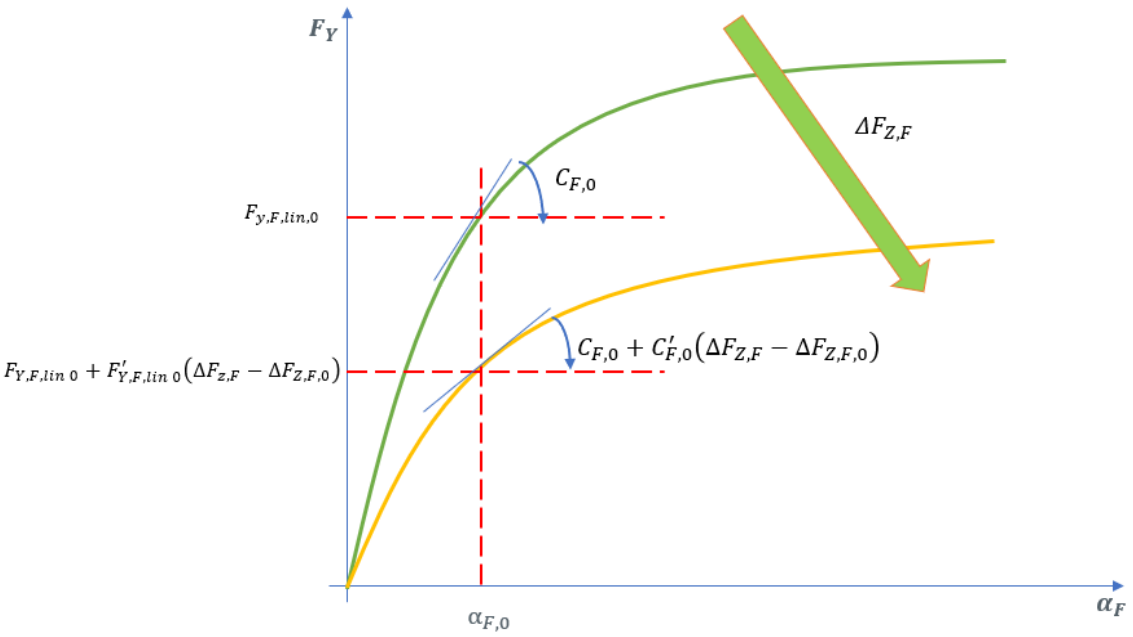

Figure 5.10: Linearization of the lateral force on the front axle

$C_{F,0}$ is the nominal value of cornering stiffness with respect to the linearization point; essentially the tyre model, used in this linearization model, considers the tyre characteristic as a line tangent to the actual lateral force characteristic at the linearization point. As consequence the lateral force is given by the linearized value of lateral force plus the cornering stiffness multiplied for the variation of cornering stiffness with respect to the linearization point.

To formulate the novel single-track vehicle model, it is not only considered the variation of cornering stiffness with the variation of vertical load; because if it is considered the load transfer on the front axle, it is possible to have that axle is working in another point that is characterized by different values of cornering stiffness. The value of cornering stiffness is equal to the previous value of cornering stiffness plus the gradient of cornering stiffness with respect to the load transfer multiplied by the load transfer difference from the linearization point.

$$C_F = C_F(\Delta F_{Z,F})$$

$$C_F \approx C_{F,0} + C'_{F,0}(\Delta F_{Z,F} - \Delta F_{Z,F,0})$$

What is also considered, it is the fact the lateral force, that corresponds to the linearization point, changes with the load transfer, $\Delta F_{Z,F}$, on the respective axle. Instead of having a linearization point, that could be F_{Y,F_0}, there is a linearization point, $F_{Y,F,lin}$, that is the new

lateral force given by the previous lateral force plus the gradient of the lateral force with respect to the load transfer multiplied by the load transfer variation.

$$F_{Y,F,\,lin} = F_{Y,F,\,lin}\left(\Delta F_{Z,F}\right)$$

$$F_{Y,F,\,lin} = F_{Y,F,\,lin,0} + F'_{Y,\,F,\,lin,\,0}\left(\Delta F_{Z,F} - \Delta F_{Z,F,0}\right)$$

In this way the single-track model is reformulated and includes the two standard equations, that are the lateral force balance equation and the yaw moment balance equation, in-order to express the lateral force on the front and rear axles by considering the variation of both the cornering stiffness and the lateral force on the axle as a function of vertical load transfer. At other two equations, it also considered the roll moment balance equation.

As consequence there is the lateral force on the front axle as a function of slip angle and the load transfer on that axle; it is given by the lateral force at the nominal value of slip angle plus the cornering stiffness multiplied by the difference between the actual slip angle and the slip angle at the linearization point. Then cornering stiffness and value of lateral force with respect which it is considered the cornering stiffness are expressed as a function of vertical load transfer. The equations below represent the new model of the linearization of the lateral forces:

$$F_{Y,F} = F_{Y,F}\left(\alpha_F, \Delta F_{Z,F}\right) \approx F_{Y,F,\,lin} + C_F\left(\alpha_F - \alpha_{F,\,0}\right)$$

In this way the lateral force on the front axle is given by the lateral force on the linearization point plus the lateral force gradient with respect to the load transfer on that axle, multiplied by the actual load transfer and the load transfer on the linearization point, plus the cornering stiffness on that axle that includes the nominal value of cornering stiffness and the gradient of the cornering stiffness with respect to the vertical load variation, multiplied by the vertical load variation with respect the nominal load transfer, multiplied by the slip angle difference with respect the nominal point in terms of slip angle. By these considerations, the new lateral force is given by:

$$\begin{aligned} F_{Y,F} \approx F_{Y,F,\,lin,0} + F'_{Y,\,F,lin,0}\left(\Delta F_{Z,F} - \Delta F_{Z,F,0}\right) \\ + \left(\alpha_F - \alpha_{F,0}\right)\left[C_{F,0} + C'_{F,0}\left(\Delta F_{Z,F} - \Delta F_{Z,F,0}\right)\right] \end{aligned}$$

With

$$\Delta F_{Z,F} = \frac{K_F\theta + D_F\dot{\theta} + M_{ANTI-ROLL,\,ACT,F}}{T_F}$$

For small value of d_F. By substituting the expression of α_F, in the previous expression, the lateral force, on the front axle is written as:

$$F_{Y,F} \approx F_{Y,F,\,lin,0} + F'_{Y,\,F,lin,0}\left(\frac{K_F\theta + D_F\dot{\theta} + M_{ANTI-ROLL,\,ACT,F}}{T_F} - \Delta F_{Z,F,0}\right) + \left(\beta + \frac{a}{V}r - \delta - \alpha_{F,0}\right)\left[C_{F,0} + C'_{F,0}\left(\frac{K_F\theta + D_F\dot{\theta} + M_{ANTI-ROLL,\,ACT,F}}{T_F} - \Delta F_{Z,F,0}\right)\right]$$

By considering as state variables the parameters, r, β, θ, $\dot{\theta}$ and as inputs δ, $M_{ANTI-ROLL,\,ACT,F}$ and $M_{ANTI-ROLL,\,ACT,R}$, the following terms are linearized through Taylor expansion:

$$\delta\theta = \delta_0\theta_0 + \theta_0(\delta - \delta_0) + \delta_0(\theta - \theta_0)$$

$$\delta\dot{\theta} = \delta_0\dot{\theta}_0 + \dot{\theta}_0(\delta - \delta_0) + \delta_0\left(\dot{\theta} - \dot{\theta}_0\right)$$

$$\delta M_{ANTI-ROLL,\,ACT,F} = \delta_0 M_{ANTI-ROLL,\,ACT,F_0} + M_{ANTI-ROLL,\,ACT,F_0}(\delta - \delta_0) + \delta_0\left(M_{ANTI-ROLL,\,ACT,F} - M_{ANTI-ROLL,\,ACT,F_0}\right)$$

$$\beta\theta = \beta_0\theta_0 + \theta_0(\beta - \beta_0) + \beta_0(\theta - \theta_0)$$

$$\beta\dot{\theta} = \beta_0\dot{\theta}_0 + \dot{\theta}_0(\beta - \beta_0) + \beta_0\left(\dot{\theta} - \dot{\theta}_0\right)$$

$$\beta\, M_{ANTI-ROLL,\,ACT,F} = \beta_0 M_{ANTI-ROLL,\,ACT,F_0} + M_{ANTI-ROLL,\,ACT,F_0}(\beta - \beta_0) + \beta_0\left(M_{ANTI-ROLL,\,ACT,F} - M_{ANTI-ROLL,\,ACT,F_0}\right)$$

$$r\theta = r_0\theta_0 + \theta_0(r - r_0) + r_0(\theta - \theta_0)$$

$$r\dot{\theta} = r_0\dot{\theta}_0 + \dot{\theta}_0(r - r_0) + r_0\left(\dot{\theta} - \dot{\theta}_0\right)$$

$$r M_{ANTI-ROLL,\,ACT,F} = r_0 M_{ANTI-ROLL,\,ACT,F_0} + M_{ANTI-ROLL,\,ACT,F_0}(r - r_0) + r_0\left(M_{ANTI-ROLL,\,ACT,F} - M_{ANTI-ROLL,\,ACT,F_0}\right)$$

By carrying out all the calculations, considering all the contributions, the lateral force on the front axle is given by the equation below.

$$
\begin{aligned}
F_{Y,F} \approx \beta & \left(C_{F,0} - C'_{F,0}\Delta F_{Z,F,0} + \frac{C'_{F,0}K_F\theta_0}{T_F} + \frac{C'_{F,0}D_F\dot{\theta}_0}{T_F} + \frac{C'_{F,0}M_{ANTI-ROLL,\,ACT,F_0}}{T_F} \right) \\
& + r\left(\frac{a}{V}C_{F,0} - \frac{a}{V}C'_{F,0}\Delta F_{Z,F,0} + \frac{a}{V}\frac{C'_{F,0}K_F\theta_0}{T_F} + \frac{a}{V}\frac{C'_{F,0}D_F\dot{\theta}_0}{T_F} \right. \\
& \left. + \frac{a}{V}\frac{C'_{F,0}M_{ANTI-ROLL,\,ACT,F_0}}{T_F} \right) \\
& + \theta\left(-\frac{C'_{F,0}K_F\delta_0}{T_F} + \frac{C'_{F,0}K_F\beta_0}{T_F} + \frac{C'_{F,0}K_F a r_0}{VT_F} + \frac{K_F\left(F'_{Y,\,F,lin,0} - C'_{F,0}\alpha_{F,0}\right)}{T_F} \right) \\
& + \dot{\theta}\left(-\frac{C'_{F,0}D_F\delta_0}{T_F} + \frac{C'_{F,0}D_F\beta_0}{T_F} + \frac{C'_{F,0}D_F a r_0}{VT_F} + \frac{D_F\left(F'_{Y,\,F,lin,0} - C'_{F,0}\alpha_{F,0}\right)}{T_F} \right) \\
& + \delta\left(-C_{F,0} + C'_{F,0}\Delta F_{Z,F,0} - \frac{C'_{F,0}K_F\theta_0}{T_F} - \frac{C'_{F,0}D_F\dot{\theta}_0}{T_F} \right. \\
& \left. - \frac{C'_{F,0}M_{ANTI-ROLL,\,ACT,F_0}}{T_F} \right) \\
& + M_{ANTI-ROLL,\,ACT,F}\left(-\frac{C'_{F,0}\delta_0}{T_F} + \frac{C'_{F,0}\beta_0}{T_F} + \frac{C'_{F,0}a r_0}{VT_F} \right. \\
& \left. + \frac{\left(F'_{Y,\,F,lin,0} - C'_{F,0}\alpha_{F,0}\right)}{T_F} \right) + const_F
\end{aligned}
$$

It is a function by the side slip angle, β, the yaw rate of the car, r, roll angle, θ, roll rate, $\dot{\theta}$, steering angle, δ, and the anti-roll moment on the front axle, $M_{ANTI-ROLL,ACT,\,F}$.

It is done the same job for the lateral force on the rear axle. By considering the expression below:

$$
\begin{aligned}
F_{Y,R} \approx F_{Y,R,\,lin,0} & + F'_{Y,\,R,lin,0}\left(\Delta F_{Z,R} - \Delta F_{Z,R,0}\right) \\
& + \left(\alpha_R - \alpha_{R,0}\right)\left[C_{R,0} + C'_{R,0}\left(\Delta F_{Z,R} - \Delta F_{Z,R,0}\right)\right]
\end{aligned}
$$

With

$$
\Delta F_{Z,R} = \frac{K_R\theta + D_R\dot{\theta} + M_{ANTI-ROLL,\,ACT,R}}{T_R}
$$

For small value of d_R. It is possible to have the final expression of the lateral force on the rear axle by the following equation, by combing all the equations and by using the Taylor expansion:

$$\begin{aligned} F_{Y,R} \approx \beta & \left(C_{R,0} - C'_{R,0}\Delta F_{Z,R,0} + \frac{C'_{R,0}K_R\theta_0}{T_R} + \frac{C'_{R,0}D_R\dot{\theta}_0}{T_R} + \frac{C'_{R,0}M_{ANTI-ROLL,\,ACT,R_0}}{T_R} \right) \\ & + r\left(-\frac{b}{V}C_{R,0} + \frac{b}{V}C'_{R,0}\Delta F_{Z,R,0} - \frac{b}{V}\frac{C'_{R,0}K_R\theta_0}{T_R} - \frac{b}{V}\frac{C'_{R,0}D_R\dot{\theta}_0}{T_R} \right. \\ & \left. - \frac{b}{V}\frac{C'_{R,0}M_{ANTI-ROLL,\,ACT,R_0}}{T_R} \right) \\ & + \theta\left(\frac{C'_{R,0}K_R\beta_0}{T_R} - \frac{C'_{R,0}K_Rbr_0}{VT_R} + \frac{K_R\left(F'_{Y,\,R,lin,0} - C'_{R,0}\alpha_{R,0}\right)}{T_R} \right) \\ & + \dot{\theta}\left(\frac{C'_{R,0}D_R\beta_0}{T_R} - \frac{C'_{R,0}D_Rbr_0}{VT_R} + \frac{D_R\left(F'_{Y,\,R,lin,0} - C'_{R,0}\alpha_{R,0}\right)}{T_R} \right) \\ & + M_{ANTI-ROLL,\,ACT,R}\left(\frac{C'_{R,0}\beta_0}{T_R} - \frac{C'_{R,0}br_0}{VT_R} + \frac{\left(F'_{Y,\,r,lin,0} - C'_{R,0}\alpha_{F,0}\right)}{T_R} \right) \\ & + const_R \end{aligned}$$

In this way it is possible to obtain the updated equations of motion of the model, namely the lateral force balance equation, the yaw moment balance equation and the roll moment balance equation.

5.4.3 Updated equations in single-track vehicle model

The yaw moment balance and the lateral balance equations are the two standard equations of the single-track model: as said before, it also added the roll moment balance around the roll axis. For small values of roll angle, d_F and d_R, it can be written as:

$$\begin{aligned} J_X\ddot{\theta} = ma_yh + mgh\theta - K_F\theta - D_F\dot{\theta} - M_{ANTI-ROLL,ACT,F} - K_R\theta - D_R\dot{\theta} \\ - M_{ANTI-ROLL,ACT,R} \end{aligned}$$

In fact, if θ is very low, $\sin\theta \approx \theta$ and $\cos\theta \approx 1$. The Figure shows the sign conventions for the roll angle, by considering a rear view of the vehicle body.

Moreover, in the yaw moment balance equations, it also considered an external moment $M_{Z,ext}$ caused by a torque-vectoring, in the case the car owns it.

The updated equations system becomes:

$$\begin{cases} mV(\dot{\beta}+r) = F_{Y,F} + F_{Y,R} \\ J_Z\dot{r} = F_{Y,F}a - F_{Y,R}b + M_{Z,ext} \\ J_X\ddot{\theta} = mV(\dot{\beta}+r)h + mgh\theta - K_F\theta - D_F\dot{\theta} - M_{ANTI-ROLL,ACT,F} - K_R\theta - D_R\dot{\theta} - M_{ANTI-ROLL,ACT,R} \end{cases}$$

By substituting the linearized lateral forces, calculated in the previous paragraph, the three equations of the above system are computed as:

$$\begin{aligned} \dot{\beta} = \frac{1}{mV}\Bigg\{ & \beta\left(C_{F,0} - C'_{F,0}\Delta F_{Z,F,0} + \frac{C'_{F,0}K_F\theta_0}{T_F} + \frac{C'_{F,0}D_F\dot{\theta}_0}{T_F} + \frac{C'_{F,0}M_{ANTI-ROLL,\,ACT,F_0}}{T_F} + C_{R,0}\right. \\ & \left. - C'_{R,0}\Delta F_{Z,R,0} + \frac{C'_{R,0}K_R\theta_0}{T_R} + \frac{C'_{R,0}D_R\dot{\theta}_0}{T_R} + \frac{C'_{R,0}M_{ANTI-ROLL,\,ACT,R_0}}{T_R}\right) \\ & + r\left(\frac{a}{V}C_{F,0} - \frac{a}{V}C'_{F,0}\Delta F_{Z,F,0} + \frac{a}{V}\frac{C'_{F,0}K_F\theta_0}{T_F} + \frac{a}{V}\frac{C'_{F,0}D_F\dot{\theta}_0}{T_F}\right. \\ & + \frac{a}{V}\frac{C'_{F,0}M_{ANTI-ROLL,\,ACT,F_0}}{T_F} - \frac{b}{V}C_{R,0} + \frac{b}{V}C'_{R,0}\Delta F_{Z,R,0} - \frac{b}{V}\frac{C'_{R,0}K_R\theta_0}{T_R} \\ & \left. - \frac{b}{V}\frac{C'_{R,0}D_R\dot{\theta}_0}{T_R} - \frac{b}{V}\frac{C'_{R,0}M_{ANTI-ROLL,\,ACT,R_0}}{T_R} - mV\right) \\ & + \theta\left(-\frac{C'_{F,0}K_F\delta_0}{T_F} + \frac{C'_{F,0}K_F\beta_0}{T_F} + \frac{C'_{F,0}K_Far_0}{VT_F} + \frac{K_F\left(F'_{Y,\,F,lin,0} - C'_{F,0}\alpha_{F,0}\right)}{T_F}\right. \\ & \left. + \frac{C'_{R,0}K_R\beta_0}{T_R} - \frac{C'_{R,0}K_Rbr_0}{VT_R} + \frac{K_R\left(F'_{Y,\,R,lin,0} - C'_{R,0}\alpha_{R,0}\right)}{T_R}\right) \\ & + \dot{\theta}\left(-\frac{C'_{F,0}D_F\delta_0}{T_F} + \frac{C'_{F,0}D_F\beta_0}{T_F} + \frac{C'_{F,0}D_Far_0}{VT_F} + \frac{D_F\left(F'_{Y,\,F,lin,0} - C'_{F,0}\alpha_{F,0}\right)}{T_F}\right. \\ & \left. + \frac{C'_{R,0}D_R\beta_0}{T_R} - \frac{C'_{R,0}D_Rbr_0}{VT_R} + \frac{D_R\left(F'_{Y,\,R,lin,0} - C'_{R,0}\alpha_{R,0}\right)}{T_R}\right) \\ & + \delta\left(-C_{F,0} + C'_{F,0}\Delta F_{Z,F,0} - \frac{C'_{F,0}K_F\theta_0}{T_F} - \frac{C'_{F,0}D_F\dot{\theta}_0}{T_F} - \frac{C'_{F,0}M_{ANTI-ROLL,\,ACT,F_0}}{T_F}\right) \\ & + M_{ANTI-ROLL,\,ACT,F}\left(-\frac{C'_{F,0}\delta_0}{T_F} + \frac{C'_{F,0}\beta_0}{T_F} + \frac{C'_{F,0}ar_0}{VT_F} + \frac{\left(F'_{Y,\,F,lin,0} - C'_{F,0}\alpha_{F,0}\right)}{T_F}\right) \\ & + M_{ANTI-ROLL,\,ACT,R}\left(\frac{C'_{R,0}\beta_0}{T_R} - \frac{C'_{R,0}br_0}{VT_R} + \frac{\left(F'_{Y,\,r,lin,0} - C'_{R,0}\alpha_{F,0}\right)}{T_R}\right) + const_F \\ & + const_R\Bigg\} \end{aligned}$$

$$\dot{r} = \frac{1}{J_z}\Bigg\{\beta\left[a\left(C_{F,0} - C'_{F,0}\Delta F_{Z,F,0} + \frac{C'_{F,0}K_F\theta_0}{T_F} + \frac{C'_{F,0}D_F\dot{\theta}_0}{T_F} + \frac{C'_{F,0}M_{ANTI-ROLL,\,ACT,F_0}}{T_F}\right)\right.$$
$$- b\left(C_{R,0} - C'_{R,0}\Delta F_{Z,R,0} + \frac{C'_{R,0}K_R\theta_0}{T_R} + \frac{C'_{R,0}D_R\dot{\theta}_0}{T_R}\right.$$
$$\left.\left. + \frac{C'_{R,0}M_{ANTI-ROLL,\,ACT,R_0}}{T_R}\right)\right]$$
$$+ r\left[a\left(\frac{a}{V}C_{F,0} - \frac{a}{V}C'_{F,0}\Delta F_{Z,F,0} + \frac{a}{V}\frac{C'_{F,0}K_F\theta_0}{T_F} + \frac{a}{V}\frac{C'_{F,0}D_F\dot{\theta}_0}{T_F}\right.\right.$$
$$\left. + \frac{a}{V}\frac{C'_{F,0}M_{ANTI-ROLL,\,ACT,F_0}}{T_F}\right)$$
$$- b\left(-\frac{b}{V}C_{R,0} + \frac{b}{V}C'_{R,0}\Delta F_{Z,R,0} - \frac{b}{V}\frac{C'_{R,0}K_R\theta_0}{T_R} - \frac{b}{V}\frac{C'_{R,0}D_R\dot{\theta}_0}{T_R}\right.$$
$$\left.\left. - \frac{b}{V}\frac{C'_{R,0}M_{ANTI-ROLL,\,ACT,R_0}}{T_R}\right)\right]$$
$$+ \theta\left[a\left(-\frac{C'_{F,0}K_F\delta_0}{T_F} + \frac{C'_{F,0}K_F\beta_0}{T_F} + \frac{C'_{F,0}K_F a r_0}{VT_F}\right.\right.$$
$$\left. + \frac{K_F\left(F'_{Y,\,F,lin,0} - C'_{F,0}\alpha_{F,0}\right)}{T_F}\right)$$
$$\left. - b\left(\frac{C'_{R,0}K_R\beta_0}{T_R} - \frac{C'_{R,0}K_R b r_0}{VT_R} + \frac{K_R\left(F'_{Y,\,R,lin,0} - C'_{R,0}\alpha_{R,0}\right)}{T_R}\right)\right]$$
$$+ \dot{\theta}\left[a\left(-\frac{C'_{F,0}D_F\delta_0}{T_F} + \frac{C'_{F,0}D_F\beta_0}{T_F} + \frac{C'_{F,0}D_F a r_0}{VT_F}\right.\right.$$
$$\left. + \frac{D_F\left(F'_{Y,\,F,lin,0} - C'_{F,0}\alpha_{F,0}\right)}{T_F}\right)$$
$$\left. - b\left(\frac{C'_{R,0}D_R\beta_0}{T_R} - \frac{C'_{R,0}D_R b r_0}{VT_R} + \frac{D_R\left(F'_{Y,\,R,lin,0} - C'_{R,0}\alpha_{R,0}\right)}{T_R}\right)\right]$$
$$+ \delta a\left(-C_{F,0} + C'_{F,0}\Delta F_{Z,F,0} - \frac{C'_{F,0}K_F\theta_0}{T_F} - \frac{C'_{F,0}D_F\dot{\theta}_0}{T_F}\right.$$
$$\left. - \frac{C'_{F,0}M_{ANTI-ROLL,\,ACT,F_0}}{T_F}\right)$$
$$+ M_{ANTI-ROLL,\,ACT,F}\,a\left(-\frac{C'_{F,0}\delta_0}{T_F} + \frac{C'_{F,0}\beta_0}{T_F} + \frac{C'_{F,0}a r_0}{VT_F}\right.$$
$$\left. + \frac{\left(F'_{Y,\,F,lin,0} - C'_{F,0}\alpha_{F,0}\right)}{T_F}\right)$$

$$- M_{ANTI-ROLL,\,ACT,R} b \left(\frac{C'_{R,0}\beta_0}{T_R} - \frac{C'_{R,0} b r_0}{V T_R} + \frac{\left(F'_{Y,\,r,lin,0} - C'_{R,0}\alpha_{F,0}\right)}{T_R} \right)$$

$$+ const_F a - const_R b + M_{Z,ext} \Bigg\}$$

$$\ddot{\theta} = \frac{h}{J_x} \Bigg[\beta \left(C_{F,0} - C'_{F,0}\Delta F_{Z,F,0} + \frac{C'_{F,0}K_F\theta_0}{T_F} + \frac{C'_{F,0}D_F\dot{\theta}_0}{T_F} + \frac{C'_{F,0}M_{ANTI-ROLL,\,ACT,F_0}}{T_F} + C_{R,0} \right.$$

$$\left. - C'_{R,0}\Delta F_{Z,R,0} + \frac{C'_{R,0}K_R\theta_0}{T_R} + \frac{C'_{R,0}D_R\dot{\theta}_0}{T_R} + \frac{C'_{R,0}M_{ANTI-ROLL,\,ACT,R_0}}{T_R} \right)$$

$$+ r \left(\frac{a}{V} C_{F,0} - \frac{a}{V} C'_{F,0}\Delta F_{Z,F,0} + \frac{a}{V}\frac{C'_{F,0}K_F\theta_0}{T_F} + \frac{a}{V}\frac{C'_{F,0}D_F\dot{\theta}_0}{T_F} \right.$$

$$+ \frac{a}{V}\frac{C'_{F,0}M_{ANTI-ROLL,\,ACT,F_0}}{T_F} - \frac{b}{V} C_{R,0} + \frac{b}{V} C'_{R,0}\Delta F_{Z,R,0} - \frac{b}{V}\frac{C'_{R,0}K_R\theta_0}{T_R}$$

$$\left. - \frac{b}{V}\frac{C'_{R,0}D_R\dot{\theta}_0}{T_R} - \frac{b}{V}\frac{C'_{R,0}M_{ANTI-ROLL,\,ACT,R_0}}{T_R} \right)$$

$$+ \theta \left(- \frac{C'_{F,0}K_F\delta_0}{T_F} + \frac{C'_{F,0}K_F\beta_0}{T_F} + \frac{C'_{F,0}K_F a r_0}{V T_F} + \frac{K_F\left(F'_{Y,\,F,lin,0} - C'_{F,0}\alpha_{F,0}\right)}{T_F} \right.$$

$$\left. + \frac{C'_{R,0}K_R\beta_0}{T_R} - \frac{C'_{R,0}K_R b r_0}{V T_R} + \frac{K_R\left(F'_{Y,\,R,lin,0} - C'_{R,0}\alpha_{R,0}\right)}{T_R} + \frac{mg - K_F - K_R}{h} \right)$$

$$+ \dot{\theta} \left(- \frac{C'_{F,0}D_F\delta_0}{T_F} + \frac{C'_{F,0}D_F\beta_0}{T_F} + \frac{C'_{F,0}D_F a r_0}{V T_F} + \frac{D_F\left(F'_{Y,\,F,lin,0} - C'_{F,0}\alpha_{F,0}\right)}{T_F} \right.$$

$$\left. + \frac{C'_{R,0}D_R\beta_0}{T_R} - \frac{C'_{R,0}D_R b r_0}{V T_R} + \frac{D_R\left(F'_{Y,\,R,lin,0} - C'_{R,0}\alpha_{R,0}\right)}{T_R} + \frac{-D_F - D_R}{h} \right)$$

$$+ \delta \left(-C_{F,0} + C'_{F,0}\Delta F_{Z,F,0} - \frac{C'_{F,0}K_F\theta_0}{T_F} - \frac{C'_{F,0}D_F\dot{\theta}_0}{T_F} - \frac{C'_{F,0}M_{ANTI-ROLL,\,ACT,F_0}}{T_F} \right)$$

$$+ M_{ANTI-ROLL,\,ACT,F} \left(- \frac{C'_{F,0}\delta_0}{T_F} + \frac{C'_{F,0}\beta_0}{T_F} + \frac{C'_{F,0} a r_0}{V T_F} + \frac{\left(F'_{Y,\,F,lin,0} - C'_{F,0}\alpha_{F,0}\right)}{T_F} \right.$$

$$\left. - \frac{1}{h} \right) + M_{ANTI-ROLL,\,ACT,R} \left(\frac{C'_{R,0}\beta_0}{T_R} - \frac{C'_{R,0} b r_0}{V T_R} + \frac{\left(F'_{Y,\,r,lin,0} - C'_{R,0}\alpha_{F,0}\right)}{T_R} - \frac{1}{h} \right)$$

$$+ const_F + const_R \Bigg]$$

By considering the state-space form of the system, defined in paragraph 5.4.1, the inputs of the system are the steering angle, δ, the active anti-roll moment on the front axle, $M_{ANTI-ROLL,\,ACT,F}$, the active anti-roll moment on the rear axle, $M_{ANTI-ROLL,\,ACT,R}$ and the external yaw moment caused by a torque-vectoring system, $M_{Z,ext}$. The state variables are the sideslip angle of the vehicle, β, the yaw rate, r, the roll angle, θ and the roll rate, $\dot{\theta}$. The vectors $\boldsymbol{x(t)}$ and $\boldsymbol{u(t)}$ are defined as:

$$\boldsymbol{x(t)} = \begin{pmatrix} \beta \\ r \\ \theta \\ \dot{\theta} \end{pmatrix}$$

$$\boldsymbol{u(t)} = \begin{pmatrix} \delta \\ M_{ANTI-ROLL,ACT,F} \\ M_{ANTI-ROLL,ACT,R} \\ M_{Z,ext} \end{pmatrix}$$

5.4.4 Further analysis on tyre

Further analysis on tyre behaviour are carried out to parameterize the single-track vehicle model. It is presented a method for the derivation of the numerical values of the parameters to be used in the single-track vehicle model.

In Figure 5.11, it is possible to note the front lateral tyre force as a function of slip angle for different values of vertical load and the behaviour makes sense: there is an increase of cornering stiffness when the vertical load increases to a certain extent when there is a saturation of the tyre. There is the minus sine because, according to the sign conventions, used in the model there is a positive slip angle produces a negative lateral tyre force.

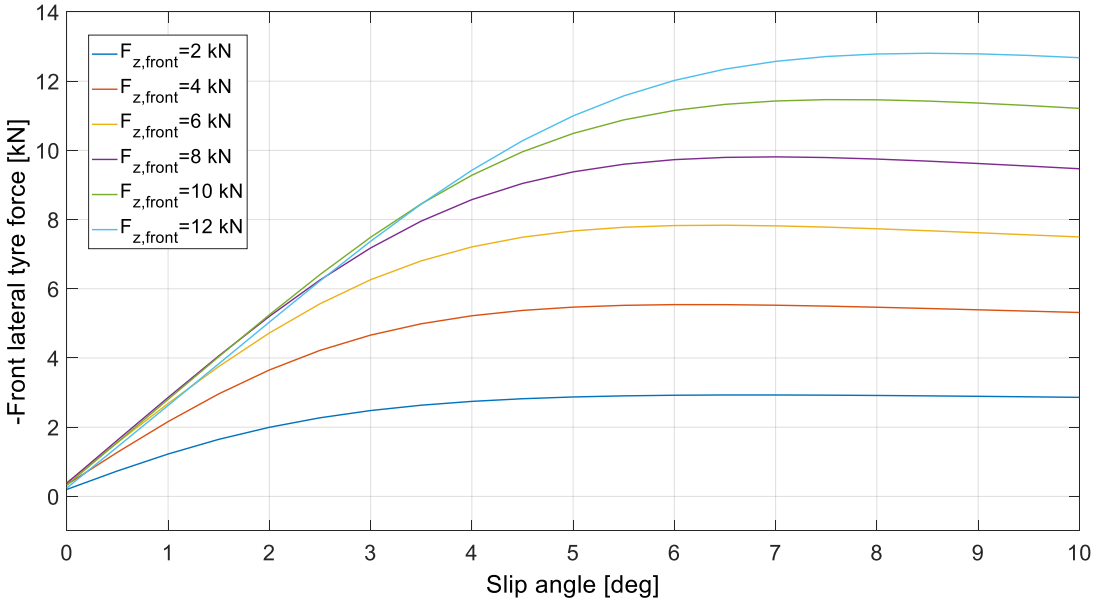

Figure 5.11: Lateral force on the front tyre as a function of slip angle for different values of vertical load

The Figure 5.12 is the plot of cornering stiffness of an individual tyre as a function of vertical load on a tyre and for different values of slip angles: essentially the cornering

stiffness is normally an increasing function of vertical load except for the case of very large values of slip angles.

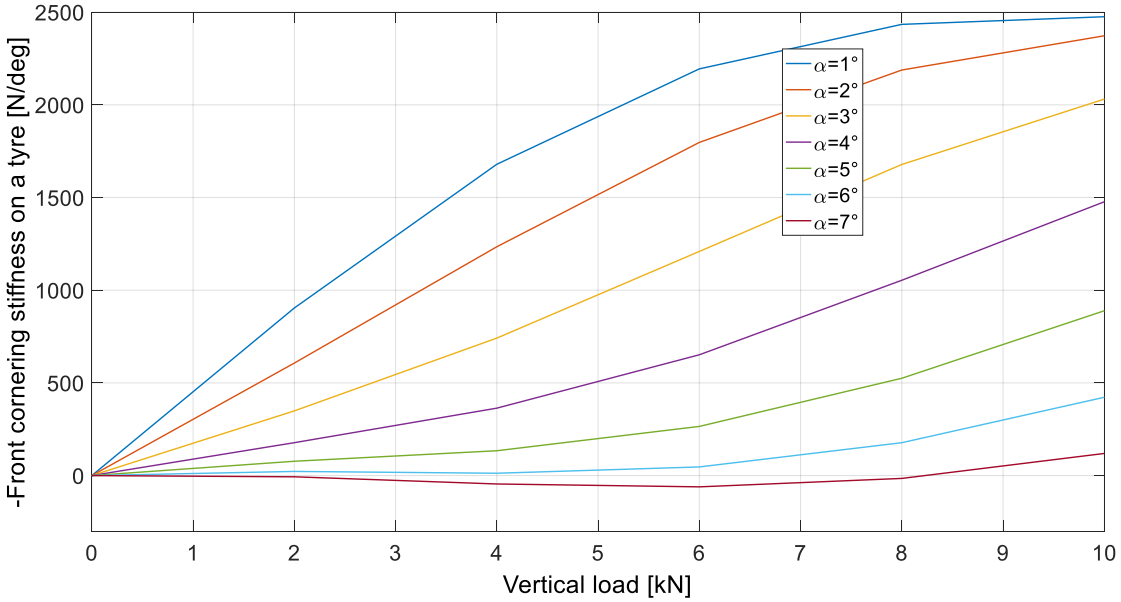

Figure 5.12: Cornering stiffness on the front tyre as a function of vertical load for different values of slip angle

By combing the characteristics of two front tyres, the Figure 5.13 shows a plot of the lateral force on the front axle as a function of slip angle on the front axle for different values of front load transfer: this characteristic is decreasing when the load transfer on the front axle is increased.

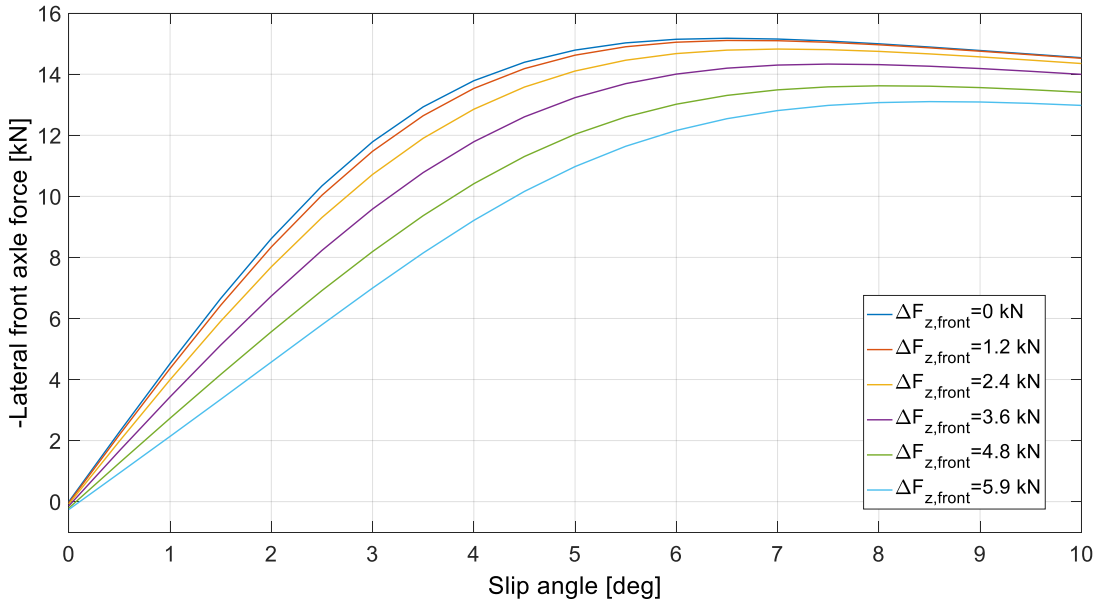

Figure 5.13: Lateral force on the front axle as a function of slip angle for different values of front load transfer function

In Figure 5.14, it is plotted the lateral force on the front axle as a function of load transfer and clearly it is possible to note that whatever is the slip angle, there is a decrease of this lateral force characteristic.

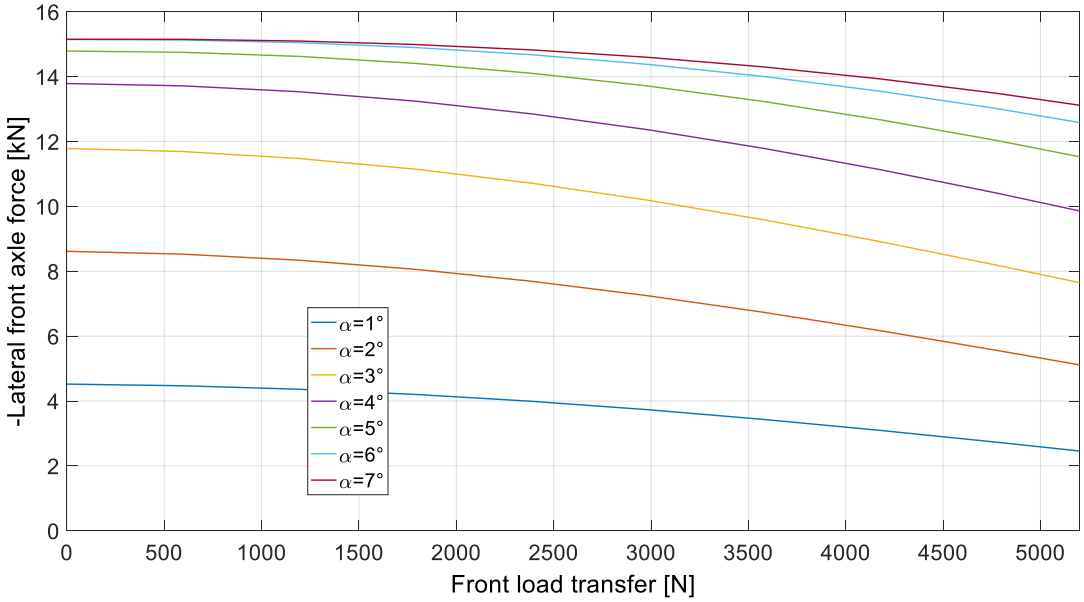

Figure 5.14: Lateral force on the front axle as a function of load transfer for different values of slip angle

In Figure 5.15, it is represented the lateral force gradient on the front axle, that is the variation of the lateral force with respect to the load transfer caused by the lateral acceleration: this gradient tells how much the lateral force on the axle is reduced in absolute value because of the effect on the load transfer on the axle, which is the parameter included in the single- track vehicle model.

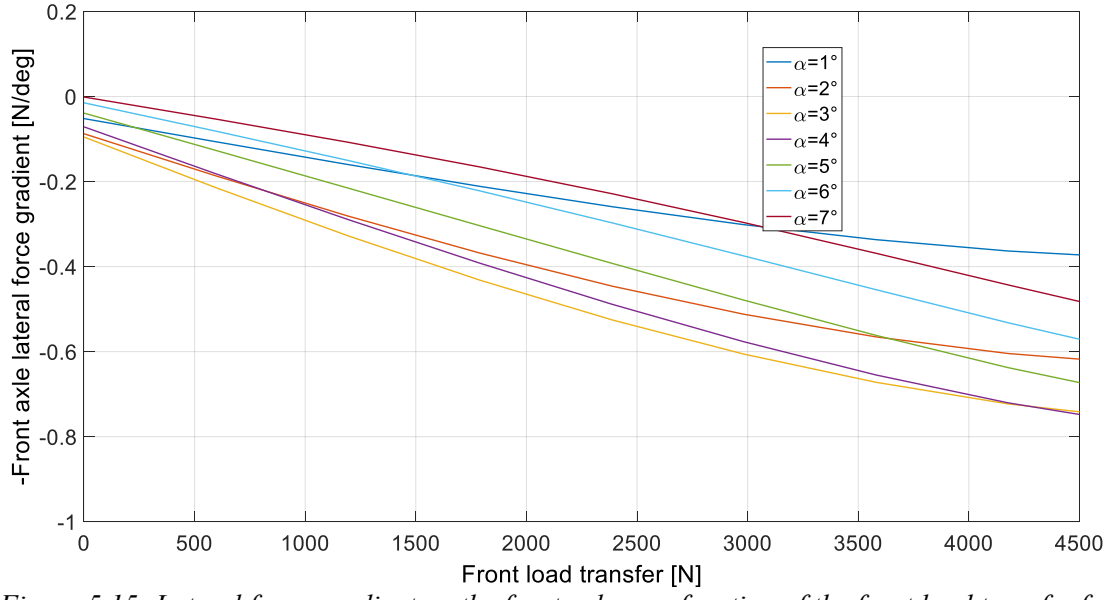

Figure 5.15: Lateral force gradient on the front axle as a function of the front load transfer for different values of slip angle

In Figure 5.16, there is the plot of cornering stiffness as a function of load transfer for different values of slip angle.

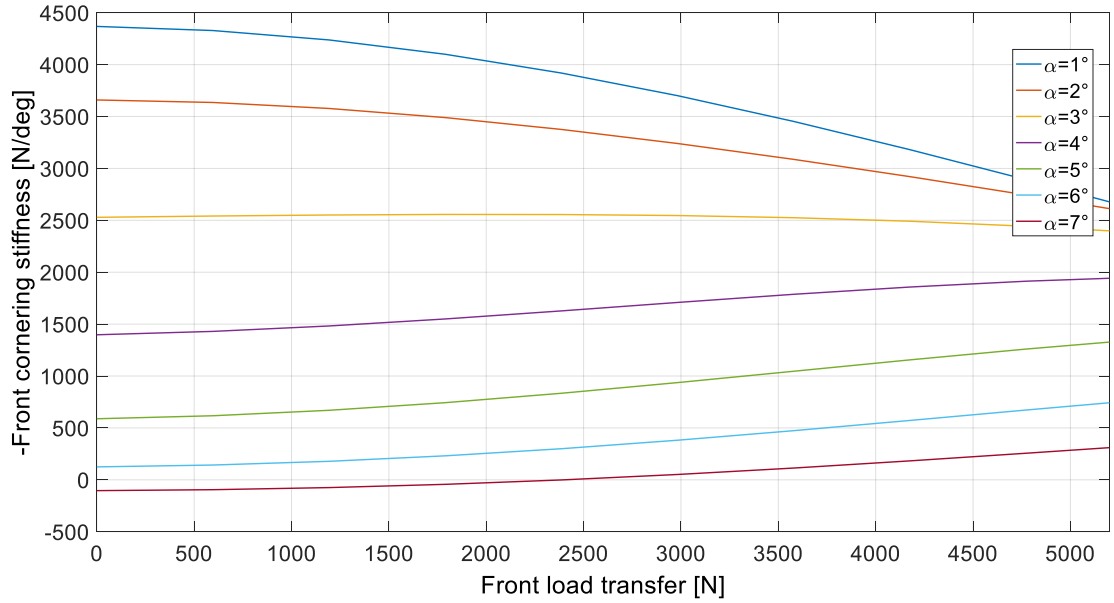

Figure 5.16: Cornering stiffness on the front axle as a function of front load transfer for different values of slip angle

It is interesting to observe that the cornering stiffness in absolute value decreases with the load transfer as expected from the textbooks for small values of slip angle, but for the specific tyres for high values of slip angles the cornering stiffness on the axle is actually increased with the front load transfer. However, the total lateral force on the axle decreases with the load transfer because of the effect of the variation of linearization point that is included in the single-track model formulation.

In Figure 5.17 there is the cornering stiffness gradient on the front axle, that is the variation of the cornering stiffness per unit variation of the lateral load transfer on the front axle.

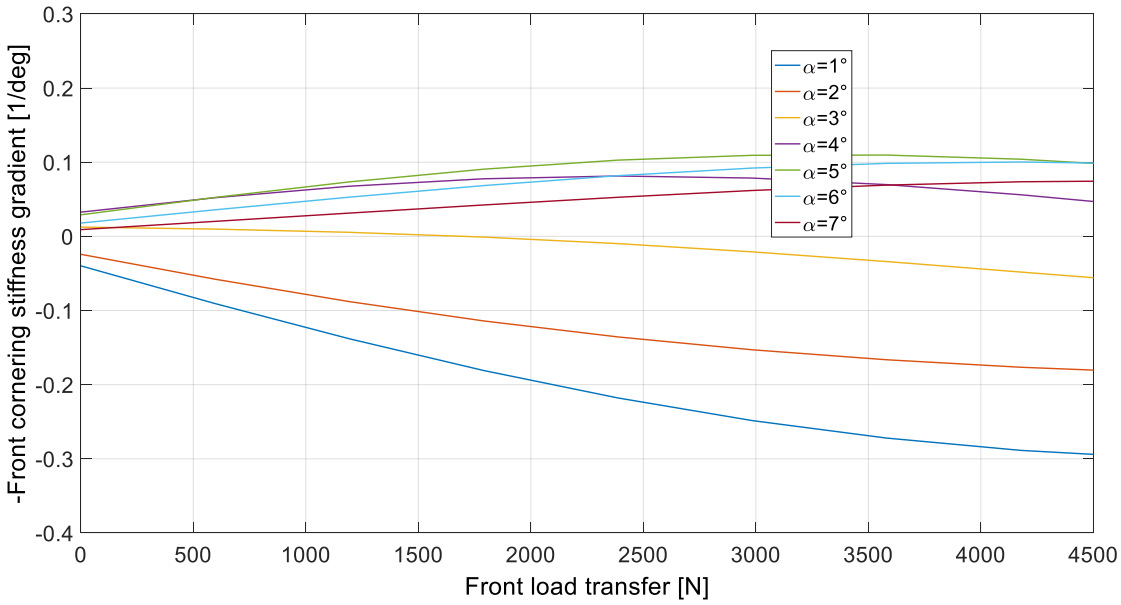

Figure 5.17: Cornering stiffness gradient on the front axle as a function of front load transfer for different values of slip angle

Similar results are reached for the rear tyre, of with results are not reported in this thesis.

By using the same data included in the Simulink file of the non-linear model, the results reached by the MATLAB File of the quasi static model are used, in-order-to parameterize the single-track vehicle model.

For the parametrization three lateral acceleration values of interest are considered: a first set of values included on the top part of the table are produced by the quasi-static model, with the reference understeer characteristic, and the respect lateral accelerations.

By using the tyre-tool, it is possible to calculate the tyre related parameters for the linearized single the track vehicle model, shown in Table 5.2: these values are the nominal value of the cornering stiffness on the front and rear axle, the cornering stiffness gradients and the lateral force gradients on the front axle and rear axle.

It is possible to observe that whilst the lateral force gradients are always negative for the three values of lateral acceleration, which means that the lateral force is a decreasing function of the lateral load transfer on the axle, the cornering stiffness gradient changes sign when different lateral accelerations are considered. In particular, for low and medium lateral accelerations and slip angles, the cornering stiffness gradient is positive but since, according to the signs conventions used the cornering stiffness is negative, the absolute value of cornering stiffness is a decreasing function of the load transfer. For high values of

lateral acceleration, because of this peculiar tyre behaviour, the cornering stiffness gradient is negative which means the cornering stiffness is, in absolute value, an increasing function of lateral load transfer.

$a_y = 3\ {}^{m}/_{s^2}$	$a_y = 6\ {}^{m}/_{s^2}$	$a_y = 9\ {}^{m}/_{s^2}$
$F_{Y,F,lin,0} = 3729.8\ N$	$F_{Y,F,lin,0} = 7397.3\ N$	$F_{Y,F,lin,0} = 11079.0\ N$
$F_{Y,rR,lin,0} = 3829\ N$	$F_{Y,rR,lin,0} = 7717.6\ N$	$F_{Y,rR,lin,0} = 11702.0\ N$
$\alpha_{F,0} = 0.83°$	$\alpha_{F,0} = 1.86°$	$\alpha_{F,0} = 3.76°$
$\alpha_{R,0} = 0.53°$	$\alpha_{R,0} = 1.27°$	$\alpha_{R,0} = 2.73°$
$\Delta F_{Z,F,0} = 1166.4\ N$	$\Delta F_{Z,F,0} = 2411.9\ N$	$\Delta F_{Z,F,0} = 3808.5\ N$
$\Delta F_{Z,R,0} = 1888.9\ N$	$\Delta F_{Z,R,0} = 3694.8\ N$	$\Delta F_{Z,R,0} = 5390.4\ N$
$\theta_0 = 1.89$	$\theta_0 = 3.77$	$\theta_0 = 5.79$
$r_0 = 6.19\ {}^{°}/_{s}$	$r_0 = 12.33\ {}^{°}/_{s}$	$r_0 = 18.6\ {}^{°}/_{s}$
$\beta_0 = 0.22\,°$	$\beta_0 = 0.65\,°$	$\beta_0 = 1.8\,°$
$M_{ANTI-ROLL,ACT,F,0} = 1133.3\ Nm$	$M_{ANTI-ROLL,ACT,F,0} = 2412.5\ Nm$	$M_{ANTI-ROLL,ACT,F,0} = 3938.6\ Nm$
$M_{ANTI-ROLL,ACT,R,0} = 2448.2\ Nm$	$M_{ANTI-ROLL,ACT,R,0} = 4738.4\ Nm$	$M_{ANTI-ROLL,ACT,R,0} = 6815.5\ Nm$
$\delta_0 = 0.95\,°$	$\delta_0 = 1.9\,°$	$\delta_0 = 3\,°$
$C_{F,0} = -4349.4\ {}^{N}/_{°}$	$C_{F,0} = -3560.7\ {}^{N}/_{°}$	$C_{F,0} = -2035.2\ {}^{N}/_{°}$
$C'_{F,0} = 0.14\ {}^{1}/_{°}$	$C'_{F,0} = 0.25\ {}^{1}/_{°}$	$C'_{F,0} = -0.081\ {}^{1}/_{°}$
$C_{R,0} = -6650.5\ {}^{N}/_{°}$	$C_{R,0} = -5236.1\ {}^{N}/_{°}$	$C_{R,0} = -3254.1\ {}^{N}/_{°}$
$C'_{R,0} = 0.42\ {}^{1}/_{°}$	$C'_{R,0} = 0.47\ {}^{1}/_{°}$	$C'_{R,0} = -0.063\ {}^{1}/_{°}$
$F'_{Y,F,lin,0} = -0.15$	$F'_{Y,F,lin,0} = -0.71$	$F'_{Y,F,lin,0} = -1.1$
$F'_{Y,R,lin,0} = -0.25$	$F'_{Y,R,lin,0} = -0.87$	$F'_{Y,R,lin,0} = -1.4$
$f_0 = 0.32$	$f_0 = 0.34$	$f_0 = 0.37$

Table 5.2: Parameter values from the-quasi static model and tyre analysis (active vehicle)

5.5 Results with updated single-track vehicle model

In this paragraph it is possible to have a look of the open-loop response with a linearized single-track vehicle model included the yaw rate and the roll dynamic of the vehicle.

In Figure 5.18, the frequency response of yaw rate over the steering angle is reported for $a_y = 3\,{}^{m}/_{s^2}$ and $V = 100\ {}^{km}/_{h}$. This plot helps to understand which the impact of this novel formulation of the single-track vehicle model is: the case with no contributions refers to the standard single-track vehicle model whilst the case with cornering stiffness and lateral force gradient contributions is the complete model; there are other two cases where it is considered only the lateral force gradient contribution and only the cornering stiffness gradient contribution. For this first analysis, it is possible to note that the impact is not substantial because all the lines are really close among them.

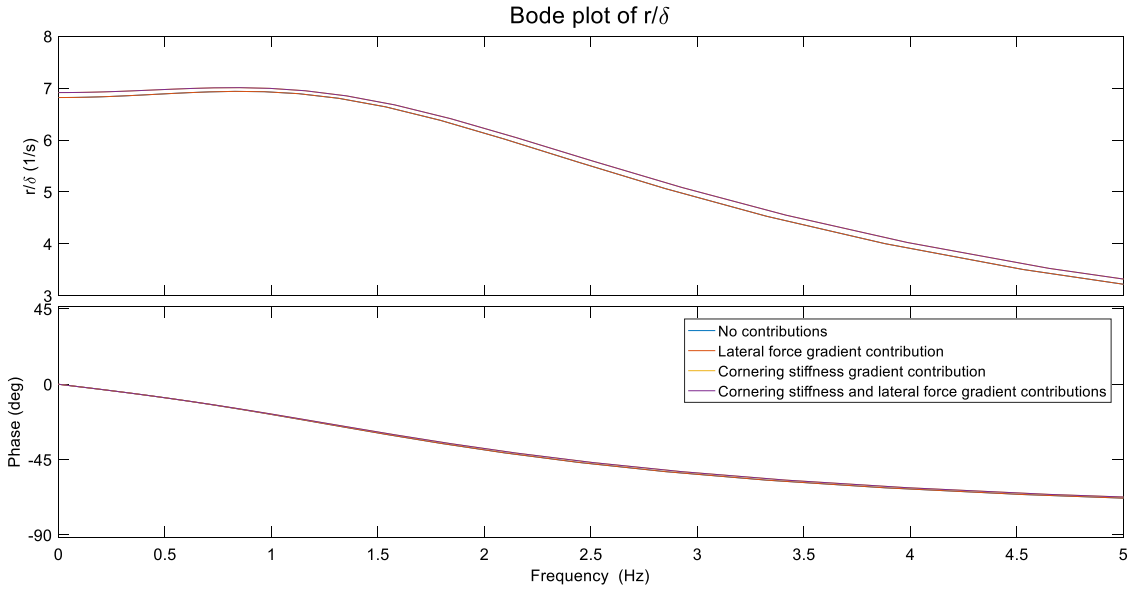

Figure 5.18: Frequency response of yaw rate over delta for $a_y = 3\,{}^{m}/_{s^2}$ *and* $V = 100\ {}^{km}/_{h}$

The actual power of this new formulation is that allows to consider the effect of the anti-roll moment from the actuation system on the front axle on the yaw rate response on the vehicle; the bode diagram, in Figure 5.19, represents the yaw rate over the anti-roll moment imposed by the front suspension system and again here there are considered different cases.

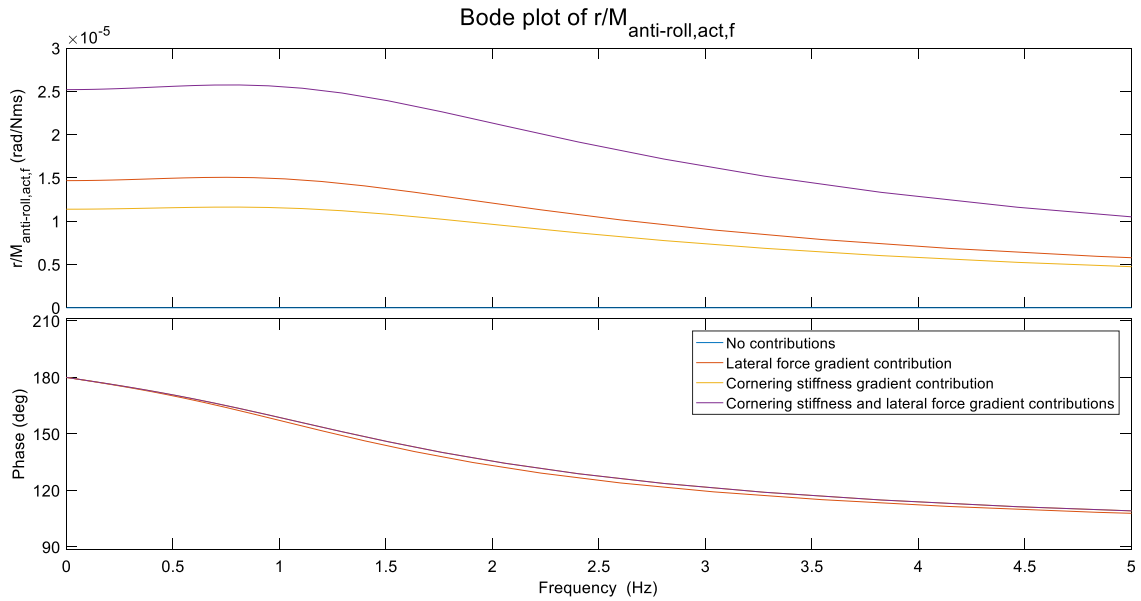

Figure 5.19: Frequency response of yaw rate over front active anti-roll moment at at $a_y = 6\,{}^{m}/_{s^2}$ *and V = 100* ${}^{km}/_{h}$

The case with no contributions, which corresponds to the standard single-track model, is characterized by zero gain because in a conventional model, the anti-roll moment doesn't have any effect on the yaw rate response on the vehicle. It is possible to see the impact of the yaw rate response of the vehicle of the front anti-roll moment and the impact of the variation of the cornering stiffness that corresponds to the orange line in the plot. The contribution of lateral force gradient contribution corresponds to the red line whilst the violet line refers to the single-track vehicle model with both the variation of the cornering stiffness and lateral forces on the linearization point.

The initial value of phase angle is 180 degrees, because as expected, if in steady state condition the anti-roll moment on the front axle increases the vehicle is more understeering than and so a decrease yaw rate of the vehicle. The yaw rate variation is negative when there is an increasement of the anti-roll moment on the front axle.

In Figure 5.20, it is showed the bode diagram of the yaw rate over the anti-roll moment on the actuation system on the rear axle; in this case the phase angle starts from zero because if the load transfer on the rear axle increases the vehicle becomes less understeering and it has a higher yaw rate.

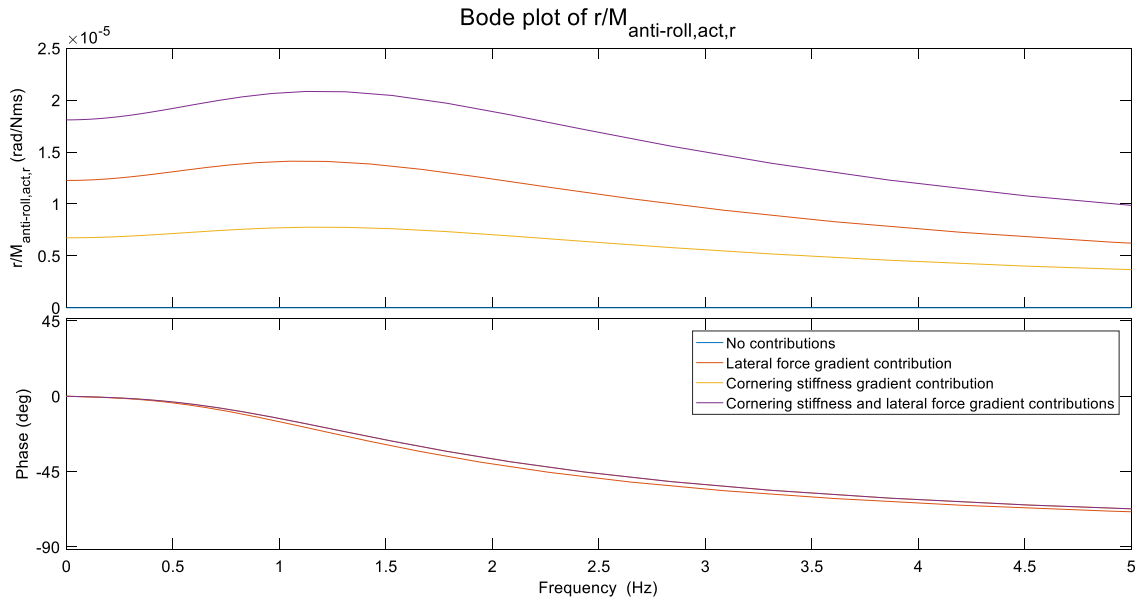

Figure 5.20: Frequency response of yaw rate over rear anti-roll moment at $a_y = 6\,{}^{m}/_{s^2}$ *and V = 100* ${}^{km}/_{h}$

Some kind of analyses are computed, for example for $a_y = 9\ {}^{m}/_{s^2}$: in Figure 5.21 it is showed the diagram of the yaw rate over the anti-roll moment on the front axle.

In this plot it is possible to see that the cornering stiffness increases with the load transfer and in fact the phase angle starts from zero in the frequency response but, because of the effect of the lateral force gradient, there is a reduction of the steady state value of the yaw rate. In fact, the red characteristic, that corresponds to only the lateral force gradient contribution, starts from a phase angle of 180 degree and by considering the two contributions together, the effect of the lateral force gradient is the prevalent one.

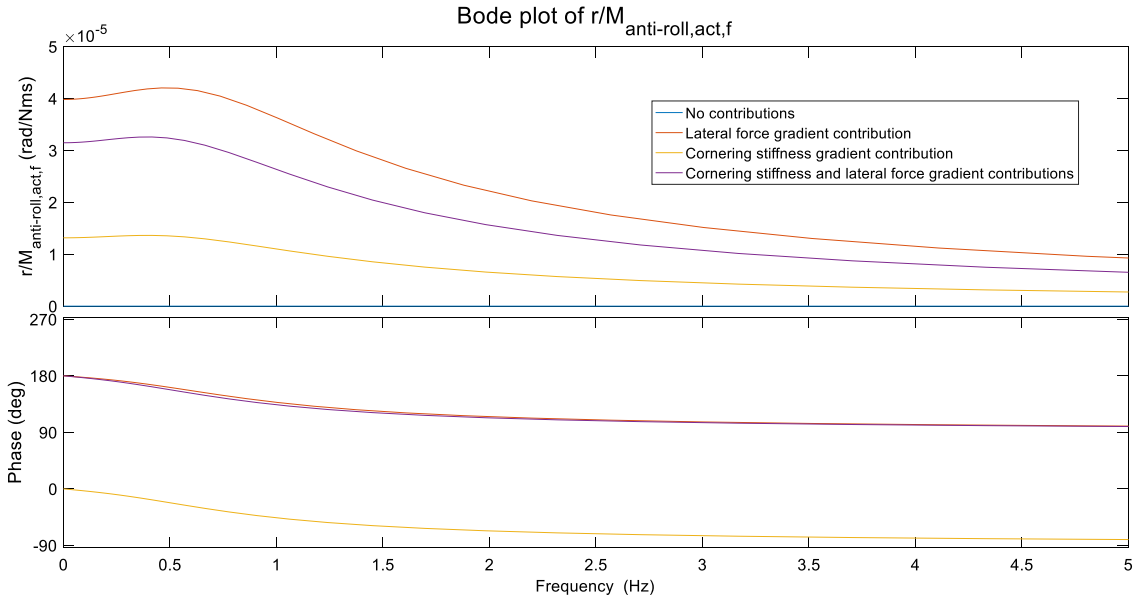

Figure 5.21: Frequency response of yaw rate over front anti-roll moment at $a_y = 9\,{}^{m}/_{s^2}$ *and* $V = 100\,{}^{km}/_{h}$

For the bode diagram of the yaw rate over rear anti-roll moment, in Figure 5.22, the cornering stiffness gradient contribution, since there is an increase of the cornering stiffness on the axle with the load transfer, would tend to reduce the yaw rate but on the other hand the lateral force gradient contribution provokes an increasement of the yaw rate; the second effect is prevalent over the first one, so the result characteristic is the violet one.

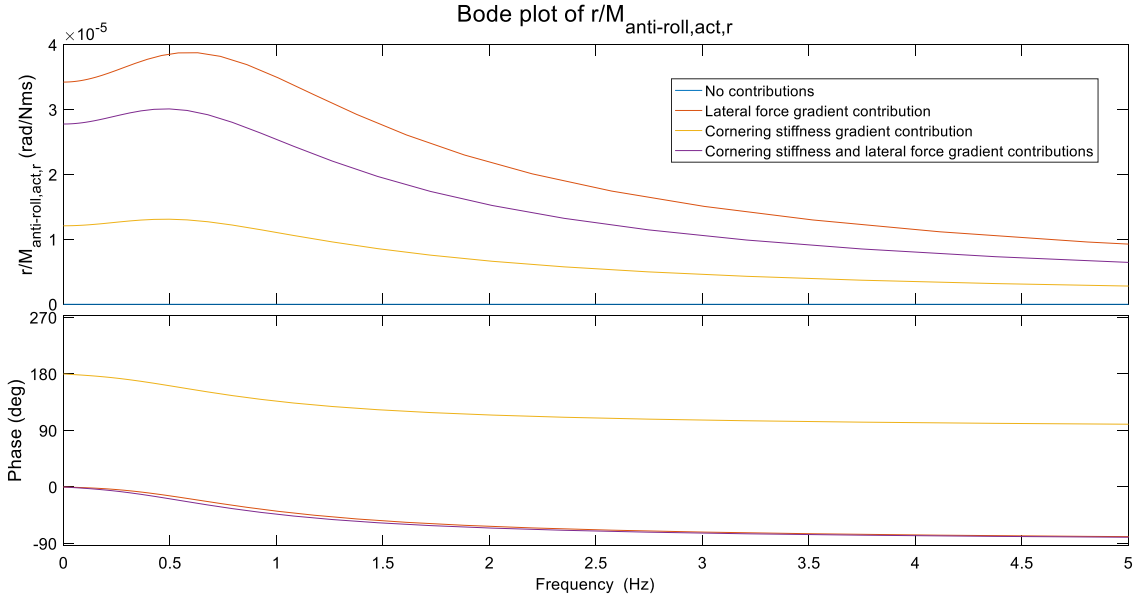

Figure 5.22: Frequency response of yaw rate over rear anti-roll moment at $a_y = 9\,{}^{m}/_{s^2}$ *and* $V = 100\,{}^{km}/_{h}$

After these checks, several diagrams are plotted as with the complete model for different values of speed of the vehicle. In Figure 5.23, for example, there is the frequency response of the yaw rate over front anti-roll moment for $a_y = 3\,{}^{m}/_{s^2}$: as expected if a M_F increases, r decreases according to the front-to-total roll stiffness distribution control strategy and vice versa for the rear axle.

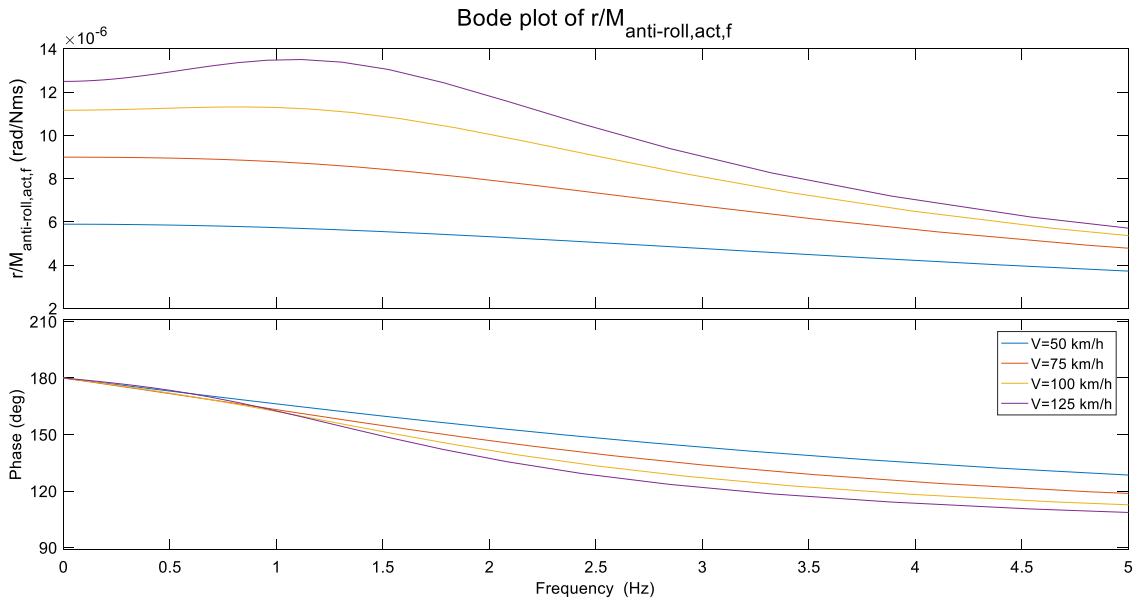

Figure 5.23: Frequency response of yaw rate over front-anti roll moment at $a_y = 3\,{}^{m}/_{s^2}$ *and different vehicle speeds*

As a term of comparison, in the single-track vehicle model an external yaw moment is included as input, such that in the plot of Figure 5.24 the frequency response of the yaw rate over the external yaw moment is represented. It is interesting to observe the steady state values of the gains caused by an external yaw moment with respect to the steady state values of the gains caused by an external anti-roll moment caused by the suspension system to understand the relative effectiveness of using the front-to-total roll distribution control in order to control the yaw rate of the vehicle rather than a torque vectoring controller.

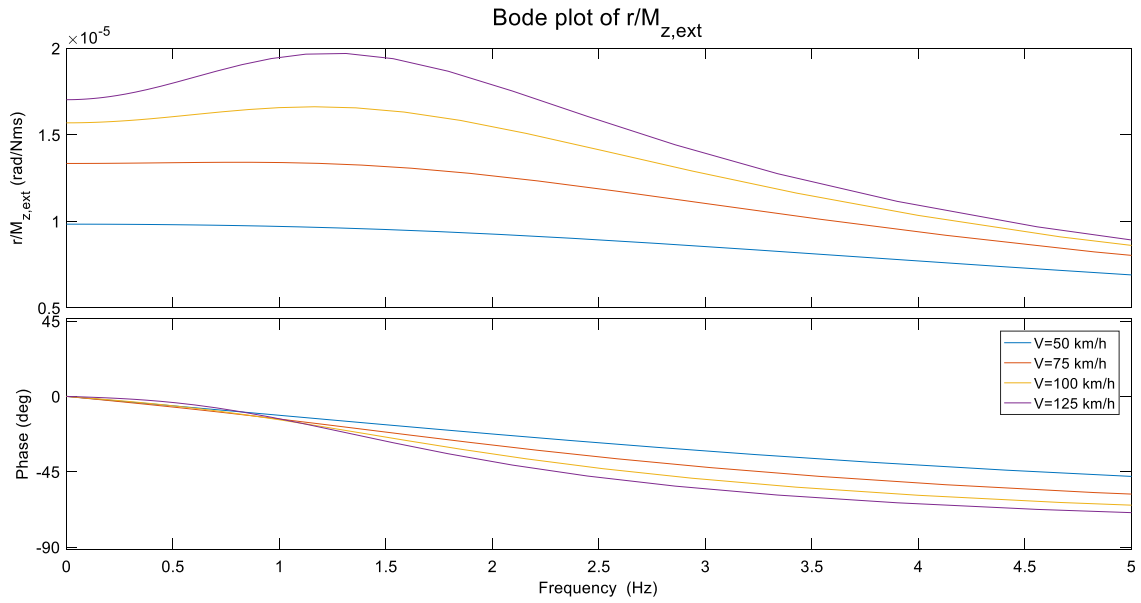

Figure 5.24: Frequency response of yaw rate over external yaw moment at moment at $a_y = 3\,{}^{m}/_{s^2}$ *and different vehicle speeds*

All the analyses are carry out for all the values of lateral acceleration involved not all showed in this thesis.

In Table 5.3 the values of the steady state gains of the transfer functions for each lateral acceleration and different speeds are showed: for example, ${}^{r}/_{M_z}$ is the steady state value of the yaw rate gain when a torque vectoring control is applied, and it means there is variation of 0.9 over 10^{-5} ${}^{rad}/_{s}$ when 1 Nm of external yaw moment is applied. These steady state values are compared with the gains of r over M_F and M_R: for example, at $V = 50$ ${}^{km}/_{h}$ and $a_y = 3\,{}^{m}/_{s^2}$ one Nm of direct yaw moment is 50% more effective to generate a yaw rate variation than a variation of anti-roll moment.

By considering another situation, for example $a_y = 6\,{}^{m}/_{s^2}$ and for each speed involved, 1 Nm of anti-roll moment can even have a larger effect than 1 Nm of direct yaw moment. This analysis is interesting to understand the effectiveness of torque vectoring control and of front-to-total roll stiffness distribution control in order to tune vehicle response.

$a_y = 3\,{}^{m}/_{s^2}$	$a_y = 6\,{}^{m}/_{s^2}$	$a_y = 9\,{}^{m}/_{s^2}$
$V = 50\ {}^{km}/_{h}$	$V = 50\,{}^{km}/_{h}$	$V = 50\ {}^{km}/_{h}$
$\frac{r}{M_{Z,ext}}(j\omega = 0) = 0.9 * 10^{-5}\ {}^{rad}/_{Nms}$ $\frac{r}{M_{Z,ext}}(j\omega = 0) = 0.6 * 10^{-5}\ {}^{rad}/_{Nms}$ $\frac{r}{M_{Z,ext}}(j\omega = 0) = 0.5 * 10^{-5}\ {}^{rad}/_{Nms}$	$\frac{r}{M_{Z,ext}}(j\omega = 0) = 1.2 * 10^{-5}\ {}^{rad}/_{Nms}$ $\frac{r}{M_{Z,ext}}(j\omega = 0) = 1.4 * 10^{-5}\ {}^{rad}/_{Nms}$ $\frac{r}{M_{Z,ext}}(j\omega = 0) = 1.3 * 10^{-5}\ {}^{rad}/_{Nms}$	$\frac{r}{M_{Z,ext}}(j\omega = 0) = 2.5 * 10^{-5}\ {}^{rad}/_{Nms}$ $\frac{r}{M_{Z,ext}}(j\omega = 0) = 2.1 * 10^{-5}\ {}^{rad}/_{Nms}$ $\frac{r}{M_{Z,ext}}(j\omega = 0) = 1.4 * 10^{-5}\ {}^{rad}/_{Nms}$
$V = 75\ {}^{km}/_{h}$	$V = 75\ {}^{km}/_{h}$	$V = 75\ {}^{km}/_{h}$
$\frac{r}{M_{Z,ext}}(j\omega = 0) = 1.3 * 10^{-5}\ {}^{rad}/_{Nms}$ $\frac{r}{M_{Z,ext}}(j\omega = 0) = 0.9 * 10^{-5}\ {}^{rad}/_{Nms}$ $\frac{r}{M_{Z,ext}}(j\omega = 0) = 0.5 * 10^{-5}\ {}^{rad}/_{Nms}$	$\frac{r}{M_{Z,ext}}(j\omega = 0) = 1.6 * 10^{-5}\ {}^{rad}/_{Nms}$ $\frac{r}{M_{Z,ext}}(j\omega = 0) = 2 * 10^{-5}\ {}^{rad}/_{Nms}$ $\frac{r}{M_{Z,ext}}(j\omega = 0) = 1.6 * 10^{-5}\ {}^{rad}/_{Nms}$	$\frac{r}{M_{Z,ext}}(j\omega = 0) = 3.5 * 10^{-5}\ {}^{rad}/_{Nms}$ $\frac{r}{M_{Z,ext}}(j\omega = 0) = 2.7 * 10^{-5}\ {}^{rad}/_{Nms}$ $\frac{r}{M_{Z,ext}}(j\omega = 0) = 2.2 * 10^{-5}\ {}^{rad}/_{Nms}$
$V = 100\ {}^{km}/_{h}$	$V = 100\ {}^{km}/_{h}$	$V = 100\ {}^{km}/_{h}$
$\frac{r}{M_{Z,ext}}(j\omega = 0) = 1.6 * 10^{-5}$ $\frac{r}{M_{Z,ext}}(j\omega = 0) = 1.1 * 10^{-5}$ $\frac{r}{M_{Z,ext}}(j\omega = 0) = 0.6 * 10^{-5}$	$\frac{r}{M_{Z,ext}}(j\omega = 0) = 1.9 * 10^{-5}\ {}^{rad}/_{Nms}$ $\frac{r}{M_{Z,ext}}(j\omega = 0) = 2.5 * 10^{-5}\ {}^{rad}/_{Nms}$ $\frac{r}{M_{Z,ext}}(j\omega = 0) = 1.8 * 10^{-5}\ {}^{rad}/_{Nms}$	$\frac{r}{M_{Z,ext}}(j\omega = 0) = 4.1 * 10^{-5}\ {}^{rad}/_{Nms}$ $\frac{r}{M_{Z,ext}}(j\omega = 0) = 3.2 * 10^{-5}\ {}^{rad}/_{Nms}$ $\frac{r}{M_{Z,ext}}(j\omega = 0) = 2.8 * 10^{-5}\ {}^{rad}/_{Nms}$
$V = 125\ {}^{km}/_{h}$	$V = 125\ {}^{km}/_{h}$	$V = 125\ {}^{km}/_{h}$
$\frac{r}{M_{Z,ext}}(j\omega = 0) = 1.7 * 10^{-5}\ {}^{rad}/_{Nms}$ $\frac{r}{M_{Z,ext}}(j\omega = 0) = 1.3 * 10^{-5}\ {}^{rad}/_{Nms}$ $\frac{r}{M_{Z,ext}}(j\omega = 0) = 0.6 * 10^{-5}\ {}^{rad}/_{Nms}$	$\frac{r}{M_{Z,ext}}(j\omega = 0) = 2.1 * 10^{-5}\ {}^{rad}/_{Nms}$ $\frac{r}{M_{Z,ext}}(j\omega = 0) = 2.8 * 10^{-5}\ {}^{rad}/_{Nms}$ $\frac{r}{M_{Z,ext}}(j\omega = 0) = 1.9 * 10^{-5}\ {}^{rad}/_{Nms}$	$\frac{r}{M_{Z,ext}}(j\omega = 0) = 4.6 * 10^{-5}\ {}^{rad}/_{Nms}$ $\frac{r}{M_{Z,ext}}(j\omega = 0) = 3.4 * 10^{-5}\ {}^{rad}/_{Nms}$ $\frac{r}{M_{Z,ext}}(j\omega = 0) = 3.2 * 10^{-5}\ {}^{rad}/_{Nms}$

Table 5.3: Values of the steady-state gain for four different speeds

CHAPTER 6

6.1 Introduction

In this chapter, at first, it is considered the vehicle with active suspension controller, but without the front to total roll stiffness distribution controller. So, it is taken a constant value of f which is the front to total roll stiffness distribution.

In the active vehicle they are considered the feedback and feedforward contributions of the controller that modify f in the time domain. The system is not-linear, and it is carried out a further linearization in order to sort out this system for a frequency domain analysis of the controller.

After the linearization in order to include the front-to-total roll stiffness distribution control with variable front-to-total distribution, the controller is designed and verified in frequency domain.

6.2 Active vehicle without front-to-total roll stiffness distribution controller

The system showed in Figure 6.1 receives as input the parameter f, which is the output of the controller and it used to calculate the stiffness contribution of the anti-roll moment of the active suspension system. This control structure emulates the active suspension that provides a constant passive damping, a linear behaviour in terms of anti-roll moment as a function of roll angle; then there is f, the parameter between 0 and 1, that decides how much anti-roll moment is on the front and rear axle.

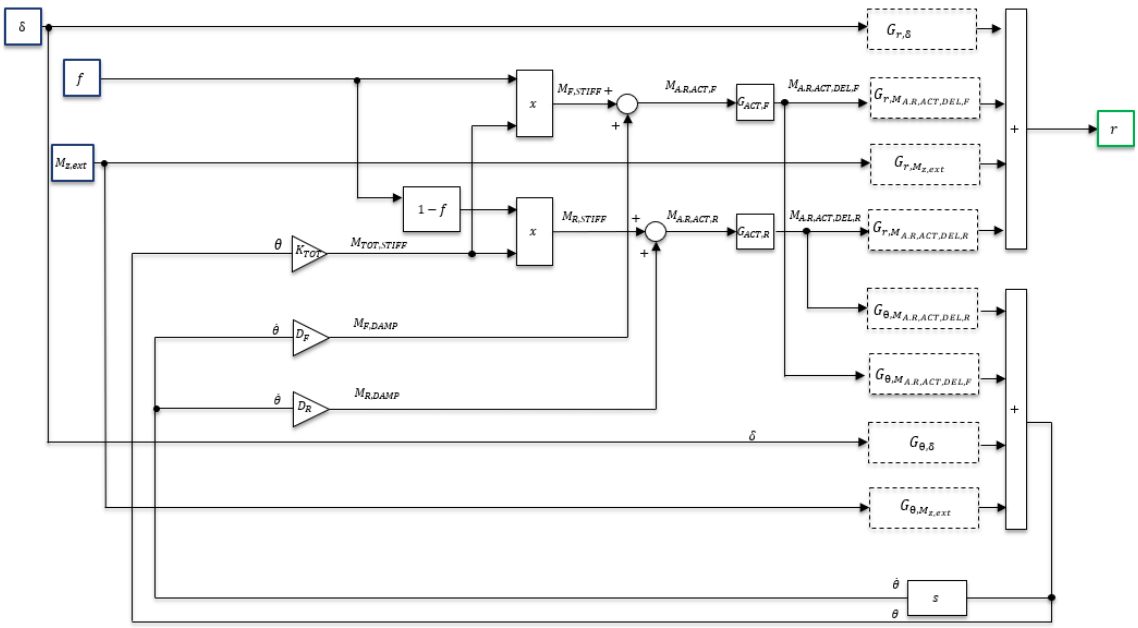

Figure 6.1: Simpifed scheme of the active vehicle without the variation of f

6.2.1 Linearization of the active system and calculation of the transfer functions

From the above control structure, it is possible to obtain and solve equations of r and θ and to linearize the equation of the anti-roll moment on the front and rear axles. The equation of r and θ are given by:

$$r = G_{r,\delta}\delta + G_{r,M_{z,ext}}M_{z,ext} + G_I\, M_{ANTI-ROLL,ACT,F} + G_{II}\, M_{ANTI-ROLL,ACT,R}$$

$$\theta = G_{\theta,\delta}\delta + G_{\theta,M_{z,ext}}M_{z,ext} + G_{III}\, M_{A.NTI-ROLL,ACT,F} + G_{IV} M_{ANTI-ROLL,ACT,R}$$

The anti-roll moment, due to the active suspension on the front axle, is given by the stiffness contribution that is a function of f plus a damping contribution and for the rear axle the anti-roll moment is related to the roll stiffness contribution multiplied by the complement of 1 of the roll stiffness distribution on the front axle plus the damping contribution on the rear axle. Their expressions are:

$$M_{A.NTI-ROLL,ACT,F} = K_{tot}\theta f + D_f\dot{\theta}$$

$$M_{A.NTI-ROLL,ACT,R} = K_{tot}\theta(1-f) + D_r\dot{\theta}$$

It is carried out the linearization to have the linearized formulation of the anti-roll moment on the front and rear axles as a function of the control input f. It results as:

$$f\theta \approx f_0\theta_0 + \frac{\partial(f\theta)}{\partial\theta}(f_0\theta_0)(\theta - \theta_0) + \frac{\partial(f\theta)}{\partial f}(f_0\theta_0)(f - f_0)$$

$$f\theta \approx f_0\theta_0 + f_0(\theta - \theta_0) + \theta_0(f - f_0)$$

$$f\theta \approx f\theta_0 + \theta f_0 - \theta_0 f_0$$

As consequence the linearized anti-roll moments are given by:

$$M_{A.NTI-ROLL,ACT,F} \approx K_{tot}\left(f\theta_0 + \theta f_0 - \theta_0 f_0\right) + D_f\dot{\theta}$$

$$M_{A.NTI-ROLL,ACT,R} \approx K_{tot}\theta - K_{tot}(f\theta_0 + \theta f_0 - \theta_0 f_0) + D_r\dot{\theta}$$

All the equations are combined to have the equations in the Laplace domains of the yaw rate of the car, r, and the roll angle, θ, as a function of steering angle, δ, as a functional by a potential yaw moment, $M_{Z,ext}$, caused by a torque vectoring and as a function of the two anti-roll moments that on their side are functions of f. The two main equations computed are:

$$r = G_{r,\delta}\delta + G_{r,M_{Z,ext}}M_{Z,ext} + G_I\left[K_{tot}(f\theta_0 + \theta f_0 - \theta_0 f_0) + D_f\dot{\theta}\right] + G_{II}\left[K_{tot}\theta - K_{tot}(f\theta_0 + \theta f_0 - \theta_0 f_0) + D_r\dot{\theta}\right]$$

$$\theta = G_{\theta,\delta}\delta + G_{\theta,M_{Z,ext}}M_{Z,ext} + G_{III}\left[K_{tot}(f\theta_0 + \theta f_0 - \theta_0 f_0) + D_f\dot{\theta}\right] + G_{IV}\left[K_{tot}\theta - K_{tot}(f\theta_0 + \theta f_0 - \theta_0 f_0) + D_r\dot{\theta}\right]$$

All the calculations are carried out to get the final expressions of the transfer functions including all the contributions, for example the actuation delays of the actuators given by the transfer functions $G_{ACT,F}$ and $G_{ACT,R}$.

At the end the following transfer functions are obtained, by substituting the equation of θ in r: the roll angle versus steering angle, $\frac{\theta(s)}{\delta(s)}$, the yaw rate versus the roll angle, $\frac{r(s)}{\delta(s)}$, the yaw rate versus the external moment, $\frac{r(s)}{M_{z,ext}(s)}$, and what is essential for control system design the transfer function yaw rate of the car over the control output f, $\frac{r(s)}{f(s)}$.

$$\frac{\theta(s)}{\delta(s)} = \frac{G_{\theta,\delta}}{1 - \left\{K_{tot}[G_{IV} + f_0(G_{III} - G_{IV})] + s\left(D_f G_{III} + D_r G_{IV}\right)\right\}}$$

$$\frac{r(s)}{\delta(s)} = G_{r,\delta} + \frac{G_{\theta,\delta}\{K_{tot}[G_{II} + f_0(G_I - G_{II})] + s(D_f G_I + D_r G_{II})\}}{1 - \{K_{tot}[G_{IV} + f_0(G_{III} - G_{IV})] + s(D_f G_{III} + D_r G_{IV})\}}$$

$$\frac{r(s)}{M_{z,ext}(s)} = G_{r,M_{z,ext}} + \frac{G_{\theta,M_{z,ext}}\{K_{tot}[G_{II} + f_0(G_I - G_{II})] + s(D_f G_I + D_r G_{II})\}}{1 - \{K_{tot}[G_{IV} + f_0(G_{III} - G_{IV})] + s(D_f G_{III} + D_f G_{IV})\}}$$

$$\frac{r(s)}{f(s)} = K_{tot}\theta_0(G_I - G_{II}) + \frac{K_{tot}\theta_0(G_{III} - G_{IV})\{K_{tot}[G_{II} + f_0(G_I - G_{II})] + s(D_f G_I + D_r G_{II})\}}{1 - \{K_{tot}[G_{IV} + f_0(G_{III} - G_{IV})] + s(D_f G_{III} + D_r G_{IV})\}}$$

Where

$$G_I = G_{r,M_{ANTI-ROLL,\,ACT,DEL,F}} G_{ACT,F}$$

$$G_{II} = G_{r,M_{ANTI-ROLL,\,ACT,DEL,R}} G_{ACT,R}$$

$$G_{III} = G_{\theta,M_{ANTI-ROLL,\,ACT,DEL,F}} G_{ACT,F}$$

$$G_{IV} = G_{\theta,M_{ANTI-ROLL,\,ACT,DEL,R}} G_{ACT,R}$$

6.2.2 Bode diagrams of passive and active vehicle with data of passive vehicle

Initial checks are carried out to verify that the results in formulation of the transfer function are correct. In Table 6.1, they are reported the main linearization points, referred to the passive vehicle, for three values of lateral acceleration.

$a_y = 3\ {}^{m}/_{s^2}$	$a_y = 6\ {}^{m}/_{s^2}$	$a_y = 9\ {}^{m}/_{s^2}$
$F_{Y,F,lin,0} = 3742.9\ N$	$F_{Y,F,lin,0} = 7434.4\ N$	$F_{Y,F,lin,0} = 3742.9\ N$
$F_{Y,rR,lin,0} = 3842.5\ N$	$F_{Y,rR,lin,0} = 7733\ N$	$F_{Y,rR,lin,0} = 3842.5\ N$
$\alpha_{F,0} = 0.85°$	$\alpha_{F,0} = 2.1°$	$\alpha_{F,0} = 0.85°$
$\alpha_{R,0} = 0.53°$	$\alpha_{R,0} = 1.2°$	$\alpha_{R,0} = 0.53$
$\Delta F_{Z,F,0} = 1649.9\ N$	$\Delta F_{Z,F,0} = 3289.7\ N$	$\Delta F_{Z,F,0} = 1649.9\ N$
$\Delta F_{Z,R,0} = 1434.4\ N$	$\Delta F_{Z,R,0} = 2871.6\ N$	$\Delta F_{Z,R,0} = 1434.4\ N$
$\theta_0 = 1.9$	$\theta_0 = 3.8$	$\theta_0 = 5.7$
$r_0 = 6.19\ {}^{°}/_{s}$	$r_0 = 12.4\ {}^{°}/_{s}$	$r_0 = 18.6\ {}^{°}/_{s}$
$\beta_0 = 0.22\ °$	$\beta_0 = 0.56\ °$	$\beta_0 = 1.33\ °$
$M_{ANTI-ROLL,ACT,F,0} = 0\ Nm$	$M_{ANTI-ROLL,ACT,F,0} = 0\ Nm$	$M_{ANTI-ROLL,ACT,F,0} = 0\ Nm$
$M_{ANTI-ROLL,ACT,R,0} = 0\ Nm$	$M_{ANTI-ROLL,ACT,R,0} = 0\ Nm$	$M_{ANTI-ROLL,ACT,R,0} = 0\ Nm$
$\delta_0 = 0.98\ °$	$\delta_0 = 2.2\ °$	$\delta_0 = 4.5\ °$

$C_{F,0} = -4237.9\ {}^{N}/_{\circ}$	$C_{F,0} = -3051.4\ {}^{N}/_{\circ}$	$C_{F,0} = -1478.5\ {}^{N}/_{\circ}$
$C'_{F,0} = 0.23\ {}^{1}/_{\circ}$	$C'_{F,0} = 0.23\ {}^{1}/_{\circ}$	$C'_{F,0} = -0.14\ {}^{1}/_{\circ}$
$C_{R,0} = -6814.1\ {}^{N}/_{\circ}$	$C_{R,0} = -5360.4\ {}^{N}/_{\circ}$	$C_{R,0} = -3880.5\ {}^{N}/_{\circ}$
$C'_{R,0} = 0.32\ {}^{1}/_{\circ}$	$C'_{R,0} = 0.46\ {}^{1}/_{\circ}$	$C'_{R,0} = 0.071\ {}^{1}/_{\circ}$
$F'_{Y,F,lin,0} = -0.23$	$F'_{Y,F,lin,0} = -0.88$	$F'_{Y,F,lin,0} = -1.2$
$F'_{Y,R,lin,0} = -0.18$	$F'_{Y,R,lin,0} = -0.74$	$F'_{Y,R,lin,0} = -1.25$
$f_0 = 0.54$	$f_0 = 0.54$	$f_0 = 0.54$

Tab 6.1: Parameters values from the quasi-static model and tyre analysis (passive vehicle)

Essentially some comparisons are made between the bode plot of the system for the passive vehicle, when it is used the simple track model formulation without considering the variation of cornering stiffness induced by the load transfer and without including the variation of lateral tyre force as a function of the load transfer which is the blue line, the bode diagram of the passive vehicle by using the more advanced model explained in chapter 5 including the variation of the cornering stiffness and the variation of the lateral tyre force on each axle as a function of load transfer. It is also considered the new formulation of the moment that implies the linearization of the anti-roll moment on the front and rear axle based on the system input f.

The Figure 6.2 shows the frequency response of ${}^{r(s)}/_{\delta(s)}$ at $V = 100\ {}^{km}/_{h}$ and $a_y = 3\ {}^{m}/_{s^2}$

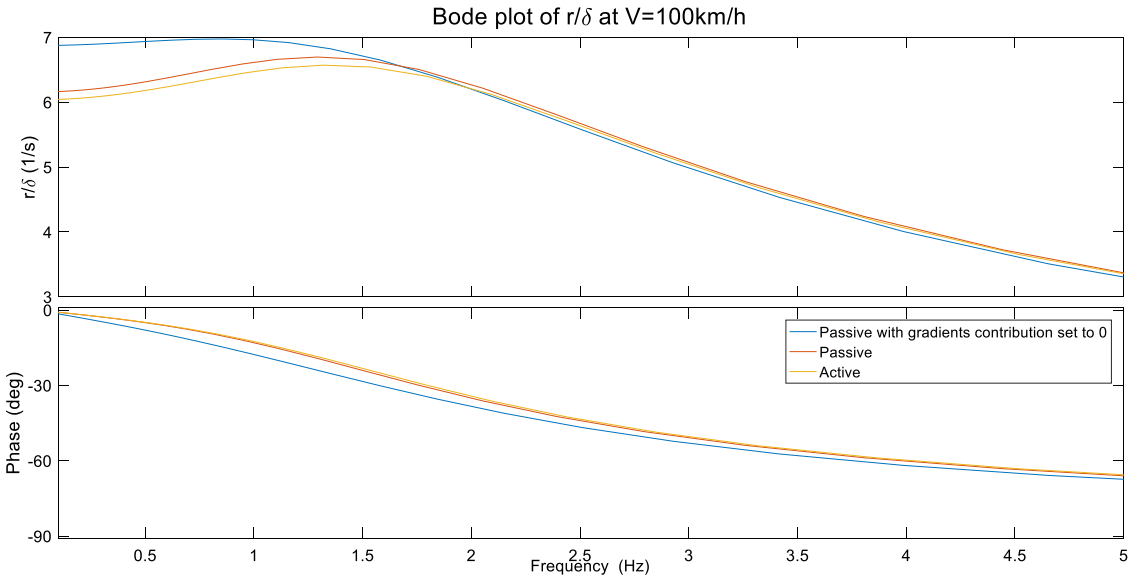

Figure 6.2: Bode plot of yaw rate over steering angle

It is possible to see that the passive vehicle and the active vehicle with the same data of the passive vehicle provide very similar results and it is what expected; these analyses are made in term of yaw rate and roll angle transfer functions. These analyses are carried out for three values of lateral acceleration: 3 $^{m}/_{s^2}$, 6 $^{m}/_{s^2}$, 9 $^{m}/_{s^2}$. The Figures 6.3 and 6.4 show results about the frequency response of $^{r(s)}/_{\delta(s)}$ and $^{r(s)}/_{\delta(s)}$ for $a_y = 9\ ^{m}/_{s^2}$.

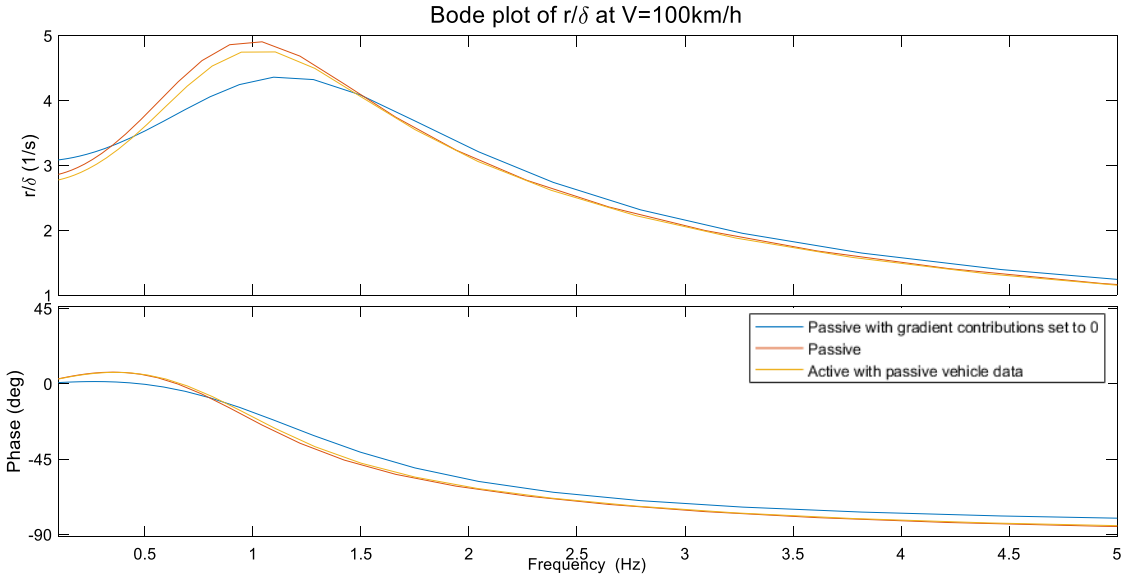

Figure 6.3: Bode diagram of yaw rate over steering angle

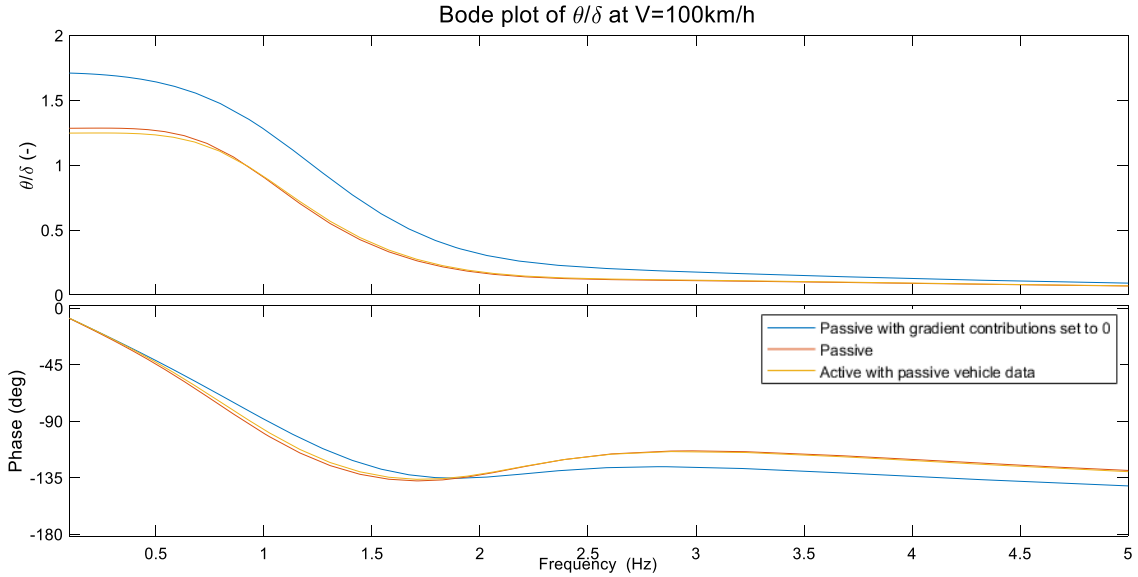

Figure 6.4: Bode diagram of yaw over steering angle

6.3 Active vehicle with PID control

The next step is to create the model in the frequency domain including the controller.

The Figure 6.5 reports the block diagram of the overall system; the inputs is the steering angle delta, then there is a linearized version of the look-up table in order to get the reference yaw rate in steady state condition and there is also a transfer function to consider the desirable dynamics of the reference yaw rate.

There is the calculation of the yaw rate error and based on the error on the yaw rate, the PID control calculates the front-to-total roll stiffness distribution parameter, f; some activation conditions, w_{a_y}, are present based on the lateral acceleration. It is also present the feedforward contribution that depends on the steering angle and it is summed to feedback contribution; in this way it is calculated f and this f is sent to the actuation system in order to calculate the yaw rate and roll angle caused by the different contributions caused by the steering angle, the anti-roll moment on the front and rear axles and the torque vectoring yaw moment if available.

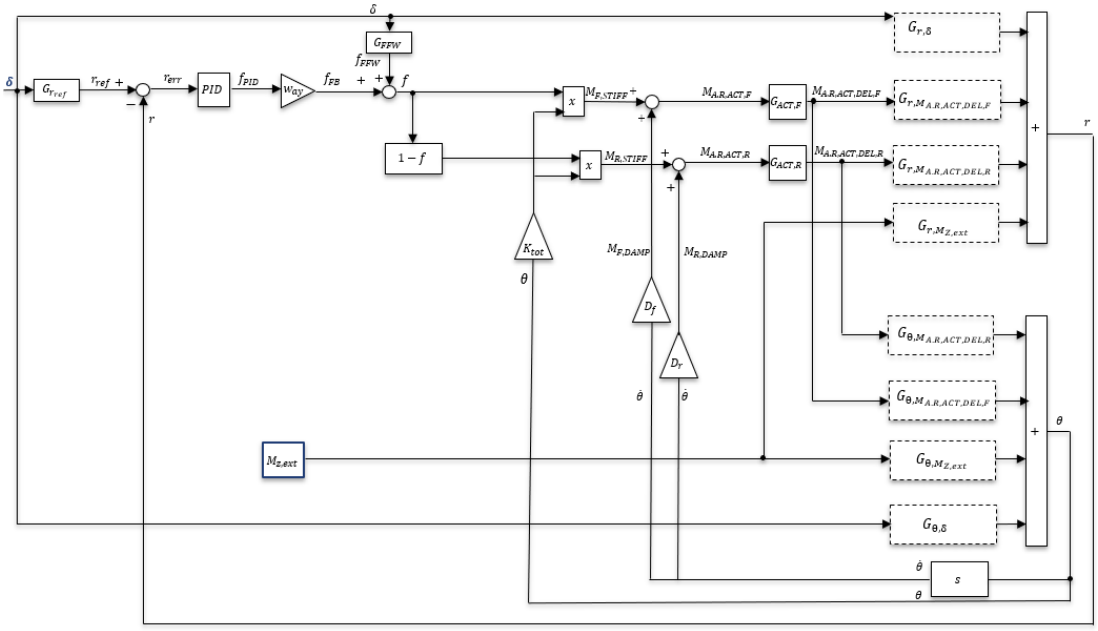

Figure 6.5: Block diagram of the vehicle with the front-to-total roll stiffness distribution controller

6.3.1 Computation of the main transfer functions

The transfer functions for the overall system are obtained including the controller: it is calculated the relations between the yaw rate, r, the roll angle, θ, and each system inputs, δ and $M_{Z,ext}$. The equations in closed-loop are:

$$r = G_{r,\delta}\delta + G_{r,M_{Z,ext}}M_{Z,ext} + G_I\, M_{ANTI-ROLL,ACT,F} + G_{II}\, M_{ANTI-ROLL,ACT,R}$$

$$\theta = G_{\theta,\delta}\delta + G_{\theta,M_{Z,ext}}M_{Z,ext} + G_{III}\, M_{ANTI-ROLL,ACT,F} + G_{IV} M_{ANTI-ROLL,ACT,R}$$

In the closed-loop system, f varies as a function of steering angle δ. It is calculated based on the error of the yaw rate r. It is possible to write the following equations by considering $w_{a_y} = 1$:

$$f = f_{FB} + f_{FFW}$$

$$f_{FB} = G_{PID} r_{err}$$

$$r_{err} = r_{ref} - r$$

A transfer function, $H_{r_{ref}}$, produces realistic and desirable yaw rate dynamics, as by equation:

$$r_{referene} = \delta G_{r_{ref}}$$

$$G_{r_{ref}} = H_{r_{ref}} G_{r_{ref,ss}}$$

The anti-roll moments on the front and rear axles, by using the previous linearization, are given by:

$$M_{ANTI-ROLL,ACT,F} \approx K_{tot}(f\theta_0 + \theta f_0 - \theta_0 f_0) + D_f\dot{\theta}$$

$$M_{ANTI-ROLL,ACT,R} \approx K_{tot}\theta - K_{tot}(f\theta_0 + \theta f_0 - \theta_0 f_0) + D_r\dot{\theta}$$

It is done a further linearization of the feedforward ratio, f_{FFW}, and of the reference yaw rate in steady state conditions, $r_{ref,ss}$, as by the equations:

$$f_{FFW} \approx f_{FFW,0} + f'_{FFW,0}(\delta - \delta_0)$$

$$r_{ref,ss} \approx r_{ref,ss,0} + r'_{ref,ss,0}(\delta - \delta_0)$$

By considering a speed, V, from the graphs $r_{ref} = r_{ref}(\delta)$, $f_{FW} = f_{FW}(\delta)$, Figure 6.6, and for each value of lateral acceleration considered, it is possible to calculate the gradients $r'_{ref,ss,0}$ and $f'_{FFW,0}$ as incremental ratio:

$$r'_{ref,ss,0} \approx \frac{r_{ref,ss} - r_{ref,ss,0}}{\delta - \delta_0}$$

$$f'_{FFW,0} \approx \frac{f_{FFW} - f_{FFW,0}}{\delta - \delta_0}$$

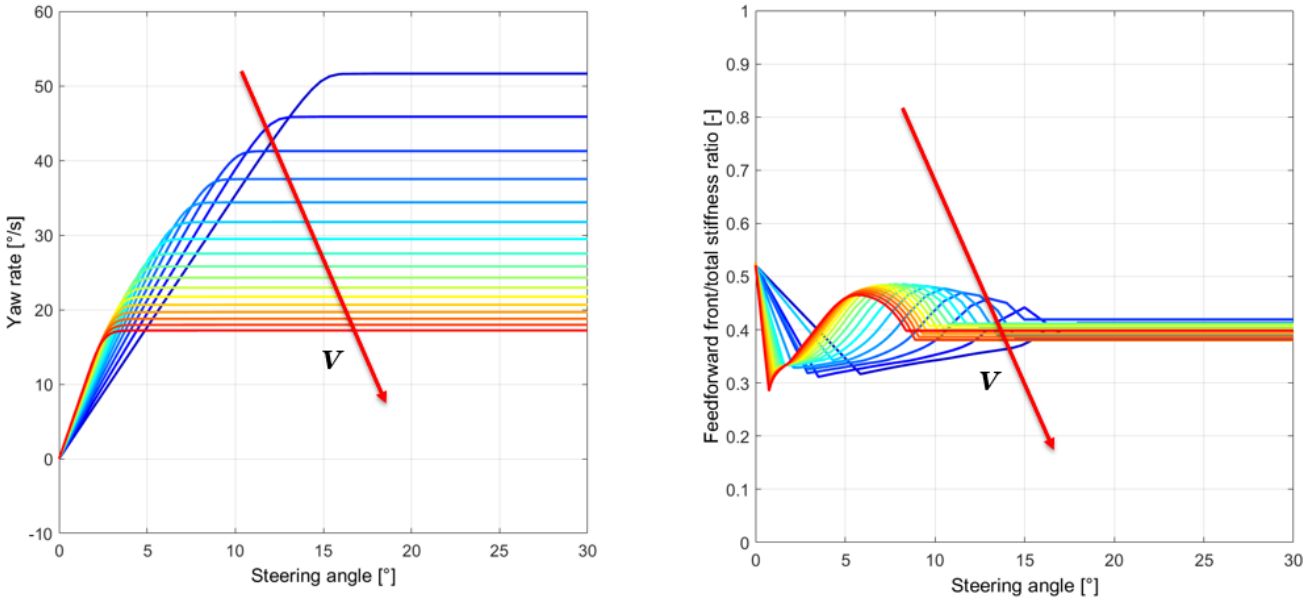

Figure 6.6: Look-up tables by the quasi-static model

By substituting the expressions above in the equation of f, the final expression of f is given by:

$$f \approx f_{FFW,0} + G_{PID} r_{ref,ss,0} H_{r_{ref}} + \delta \left(f'_{FFW,0} + G_{PID} r'_{ref,ss,0} H_{r_{ref}} \right) + \delta_0 \left(-G_{PID} r'_{ref,ss,0} H_{r_{ref}} - f'_{FFW,0} \right) - r G_{PID}$$

At the end it is computed the final equation of r, as:

$$
\begin{aligned}
& r \\
& \approx \delta G_{r,\delta} + M_{Z,ext} G_{r,M_{Z,ext}} + K_{tot} f_0 \theta_0 (G_{II} - G_I) \\
& + K_{tot} \theta_0 (G_I - G_{II}) \left[f_{FFW,0} + G_{PID} r_{ref,ss,0} H_{r_{ref}} + \delta \left(f'_{FFW,0} + G_{PID} r'_{ref,ss,0} H_{r_{ref}} \right) \right. \\
& + \delta_0 \left(-G_{PID} r'_{ref,ss,0} H_{r_{ref}} - f'_{FFW,0} \right) \\
& \left. - r G_{PID} \right] \left\{ [K_{tot} [G_{II} + f_0 (G_I - G_{II})] \right. \\
& + s(D_F G_I + D_R G_{II})] \left[\frac{1}{1 - \{K_{tot} [G_{IV} + f_0 (G_{III} - G_{IV})] + s(D_f G_{III} + D_r G_{IV})\}} \right] [\delta G_{\theta,\delta} \\
& + M_{Z,ext} G_{\theta,M_{Z,ext}} + K_{tot} f_0 \theta_0 (G_{IV} - G_{III}) + K_{tot} \theta_0 (G_{III} - G_{IV})] f_{FFW,0} \\
& + G_{PID} r_{ref,ss,0} H_{r_{ref}} + \delta \left(f'_{FFW,0} + G_{PID} r'_{ref,ss,0} H_{r_{ref}} \right) \\
& \left. + \delta_0 \left(-G_{PID} r'_{ref,ss,0} H_{r_{ref}} - f'_{FFW,0} \right) - r G_{PID} \right\}
\end{aligned}
$$

Analysis are carried to evaluate the performance of the open loop control system, in Figure 6.7, by considering the transfer function of the PID controller plus the complex model of the plant receiving as input the front-to-total roll stiffness distribution parameter.

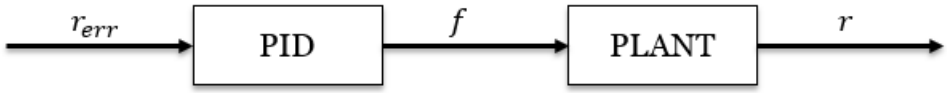

Figure 6.7: Open-loop system

It is evaluated the transfer function of the open-loop system as:

$$\frac{r(s)}{r_{err}(s)} = G_{PID} G_{PLANT}$$

The performances of the closed-loop system, shown in Figure 6.8, are evaluated by considering its transfer function, defined as:

$$\frac{r(s)}{r_{ref}(s)} = \frac{G_{PID} G_{PLANT}}{1 + G_{PID} G_{PLANT}}$$

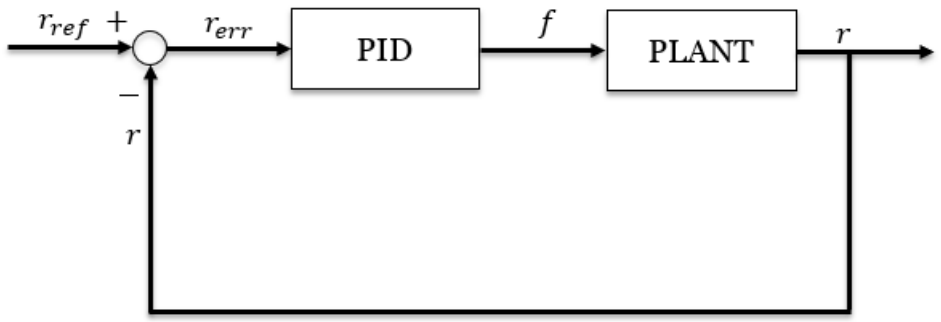

Figure 6.8: Closed-loop system

It is derived, then, the transfer function of the yaw rate of the car over the steering angle when including the feedback and feedforward contributions, shown in Figure 6.9.

$$\frac{r(s)}{\delta(s)} = \frac{G_{PLANT}\left(f'_{FFW,0} + r'_{ref,ss,0}H_{r_{ref}}G_{PID}\right)}{1 + G_{PID}G_{PLANT}}$$

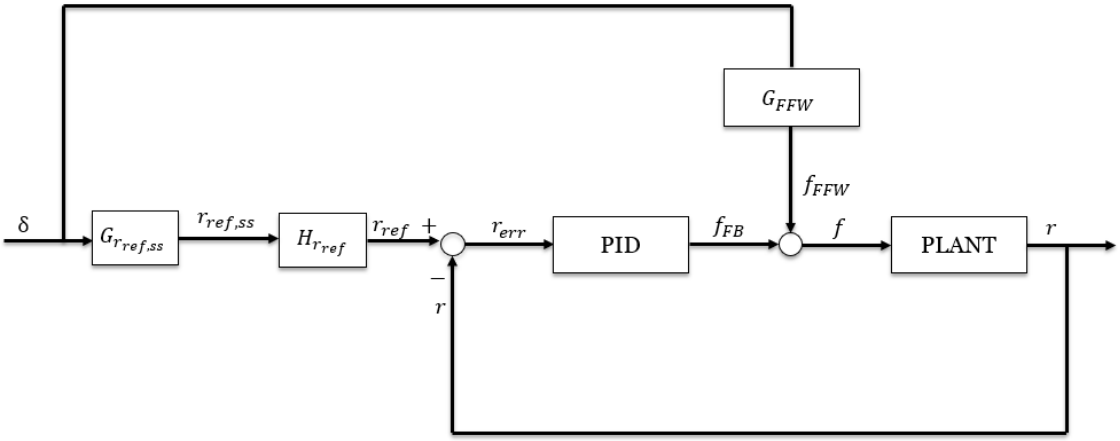

Figure 6.9: Closed-loop with feedforward and feedback contribution

6.4 Simulation results and design of the feedback contribution

In this paragraph it is explained the procedure to design the gain of the PID controller. In the first part it is used the same total roll stiffness for the active vehicle and passive vehicle; secondly it is adopted a more aggressive tuning of the gains of the controller and it is used a greater value of total roll stiffness for the active vehicle in order to have lower values of roll angle.

6.4.1: Preliminary design of the feedback contribution

At first, the Table 6.2 shows the points of the linearization for the same values of lateral acceleration, 3 $^{m}/_{s^2}$,6 $^{m}/_{s^2}$ and 9 $^{m}/_{s^2}$. At this time the values refer to the active vehicle and they are added the points of linearization of the look-up tables of the reference yaw rate and the feedforward contribution, $f'_{FFW,0}$ and $r'_{ref,ss,0}$.

$a_y = 3\ {}^{m}/_{s^2}$	$a_y = 6\ {}^{m}/_{s^2}$	$a_y = 9\ {}^{m}/_{s^2}$
$F_{Y,F,lin,0} = 3729.8\ N$	$F_{Y,F,lin,0} = 7397.3\ N$	$F_{Y,F,lin,0} = 11079.0\ N$
$F_{Y,rR,lin,0} = 3829\ N$	$F_{Y,rR,lin,0} = 7717.6\ N$	$F_{Y,rR,lin,0} = 11702.0\ N$
$\alpha_{F,0} = 0.83°$	$\alpha_{F,0} = 1.86°$	$\alpha_{F,0} = 3.76°$
$\alpha_{R,0} = 0.53°$	$\alpha_{R,0} = 1.27°$	$\alpha_{R,0} = 2.73°$
$\Delta F_{Z,F,0} = 1166.4\ N$	$\Delta F_{Z,F,0} = 2411.9\ N$	$\Delta F_{Z,F,0} = 3808.5\ N$
$\Delta F_{Z,R,0} = 1888.9\ N$	$\Delta F_{Z,R,0} = 3694.8\ N$	$\Delta F_{Z,R,0} = 5390.4\ N$
$\theta_0 = 1.89$	$\theta_0 = 3.77$	$\theta_0 = 5.79$
$r_0 = 6.19\ {}^{°}/_{s}$	$r_0 = 12.33\ {}^{°}/_{s}$	$r_0 = 18.6\ {}^{°}/_{s}$
$\beta_0 = 0.22\ °$	$\beta_0 = 0.65\ °$	$\beta_0 = 1.8\ °$
$M_{ANTI-ROLL,ACT,F,0} = 1133.3\ Nm$	$M_{ANTI-ROLL,ACT,F,0} = 2412.5\ Nm$	$M_{ANTI-ROLL,ACT,F,0} = 3938.6\ Nm$
$M_{ANTI-ROLL,ACT,R,0} = 2448.2\ Nm$	$M_{ANTI-ROLL,ACT,R,0} = 4738.4\ Nm$	$M_{ANTI-ROLL,ACT,R,0} = 6815.5\ Nm$
$\delta_0 = 0.95\ °$	$\delta_0 = 1.9\ °$	$\delta_0 = 3\ °$
$C_{F,0} = -4349.4\ {}^{N}/_{°}$	$C_{F,0} = -3560.7\ {}^{N}/_{°}$	$C_{F,0} = -2035.2\ {}^{N}/_{°}$
$C'_{F,0} = 0.14\ {}^{1}/_{°}$	$C'_{F,0} = 0.25\ {}^{1}/_{°}$	$C'_{F,0} = -0.081\ {}^{1}/_{°}$
$C_{R,0} = -6650.5\ {}^{N}/_{°}$	$C_{R,0} = -5236.1\ {}^{N}/_{°}$	$C_{R,0} = -3254.1\ {}^{N}/_{°}$
$C'_{R,0} = 0.42\ {}^{1}/_{°}$	$C'_{R,0} = 0.47\ {}^{1}/_{°}$	$C'_{R,0} = -0.063\ {}^{1}/_{°}$
$F'_{Y,F,lin,0} = -0.15$	$F'_{Y,F,lin,0} = -0.71$	$F'_{Y,F,lin,0} = -1.1$
$F'_{Y,R,lin,0} = -0.25$	$F'_{Y,R,lin,0} = -0.87$	$F'_{Y,R,lin,0} = -1.4$
$f_0 = 0.32$	$f_0 = 0.34$	$f_0 = 0.37$
$f'_{FFW,0} = 0.038\ {}^{1}/_{°}$	$f'_{FFW,0} = 0.014\ {}^{1}/_{°}$	$f'_{FFW,0} = 0.038\ {}^{1}/_{°}$
$r'_{ref,ss,0} = 6.5\ {}^{1}/_{s}$	$r'_{ref,ss,0} = 6.5\ {}^{1}/_{s}$	$r'_{ref,ss,0} = 3.7\ {}^{1}/_{s}$

Table 6.2: Parameters values from the quasi-static model and tyre analysis (active vehicle)

The Figures 6.11 and 6.12 show the bode diagrams of the open-loop transfer function: since the controller is mainly active for medium-high values of lateral acceleration, the analysis focuses on $a_y = 6\ {}^{m}/_{s^2}$ and $a_y = 9\ {}^{m}/_{s^2}$. Sensitivity simulations are carried out in order to evaluate how the open loop transfer function changes when the proportional gains or the integrative gains are varied. It is here reported only the case referred to $a_y = 6\ {}^{m}/_{s^2}$ and $V = 100\ {}^{km}/_{h}$.

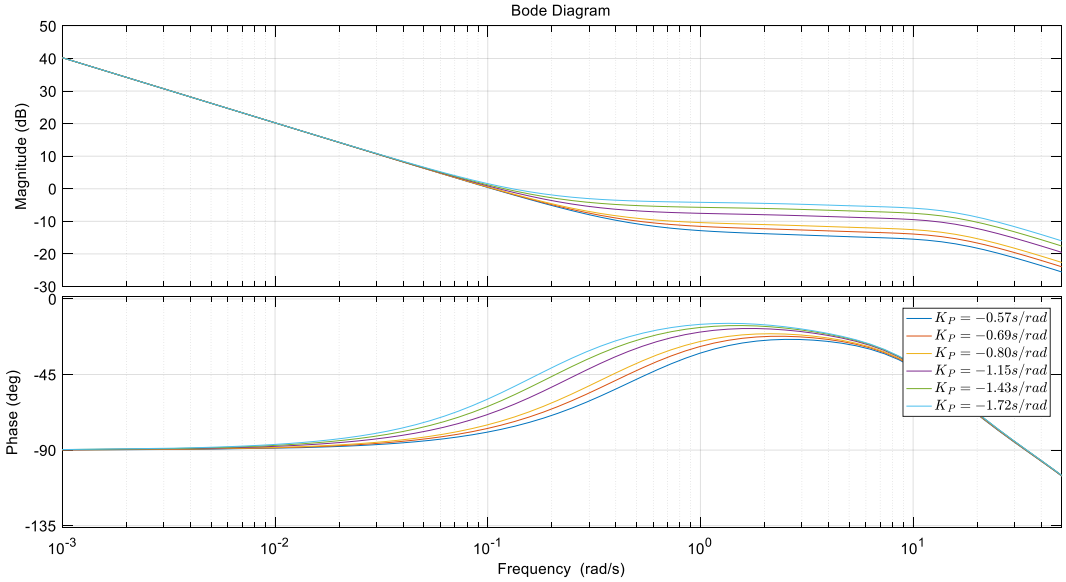

Figure 6.10: Frequency response of the open-loop transfer function for different values of K_P

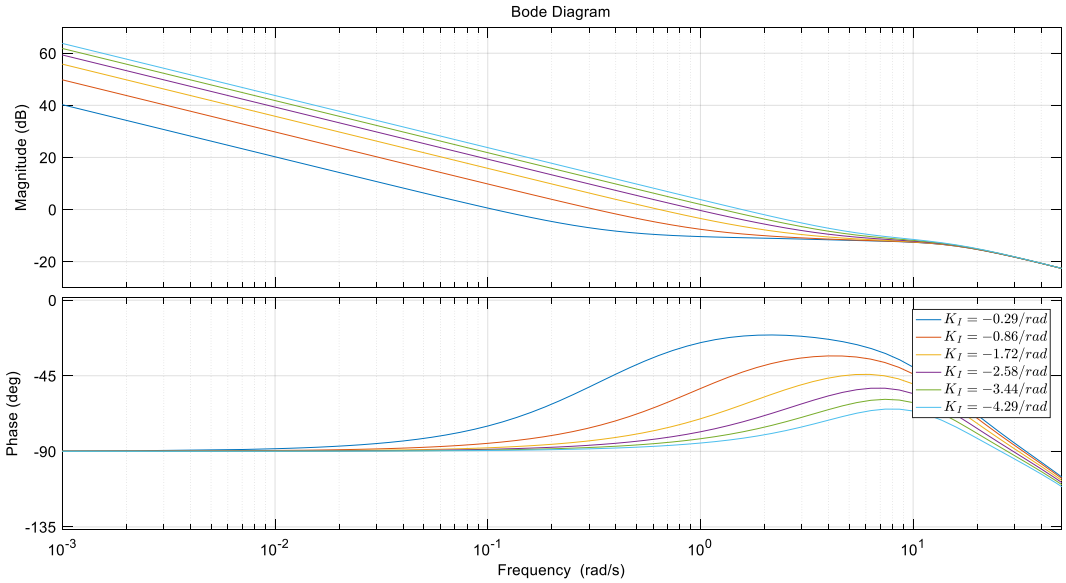

Figure 6.11: Frequency response of the open-loop transfer function for different values of K_I

It possible to see the performance of the closed-loop system, in Figure 6.12, always varying the gains of the PID controller.

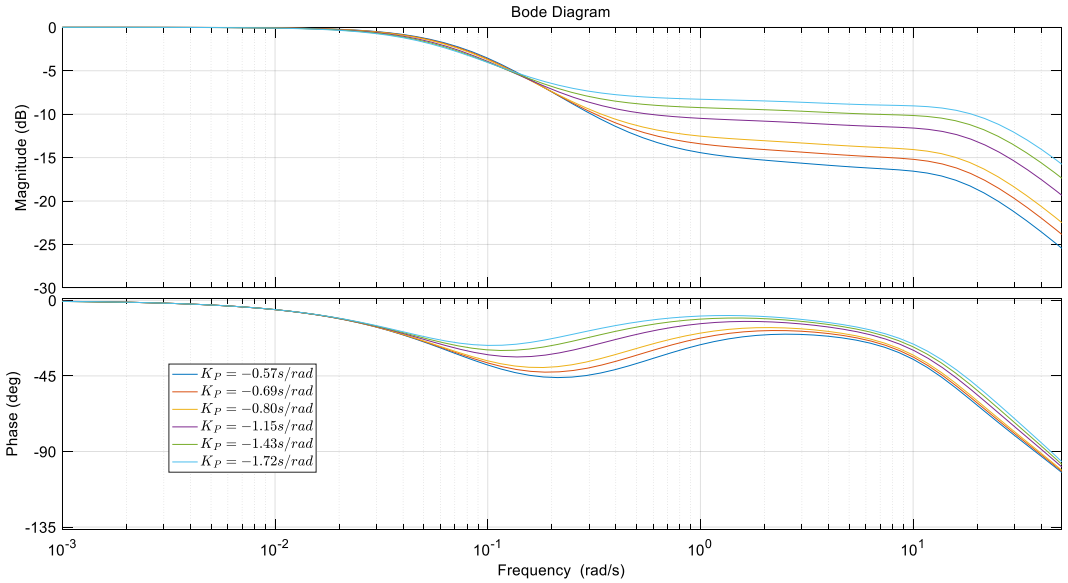

Figure 6.12: Frequency response of the closed-loop transfer function for different values of K_I

The results are summarized in the following Table 6.3 and Table 6.4, that include the values of phase margin and gain margin for different tuning of the controller gains. In this case the tuning is very conservative: in fact, the values of phase margin and gain margin are very high in order to ensure system stability rather than exaggerate with the search for high tracking performance.

$\mathbf{K_I} = -0.29\frac{1}{rad}$	$K_P = -0.69\ \frac{s}{rad}$	$K_P = -0.80\ \frac{s}{rad}$	$K_P = -1.15\ \frac{s}{rad}$	$K_P = -1.43\ \frac{s}{rad}$	$K_P = -1.72\ \frac{s}{rad}$
Gain margin	62.6 dB	53.7 dB	37.6 dB	30.1 dB	25.1 dB
Phase margin	114.5 deg	119.1 deg	134.3 deg	151.1 deg	138.9 deg

$\mathbf{K_P} = -0.80\ \frac{s}{rad}$	$K_I = -0.86\ \frac{1}{rad}$	$K_I = -1.72\ \frac{1}{rad}$	$K_I = -2.58\ \frac{1}{rad}$	$K_I = -3.44\ \frac{1}{rad}$	$K_I = -4.29\ \frac{1}{rad}$
Gain margin	53.4 dB	53.1 dB	52.7 dB	52.4 dB	52.2 dB
Phase margin	117.7 deg	115.3 deg	111.8 deg	107.3 deg	102.1 deg

Table 6.3: Gain margin and phase margin for $a_y = 6\ \frac{m}{s^2}$ and V = 100 $^{km}/_{h}$ $K_D = 0\ ^{s^2}/_{rad}$

$K_I = -0.29\frac{1}{rad}$	$K_P = -0.69\ \frac{s}{rad}$	$K_P = -0.80\ \frac{s}{rad}$	$K_P = -1.15\ \frac{s}{rad}$	$K_P = -1.43\ \frac{s}{rad}$	$K_P = -1.72\ \frac{s}{rad}$
Gain margin	73.2 dB	62.7 dB	43.9 dB	35.2 dB	29.3 dB
Phase margin	103.7 deg	106.2 deg	113.7 deg	120.3 deg	127.4 deg

$K_P = -0.80\ \frac{s}{rad}$	$K_I = -0.86\ \frac{1}{rad}$	$K_I = -1.72\ \frac{1}{rad}$	$K_I = -2.58\ \frac{1}{rad}$	$K_I = -3.44\ \frac{1}{rad}$	$K_I = -4.29\ \frac{1}{rad}$
Gain margin	62.5 dB	62.1 dB	61.7 dB	61.3 dB	60.9 dB
Phase margin	104.9 deg	103.1 deg	101.2 deg	99.4 deg	97.7 deg

Table 6.4: Gain margin and phase margin for $a_y = 9\ \frac{m}{s^2}$ and V = 100 $^{km}/_{h}$ $K_D = 0\ ^{s^2}/_{rad}$

All these values are analysed for multiple lateral accelerations, so it is possible to conclude that the controller works for a given no prating condition of the vehicle is actually stable in other operative conditions of the vehicle.

By setting some control system parameters some vehicle dynamic simulations are run with a non-linear simulation model in MATLAB Simulink. Some performance simulations are run where the passive vehicle is represented by the blue and the active vehicle is indicated as ARC.

In a ramp steer test, for example as in Figure 6.13, the understeer characteristic of the active vehicle follows the reference and in particular about the front-to-total roll stiffness ratio, as expected, the feedforward contribution that is designed by the quasi static model gets most of the contribution whilst the feedback part, that is the difference between the ARC total in the figure and the ARC FF, in steady state condition is substantially negligible.

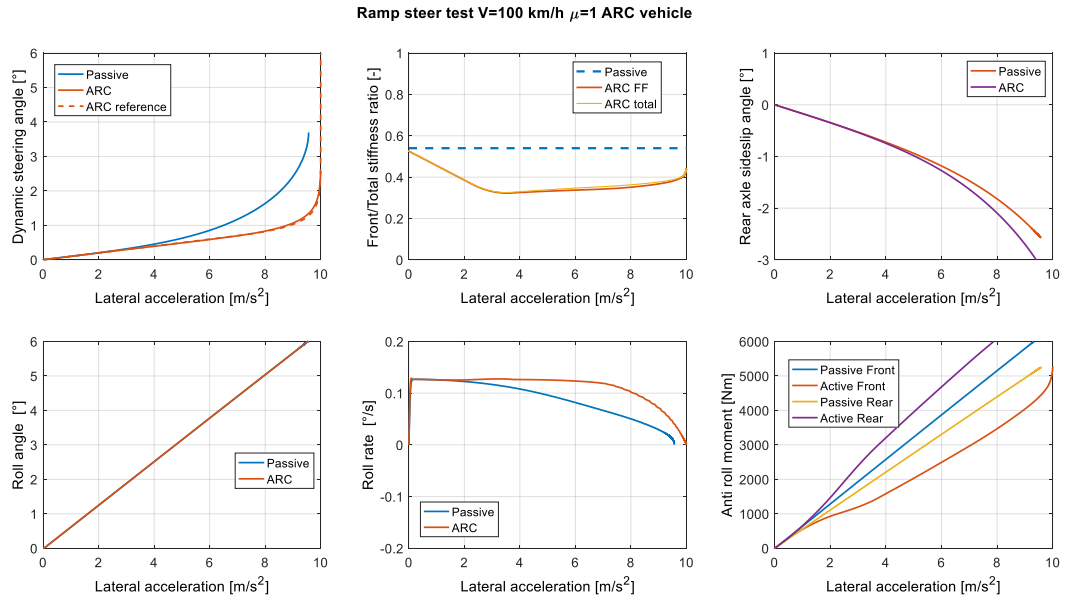

Figure 6.13: Ramp steer manoeuvre at V=100 $\frac{km}{h}$ $K_P = -1.15\,{}^{s}/_{rad}$ $K_I = -0.29\,{}^{1}/_{rad}$ *and* $K_D = 0\,{}^{s^2}/_{rad}$

Several simulations are carried out with double step steer tests with a steering wheel angle amplitude of 150 deg from an initial speed of 100 ${}^{km}/_{h}$, so it is a quite aggressive test, in Figure 6.14.

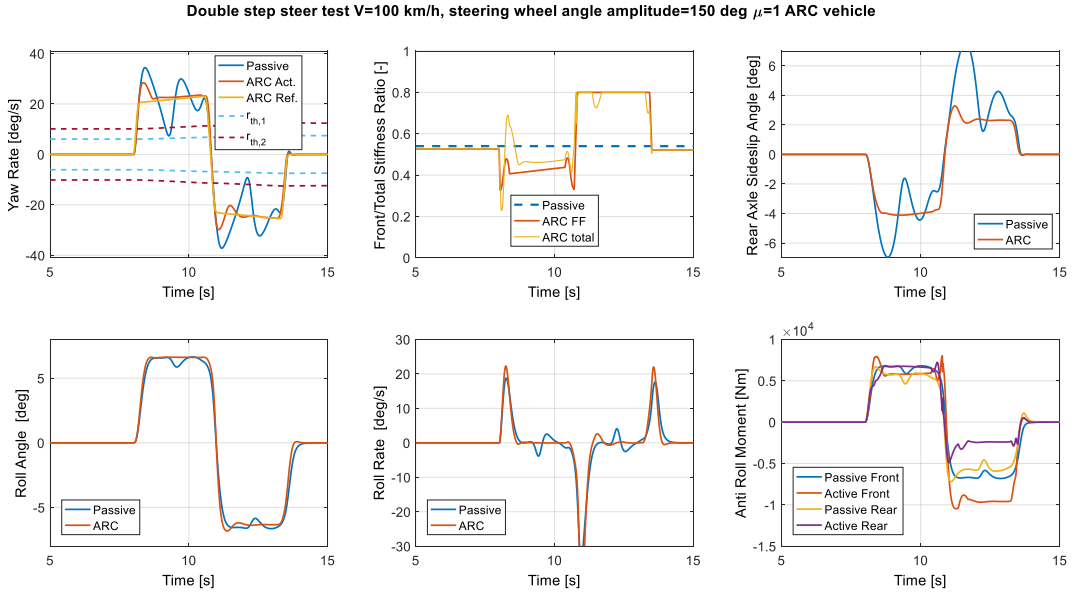

Figure 6.14: Double step steer manoeuvre at V=100 $\frac{km}{h}$ *with* $K_P = -1.72\,{}^{s}/_{rad}$, $K_I = -0.29\,{}^{1}/_{rad}$ $K_D = 0\,{}^{s^2}/_{rad}$

In this case the passive vehicle, indicated with the blue line, has significant oscillations of the yaw rate whilst these oscillations are reduced for the case of the vehicle with front to total roll stiffness distribution controller.

It also interesting to observe the time history in terms of sideslip angle on the rear axle: it is possible to see that the system with active roll controller is characterized by a significant roll damping of the sideslip angle whilst the passive vehicle has major oscillations.

In the next figures it possible to view results for different tunings of the system in these extreme manoeuvres.

Just to clarify it is carried an example of simulation in low friction conditions, in Figure 6.15: in this case, if the reference yaw rate of the car is the reference yaw rate that corresponds in high friction conditions, this means that the feedback part of the suspension controller tends to destabilise the vehicle and provokes significant values of sideslip angle.

In fact, when the rear axle slide slip angle is plotted for the passive and controlled vehicle, there is an issue with the ARC vehicle.

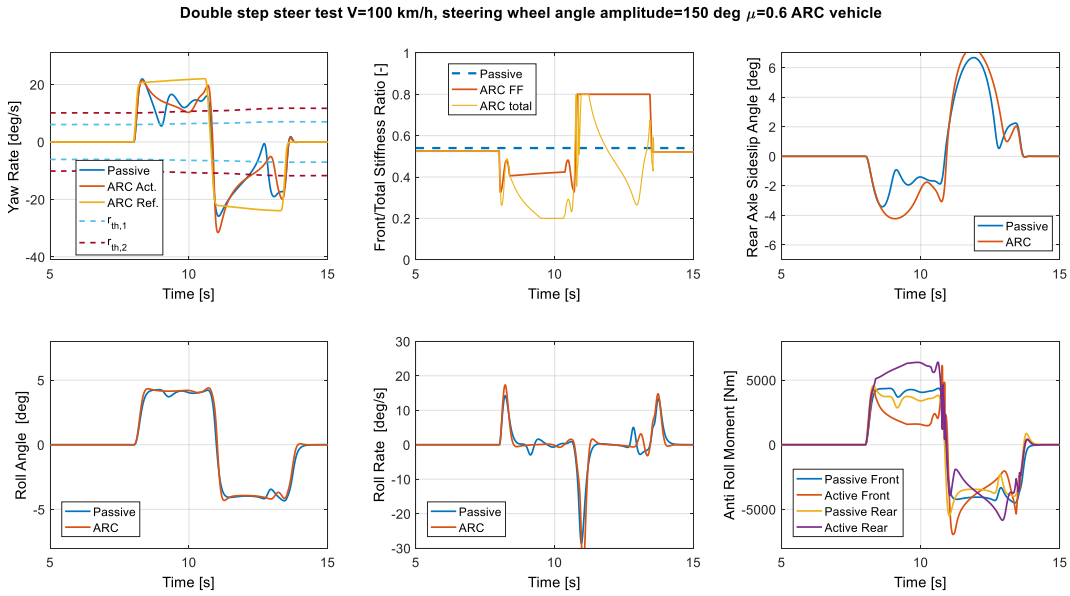

Figure 6.15: Double step steer manoeuvre at V=100 $\frac{km}{h}$ *with* $K_P = -1.15\,{}^{s}/_{rad}$, $K_I = -0.29\,{}^{1}/_{rad}$ $K_D = 0\,{}^{s^2}/_{rad}$ *with* $\mu = 0.6$

6.4.2: Modification of total roll stiffness value

The procedure adopted to have new gains of the controller, in the case of a new total roll stiffness for the active vehicle, is the design of two new look-up tables of the feedforward ratio and the reference yaw rate. By using the quasi-static model, it is designed the reference understeer characteristic for the active vehicle, in Figure 6.16; the user can act on a MATLAB interface by selecting three parameters, the understeer gradient, k_{US}, the maximum value of lateral acceleration in the linear part of the characteristic, a_y^*, and the maximum value of lateral acceleration, $a_{y,max}$.

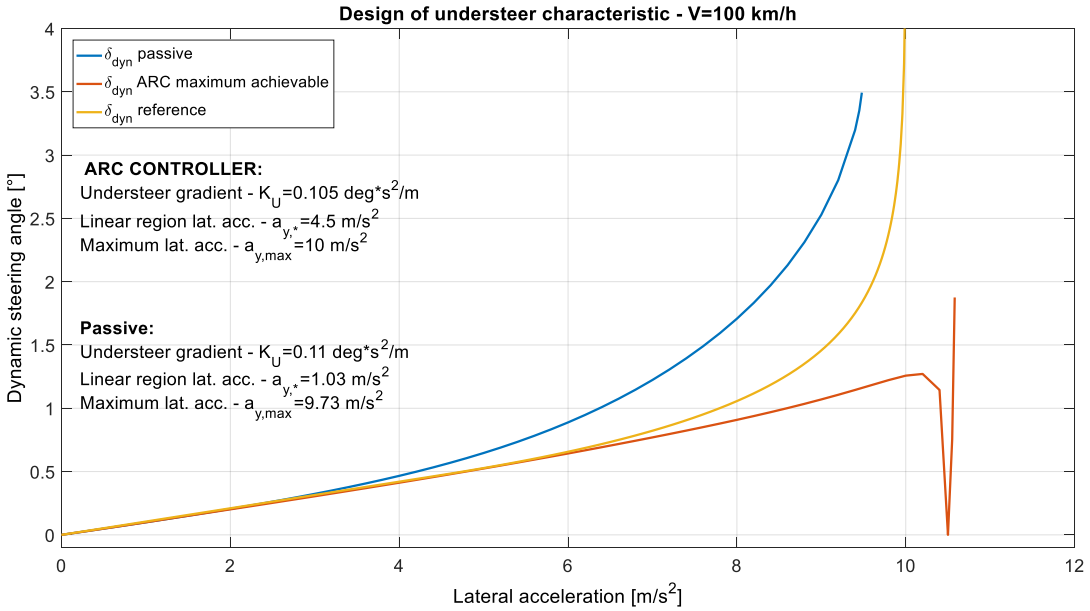

Figure 6.16: Reference understeer characteristic at $V = 100\ {}^{km}/_{h}$

The outputs of the quasi-static model are the look-up tables of the feedforward contribution ratio and reference yaw rate for different values of speed as a function of steering angle, shower in Figure 6.17.

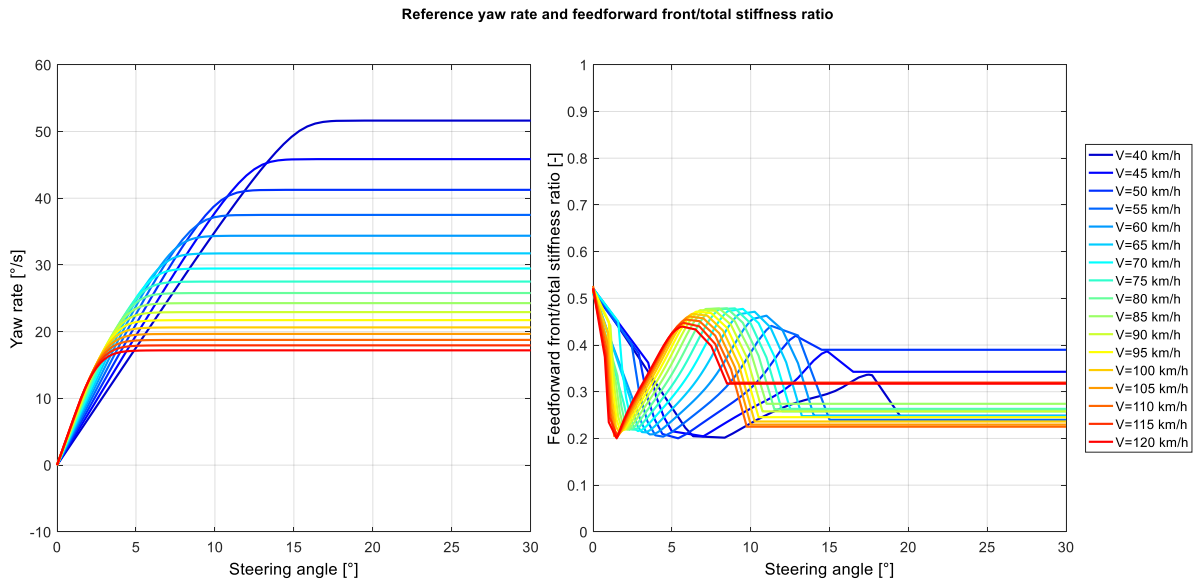

Figure 6.17: Reference yaw rate and feedforward front-to-total ratio

They are plotted the Bode diagrams of the open-loop and closed-loop transfer functions, not showed in this thesis. All the results are summarized in the following Table 6.5 and Table 6.6, in terms of values of phase margin and gain margins, for different tuning of the gain of the controller and for two values of lateral acceleration, $a_y = 6\,{}^{m}/_{s^2}, a_y = 9\,{}^{m}/_{s^2}$.

$\mathbf{K_I} = -1.43\frac{1}{\mathbf{rad}}$	$K_P = -2.87\frac{s}{rad}$	$K_P = -3.44\frac{s}{rad}$	$K_P = -4.01\frac{s}{rad}$	$K_P = -4.58\frac{s}{rad}$	$K_P = -5.16\frac{s}{rad}$
Gain Margin	38.5 dB	32.1 dB	27.5 dB	24.1 dB	21.4 dB
Phase Margin	113.5 deg	118.7 deg	124.1 deg	130.1 deg	136.5 deg

Table 6.5: Gain margin and phase margin for $a_y = 6\ \frac{m}{s^2}$ and V = 100 ${}^{km}/_{h}$ $K_D = 0\,{}^{s^2}/_{rad}$

$\mathbf{K_I} = -1.43\frac{1}{\mathbf{rad}}$	$K_P = -2.87\frac{s}{rad}$	$K_P = -3.44\frac{s}{rad}$	$K_P = -4.01\frac{s}{rad}$	$K_P = -4.58\frac{s}{rad}$	$K_P = -5.16\frac{s}{rad}$
Gain Margin	35.5 dB	29.6 dB	25.4 dB	22.2 dB	19.8 dB
Phase Margin	123.6 deg	131.2 deg	134.5 deg	124.9 deg	118.7 deg

Table 6.6: Gain margin and phase margin for $a_y = 9\ \frac{m}{s^2}$ and V = 100 ${}^{km}/_{h}$ $K_D = 0\,{}^{s^2}/_{rad}$

From the above Tables, by choosing values of $K_P = -4.01\ {}^{s}/_{rad}$, $K_P = -1.43\ {}^{1}/_{rad}$ and $K_D = 0\ {}^{s^2}/_{rad}$, they are simulated the ramp steer manoeuvre, in Figure 6.18, and double step steer manoeuvre, in Figure 6.19.

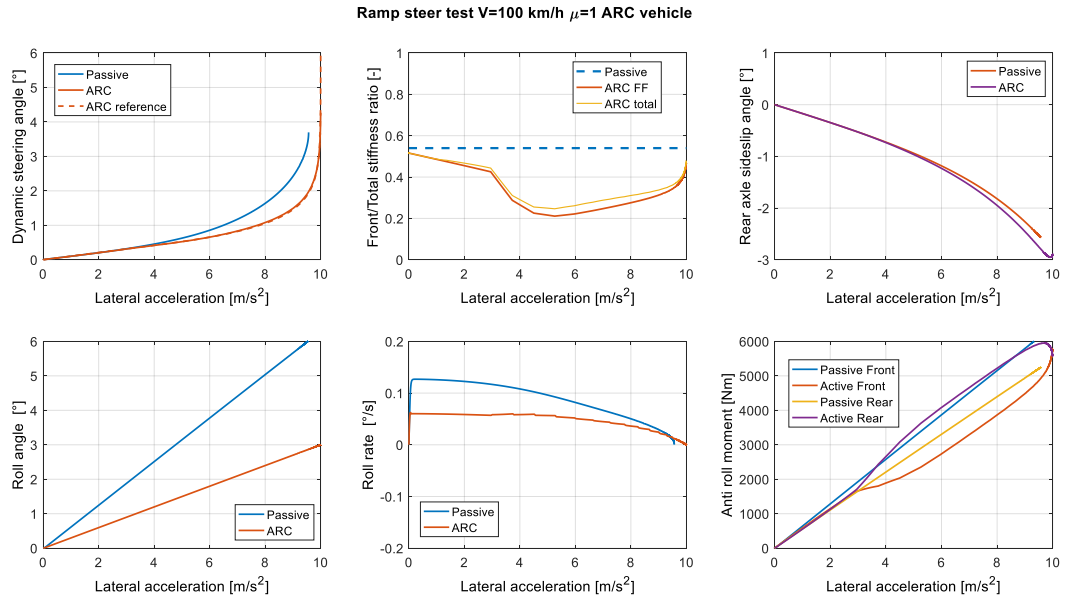

Figure 6.18: Ramp steer test manoeuvre

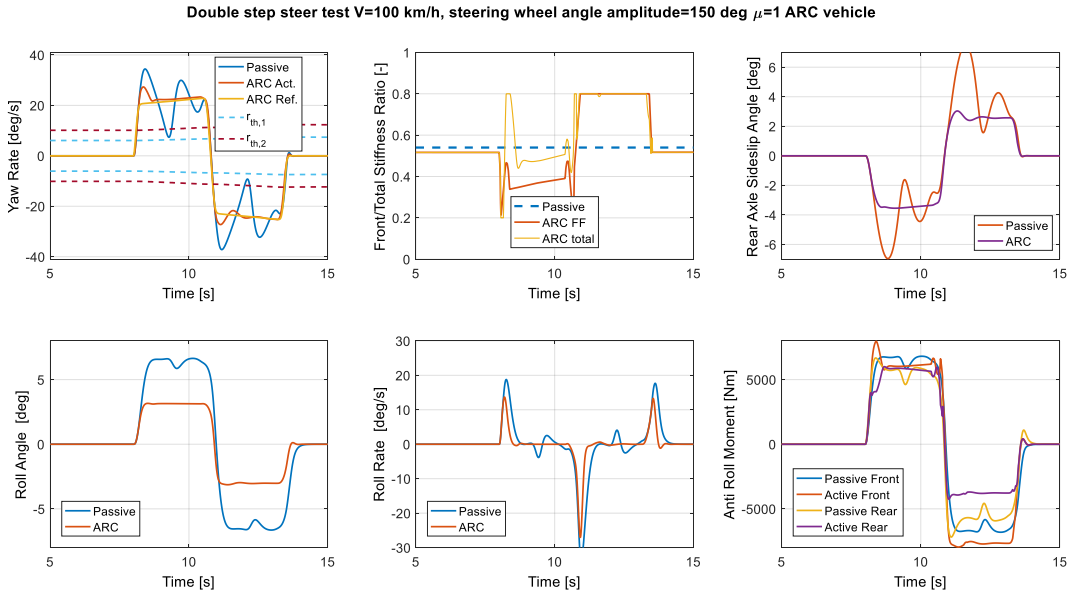

Figure 6.19: Double step steer manoeuvre

In the ramp steer test, the feedforward contribution provides the major effect in terms of front-to-total roll stiffness distribution ratio, which means that the look-up table are properly designed. In double step steer test, the active vehicle follows very well the

reference in terms of yaw rate, with respect the passive vehicle that provides several oscillations. In both tests, with a different tuning of the total roll stiffness, there is a significance difference in terms of roll angle among the vehicle with ad without controller.

CHAPTER 7

7.1 Conclusions

The aim of this thesis 'work was to verify how it is possible to enhance the dynamic response of vehicle by adopting a controllable suspension system. In particular, by varying the anti-roll moment distribution among the rear and front axle, it is possible to correct the understeer or oversteer behaviour of the vehicle.

This work has been developed at first, by implementing the controller in MATLAB-Simulink environment, then verifying that it worked, by carrying out some preliminary simulations with a real model of a vehicle validated in the last years by University of Surrey.

The controller has got two components: the feedforward ratio and the feedback contribution. The first-one is the prevalent one in steady-state conditions and it was designed by a non-linear quasi-static model. By carrying out some ramp steer manoeuvres, it is possible to see that the front-to-total feedforward ratio has got the prevalent, whilst the feedback ration is negligible. These ramp steer manoeuvres were simulated for different vehicle speeds. It is also designed the reference understeer characteristic for the active vehicle, that is less understeer with respect the passive one.

Then some sensitivity analyses, by varying the total-roll-stiffness, were performed in order to evaluate the maximum level of lateral acceleration achievable. From these studies, the effect due to the value of total roll stiffness is really low instead of the controller, which permits to modify the anti-roll moment between the front and rear axles. By using this controller, it is possible to have increasement among 7 % and 13 % of values of lateral acceleration for several values of speed investigated.

It is then carried out a study of the tyre of the vehicle, in order to plot the main characteristic of the tyre adopted. From these analyses, it was discovered that, for these tyres, the lateral force on the axle tends always to be a decreasing function with the load transfer.

This behaviour doesn't happen with the cornering stiffness; in fact, until medium values of slip angles, which correspond to medium values of lateral acceleration, the cornering stiffness decreases by increasing the load transfer. However, after a precise value of slip angle the cornering stiffness increases with the load transfer, that is totally different from it should be found in theory from the text books.

From this analysis, it was decided to formulate a novel linearization for the lateral in order to use in the single-track vehicle model for the design of the gains of the controller of the feedback contribution in transient conditions.

This novel formulation seems to be, in simulation, very powerful with respect the standard formulation, in particular if it is considered the effect of the anti-roll moments, taken as inputs of the system, on the main state variables. In fact, as expected for example, if the load transfer is major in the front axle with respect the rear axle, in steady state conditions, the yaw rate of the car tends to decrease.

Then by investigating the open-loop and closed-loop transfer function it has made a tuning of the gains of the controller and they were simulated again the ramp steer and double step steer tests. In the first manoeuvre the active vehicle is less understeer than the passive vehicle and tends to follow its reference understeer characteristic. Then the feedforward contribution has got the major effect in terms of front-to-total ratio.

In the double step steer the situation is quite critical for the passive vehicle because of its oscillations, in terms of yaw rate, with respect the active vehicle which tends to follow the reference yaw rate. In this work of thesis, it is decided to assume low values of gains of PID controller to guarantee the stability of the vehicle. Different tuning and also different values of actuators limits can permit a more aggressive response of the active vehicle.

In conclusion the future steps of this project have as aim to validate the vehicle not only in MATLAB-Simulink but also in CarMaker and then to design the controller in the new conditions.

Other future goals of this project are to carry out some experimental test, before with the passive vehicle to different values of distribution of total roll stiffness to understand the effect to have more anti-roll moment on the rear or front axle. Then the next step is to test, both in steady state manoeuvres and transient manoeuvres, the vehicle with the front-to-

total anti-roll moment distribution controller, to evaluate the potential benefit by adopting this system and to compare the results with they were reached in simulation.

References

[1] Genta G., *Meccanica dell'Autoveicolo,* Torino, LEVROTTO&BELLA, 1978.

[2] Genta G., *Motor vehicle Dynamics,* Singapore, World Scientific, 1997.

[3] Abe M., Manning. W., *Vehicle Handling Dynamics,* Oxford, Butterworth-Heinemann, 2009.

[4] Milliken W. F., Milliken D. L., *Race Car Vehicle Dynamics,* U.S.A, SAE International, 1995.

[5] Williams D. E., Haddad W. M., *Nonlinear Control of Roll Moment Distribution to Influence Vehicle Yaw Characteristics,* in *IEE Transactions on Control System Tecnology,* vol 3, no. 1, March 1995, 110-116.

[6] Oliver, Jr. et al., *Method for Enhancing Vehicle Stability,* Ford Global Technologies, Inc, Dearborn, Mich, no. 5,948,027, September 7, 1999.

[7] Burdock et al., *Vehicle Supensions,* Land Rover Group Limited, St. Helier (GB), no. US 6,471,218 B1, Oct. 29, 2002.

[8] Abe. M, *A study on effects of roll moment distribution control in active suspension on improvement of limit performance of vehicle handling*, Int. J. of Vehicle Design, vol. 15, no. 3/4/5, pp. 326–336, 1994.

[9] Hwang S. M, Park Y., *Active roll moment distribution based on predictive control*, Int. J. of Vehicle Design, vol. 16, no. 1, pp. 15–28, 1995.

[10] Shibahata Y., Shimada K., Tomari T., *Improvement of vehicle maneuverability by direct yaw moment control,* Int. J. of Vehicle Mechanics and Mobility, vol. 22, nos. 5/6, pp 465-481, 1993.

[11] De Novellis L., Sorniotti A., Gruber P., Pennycott A., *Comparison of feedback control tecniques for torque-vectoring control of fully electric vehicle,* IEE, 2014.

[12] Xu. Y, Ahmadian M., *Improving the capacity of tire normal force via variable stiffness and damping suspension system,* Journal of Terramechanics, vol. 50, no. 2, pp. 122-132, 2013.

[13] March C., Shim T., *Integrated control of suspension and front steering to enhance vehicle handling,* Journal of Automobile Engineering, vol. 221, no. 4, pp. 377-391, 2007.

[14] Wang J., Shen S., *Integrated vehicle ride control via active suspensions,* Int. J. of Vehicle Mechanics and Mobility, vol 46, no. 1, pp. 495-508, 2008.

[15] Yamamoto M., *Active control strategy for improved handling and stability,* SAE Transactions, pp 1638-1648, 1991.